

**TLE PROTEINS IN MOUSE EMBRYONIC STEM CELL
SELF RENEWAL AND EARLY LINEAGE
SPECIFICATION**

Adam F. Laing

The University of Edinburgh

2010

Declaration

I declare that:

1. This thesis was composed by me.
2. The work presented within is my own unless otherwise stated.
3. This work has not been submitted for any other degree or professional qualification except as specified.

Adam Laing

Abstract

TLE proteins are a closely related family of vertebrate corepressors. They have no intrinsic DNA binding ability, but are recruited as transcriptional repressors by other sequence specific proteins. TLE proteins and their homologues in other species have been implicated in many developmental processes including neurogenesis, haematopoiesis and the formation of major organs. They have also been implicated in early lineage specification in vertebrates but a direct role in this has not been found in mammals. The aim of my PhD is therefore to analyse the function of TLE proteins in early lineage specification and cell fate decisions using mouse embryonic stem cells (ESCs) as a model.

The investigation of this has previously been complicated, firstly by the large array of transcription factors that TLEs interact with and secondly by redundancy between similar TLE proteins hindering loss of function approaches. To circumvent these problems, I have used two complementary experimental strategies. The first was identification of point mutations in TLE1 that affect specific classes of DNA binding. Two of these mutations L743F and R534A were of particular interest and were reversibly overexpressed in ES cells to correlate phenotypes to biochemical activity. The second strategy was the mutation of the two primary TLE genes in ES cells and early mouse embryos, TLE3 and TLE4.

Complementary evidence from these approaches revealed a role for TLEs in the promotion of ES cell differentiation by repression of pluripotency/self-renewal associated genes. Additionally, neural specification was increased by TLE1 expression especially by the TLE1 point mutations, highlighting opposing roles for TLE through Wnt and Notch pathways in this process. TLE had both positive and negative effects on mesendodermal differentiation. Early mesoderm/primitive streak was increased by loss of TLE, probably through Wnt antagonism. Anterior endoderm was increased by reduced TLE, but a critical level of TLE was still necessary and TLE1 overexpression also upregulated some anterior endoderm markers suggesting both negative and positive roles for TLE proteins in this process

Acknowledgments

First of all, I would like to thank my supervisor Josh Brickman for giving me the opportunity to work in his lab on such an interesting field of science and for all his help, encouragement, support and troubleshooting abilities over these past few years.

I also thank all the members of the Brickman lab both past and present for assistance, friendship and making my time here a pleasant and memorable one, even when things were difficult for me. Special thanks go to Maurice and Fella for being such good and patient teachers and to Andrea for all her work that became the inception for my PhD project.

Also all the people at the ISCR and especially our Thursday morning developmental biology club for discussions of the science and much advice, assistance and the all the primers, constructs and antibodies etc which people kindly provided.

There are also many support staff here without whom work in the department would be impossible, and special thanks go to Jan Ure for ES cell derivation, Carol Manson for looking after my mice, Jon Rans for karyotyping and TC support and Simon Monard and Jan Vrana for FACS assistance.

I also thank our collaborators in Canada, Stefano Stifani and Manuel Buscarlet, for letting us work with them on their TLE point mutations and Susan McConnell for providing the TLE4 mice and targeting vectors.

Finally and most importantly, I thank my parents for all their love and support and for believing in my abilities.

Table of Contents

Chapter 1: General Introduction	1
1.1 Outline of vertebrate axis formation	2
1.2 Mouse early embryonic development	3
1.2 Wnt Signalling	9
1.3 Hex and TLE4	14
1.4.1 Groucho/TLE corepressors	16
1.4.2 Biochemistry of TLE proteins	18
1.4.3 Non full-length TLE proteins	22
1.4.4 TLEs in development	24
1.5 Embryonic stem cells	27
1.6 TLEs in ES cells	32
Introduction to experimental strategy and results	33
Chapter 2: Materials and Methods	36
2.1 Cloning	
2.1.1 Restriction Digests	37
2.1.2 Modification of DNA ends	37

2.1.3 Ligation of DNA fragments	37
2.1.4 DNA transformation	37
2.1.5 Preparation of Plasmid DNA	38
2.2 General Molecular Biology	
2.2.1 Preparation of genomic DNA	38
2.2.2 Agarose gel electrophoresis of DNA	38
2.2.3 Preparation of DNA from agarose gels	39
2.2.4 Preparation of RNA	39
2.2.5 cDNA synthesis	39
2.2.6 Quantitation of nucleic acids	39
2.2.7 Polymerase Chain Reaction	40
2.2.8 TOPO cloning of PCR products	40
2.2.9 Quantitative rtPCR	41
2.2.10 Sequencing of DNA	43
2.2.11 Southern Analysis	43
2.2.12 Western Analysis	44
2.2.13 Constructs	44
2.3 Cell culture and experiments	
2.3.1 Cell lines	45
2.3.2 Maintenance of Cells	45
2.3.3 Transient transfection of HEK293 cells and TOPflash assays	45
2.3.4 Stable transfection of ES cells	46

2.3.5 Antibody staining of cells	47
2.3.6 2i culture of ES cells	47
2.3.7 Neural Differentiation	48
2.3.8 Mesendoderm differentiation	48
2.3.9 Flow cytometry	48
2.3.10 Colony forming assays	49
2.4 Mouse experiments	
2.4.1 TLE4 ^{+LacZ} mice	49
2.4.2 β galactosidase staining of embryos	50
Chapter 3: TLE family expression in ES cells and early development and the generation of reagents to investigate their roles	51
3.1 Expression of TLEs in ES cells	52
3.2 Expression of TLE4 in early stage mouse embryos	55
3.3.1 The generation of TLE mutants with altered binding and corepression activity	58
3.3.2 Activity of point mutants and fusion proteins with respect to Wnt signalling.	59
3.3.3 Altered cofactor binding activities of TLE1 point mutations	63
3.4 Generation of TLE1 overexpression constructs	66

3.5 Generation and initial characterisation of TLE overexpressing ES cell lines	69
3.6 Derivation of TLE4 mutant ES cells	72
3.7 Construction of the TLE3 targeting vector	75
3.8.1 Generation of TLE3/TLE4 mutant ES cells	78
3.8.2 Generation of TLE1 rescued TLE3/TLE4 null cells	81
3.9 Altered TLE activity across a range of generated cell lines	83
3.10 Discussion	85
Chapter 4: The effects of altered TLE activity in ES cell self-renewal and lineage specification	87
4.1 TLE1 overexpression reduces the efficiency of self-renewal in ES cells	88
4.2 TLE mutant ES cells exhibit enhanced self-renewal ability	90
4.3 TLE1 expression results in modest reductions in some pluripotency markers	92
4.4 TLE3 and TLE4 compound mutants express high levels of pluripotency genes	92
4.5 TLE overexpressing cells are prone to differentiation in multiple lineages.	100
4.6 Differentiation of TLE mutants.	107

4.7 ES marker expression of TLE mutant cells in the 2i culture system	113
4.8 Discussion	118
Chapter 6: Final Discussion	122
Supplementary figures	127
Common Abbreviations	129
Appendix: Publication - Inhibition of Cortical Neuron Differentiation by Groucho/TLE1 Requires Interaction with WRPW, but Not Eh1, Repressor Peptides	131
References	140

List of Figures

Fig 1.1 Early mouse development

Fig 1.2 Involvement of TLEs in major signalling pathways

Fig 1.3 Schematic representation of Hex interactions with the Wnt and Nodal-related pathways.

Fig 1.4 Structure of Groucho/TLE proteins

Fig 3.1 Expression of the TLE gene family in embryonic stem cells

Fig 3.2 Expression pattern of TLE4 in early development

Fig 3.3.2 Analysis of TLE variants and point mutations for *wnt* modulating activity

Fig 3.3.3 Interaction of different TLE1 point mutations with *hes1*, *engrailed1* and TCF3

Fig 3.4 Overexpression strategy and construct design for TLE1 and point mutations

Fig 3.5 TLE expression levels in ES cell lines stably expressing CAG TLE1

Fig 3.5.2 FACS analysis of mCHERRY and GFP expression in TLE1 overexpressing and recombined subclones

Fig 3.6 Derivation of TLE4 heterozygous and homozygous mutant ES cells

Fig 3.7 Cloning of the TLE3 targeting vector

Fig 3.8.1 Targeting of the TLE3 loci in the TLE4^{lacZ/LacZ} cells

Fig 3.8.2 TLE1 expression in 34n TLE1 rescued lines

Fig 3.9 Expression of TLE genes in all experimental cell lines

Fig 4.1 Self-renewal ability of TLE overexpressing cells at colonial density

Fig 4.2 self-renewal ability of cells with reduced TLE activity at colonial density

Fig 4.3 Pluripotency and primitive endoderm marker expression in TLE1 overexpressors

Fig 4.4 Pluripotency and differentiation marker expression in TLE mutant cells

Fig 4.5.1 Neural differentiation of TLE overexpressing ES cells

Fig 4.5.2 Mesendoderm differentiation of TLE overexpressing ES cells

Fig 4.6.1 Neural Differentiation of TLE mutant ES cells

Fig 4.6.2 Mesendoderm differentiation of TLE mutant ES cells

Fig 4.7 ES marker expression of TLE mutant cells in 2i with altered CHIRON concentration

Fig 4.8 Speculative model for roles of TLEs in ES cell self renewal and lineage specification

Fig S.1.1 Summary table of gene expression changes in neural differentiation for TLE1 overexpressing and TLE mutant cells

Fig S.1.2 Summary table of gene expression changes in endodermal differentiation for TLE1 overexpressing and TLE mutant cells

Chapter 1

General Introduction

1.1 Outline of vertebrate axis formation

At the core of developmental biology is the question of how complex multicellular organisms develop from a single cell. This process involves tightly controlled growth, differentiation, patterning and morphogenesis. An unpatterned group of dividing cells first gains asymmetry, setting up the primary axes on which all further development is consequential. These are Anterior-Posterior (A-P) or “head to tail” which runs parallel to the notochord in vertebrates and the perpendicular Dorsal-Ventral or “front to back”. Specification of the position of axes may be maternally induced or decided after several cell divisions depending on species. In *Xenopus* for example, axis specification is induced by maternal determinants concentrated asymmetrically opposite the sperm entry point, specifying a signalling centre known as the Nieuwkoop centre (Harland et al. 1997). However, the frog zygotic genome does not become transcriptionally active until after initial axis specification during Mid Blastula Transition, and therefore maternal transcripts are essential determinants. Contrastingly, in the mouse, zygotic transcription starts at the 2-cell stage, suggesting the effect of any maternal RNA would be rapidly diluted out. No mammalian Nieuwkoop centre has been identified. While there have been a number of studies devoted to establishing a deterministic model for early mammalian development, their findings are controversial and cell identity does not appear to begin become fixed until compaction of the morula (Antczak and Blerkom. 1997; Zernicka-Goetz 1998; Piotrowska and Zernicka-Goetz. 2001). Whether maternally specified or self-regulative however, axis specification depends on distinct groups of cells organizing surrounding cell movement and gene expression. Pioneering work by Spemann and Mangold in 1924 led to the identification of one such group of cells in the amphibian dorsal blastopore lip that became known as the Spemann Organizer (Spemann et al. 1924). Transplantation of this can induce a complete secondary axis in a second embryo. The Organizer is itself induced by the Nieuwkoop centre. Based on related gene expression and morphology, Organizer equivalents have been found in other species such as the Early Gastrula Organizer and the later node in mouse, Hensen’s node in chick and the embryonic shield in teleosts. Further studies have shown that different parts of the organizer or different stages differed in their ability to produce a complete axis. For example, late gastrula Spemann Organizers do not induce a secondary axis with head, and in the mouse neither the node nor EGO can

induce a complete axis on its own (Tam and Steiner. 1999). These findings highlight the physical and temporal separation of different organizing activities. The organizer also initiates the initial lineage separations and cell movements that are the first morphological signs of embryonic axes and are known as gastrulation.

At gastrulation the establishment of the three embryonic germ layers first becomes apparent. All animal tissues and organs can be traced back to one of three separate lineages known as germ layers. The innermost endoderm gives rise to the digestive and respiratory tracts at the organism's core and associated organs such as liver, lungs and pancreas. Ectoderm forms the nervous system and surface epidermis. Mesoderm forms all other cell types including blood, muscle, circulatory and skeletal systems and other organs. The separation of the three germ layers occurs during the process of gastrulation. In amphibians, this starts with invagination of superficial dorsal cells towards the blastocoel cavity. This blastopore contains the organizer, which initiates the differentiation of involuting cells into separate germ layers with the first emerging cells destined to become dorsal mesoderm (Harland et al. 1997). In birds and mammals it starts with a movement of cells in the disc shaped embryo through a feature called the primitive streak, which runs along the AP axis with the organizer at its anterior end (Mikawa et al. 2004). Gastrulation in the model species the mouse will be discussed in more detail below. Rodent gastrulation (reviewed in detail below, with references) looks somewhat different, as the cells appear to move from the inside to the outside of the cup shaped embryo although this is more of a morphological than functional distinction. Although the initial topological arrangements and subsequent movements of these layers relative to each other vary between species, the basic function of gastrulation is similar across all vertebrates, from *Xenopus* to mouse.

1.2 Mouse early embryonic development

As with all multicellular organisms, mammalian development commences with the proliferation of a uniform group of equivalent cells with no apparent morphological distinctions. As the mammalian embryo is unique in having to generate both embryonic and extra-embryonic lineages, early development begins with an expansion phase

during which the progenitors of these lineages proliferate. After fertilization, the zygote begins to divide, taking around 3 days to produce the 16 cell morula. Up to the morula stage, cells from different embryos can be combined with no apparent defects in development. This demonstrates that the mammalian embryo is highly regulative compared to other vertebrates and suggests the absence of any maternal patterning system. At this stage, in a process known as compaction, the cells on the inside become specified as inner cell mass (ICM) and the outside, the extra-embryonic trophoderm. Immediately following compaction, the first overt morphological asymmetry becomes apparent with the formation of the blastocoel cavity dividing the embryo along its future proximal distal axis. The trophoderm will contribute to trophoblast and extraembryonic ectoderm, future components of the placenta. At 4.5dpc a second extra-embryonic lineage resolves itself from the inner cell mass, as the primitive endoderm (PrEn) segregates from the ICM. The PrEn will give rise to two distinct extra-embryonic lineages, the visceral and parietal endoderm and the remaining ICM will differentiate into a central epithelial structure, the epiblast. The visceral endoderm surrounds the epiblast and cells in this layer will contribute to the visceral yolk sac, while the parietal endoderm forms a second outer extra-embryonic layer known as Reichart's membrane. The cells in the epiblast will contribute to extraembryonic mesoderm and the three germ layers that will eventually form the embryo proper. Up till around 6.5dpc epiblast cells can mix extensively and the embryo appears bilaterally symmetric. This symmetry is broken at a morphological level by the process of gastrulation. As gastrulation begins, cells converge towards one side of the proximal epiblast and form the primitive streak, a structure through and in which, the morphogenetic movements of gastrulation proceed. Cells delaminate from the epiblast and ingress through the streak to generate the mesoderm, endoderm and posterior neural tube. As early primitive streak gene expression first appears in the epiblast, the distal most cells in this region have organizer activity and have been referred to as the Early Gastrula Organizer (EGO) (Tam and Steiner. 1999). Later the distal region of the primitive streak forms a morphologically recognizable structure known as the node, which has historically been associated with the organizer in other vertebrates although this was not shown until the early 1990s (Beddington 1994).

As in other vertebrates, the organizer region of the mouse embryo will have a major role in patterning the A-P axis in the neural tube. Formation of the streak at the future posterior side is the first morphological sign of the anterior-posterior axis. Epiblast cells ingress through the primitive streak and exit to form the three germ layers. Cells exiting along the midline will form axial mesoderm, definitive endoderm and floor plate of the neural tube. The axial mesoderm will form the notochord, prechordal plate and anterior endoderm; all three structures alongside the floor plate will produce signals patterning the dorsal-ventral axis. Streak derivatives migrating laterally, will generate the paraxial (somites) and lateral (blood) mesoderm. The left-right axis is not specified until gastrulation and arises from an asymmetry in the lateral plate mesoderm. This first 7.5 days of murine development is summarized in Fig 1.1 (Beddington and Robertson 1999; Rossant and Tam. 2004; Arnold and Robertson. 2009).

While streak formation is the first morphological sign of asymmetry, at least a day prior to gastrulation, anterior-posterior polarity can be detected at the level of gene expression. Canonical anterior organizer markers such as *Hex*, *Cerberus* and *VE-1* are detected at the future anterior side of the egg cylinder (Rosenquist and Martin. 1995; Belo et al. 1997; Thomas and Beddington. 1998). The expression of these and other anterior organizer or mesoderm markers such as *Dickopf*, *Lefty* and *FoxA2* begins in the primitive endoderm and then their expression becomes restricted to the distal region of the visceral endoderm (DVE). The DVE starts to migrate anteriorwards at around 6.0dpc, just before gastrulation (then becomes referred to as anterior visceral endoderm - AVE).

The molecular basis for the establishment of the DVE and the resulting future axes from the highly regulative beginning of mammalian development is still not fully understood. However, there is evidence for the involvement of TGF β signalling including BMP4 and Nodal, and Wnt signalling in the establishment and maintenance of proximal-distal polarity. The NODAL ligand is initially expressed throughout the epiblast but becomes localized to the proximal region around 5dpc. Its downstream effector SMAD2 is expressed in overlying VE that receives the Nodal signal and activates the transcription of anterior mesoderm markers such as *Cerberus* and *Lefty*. Interestingly, a large proportion of these DVE/AVE markers are also Nodal and Wnt antagonists. The role of

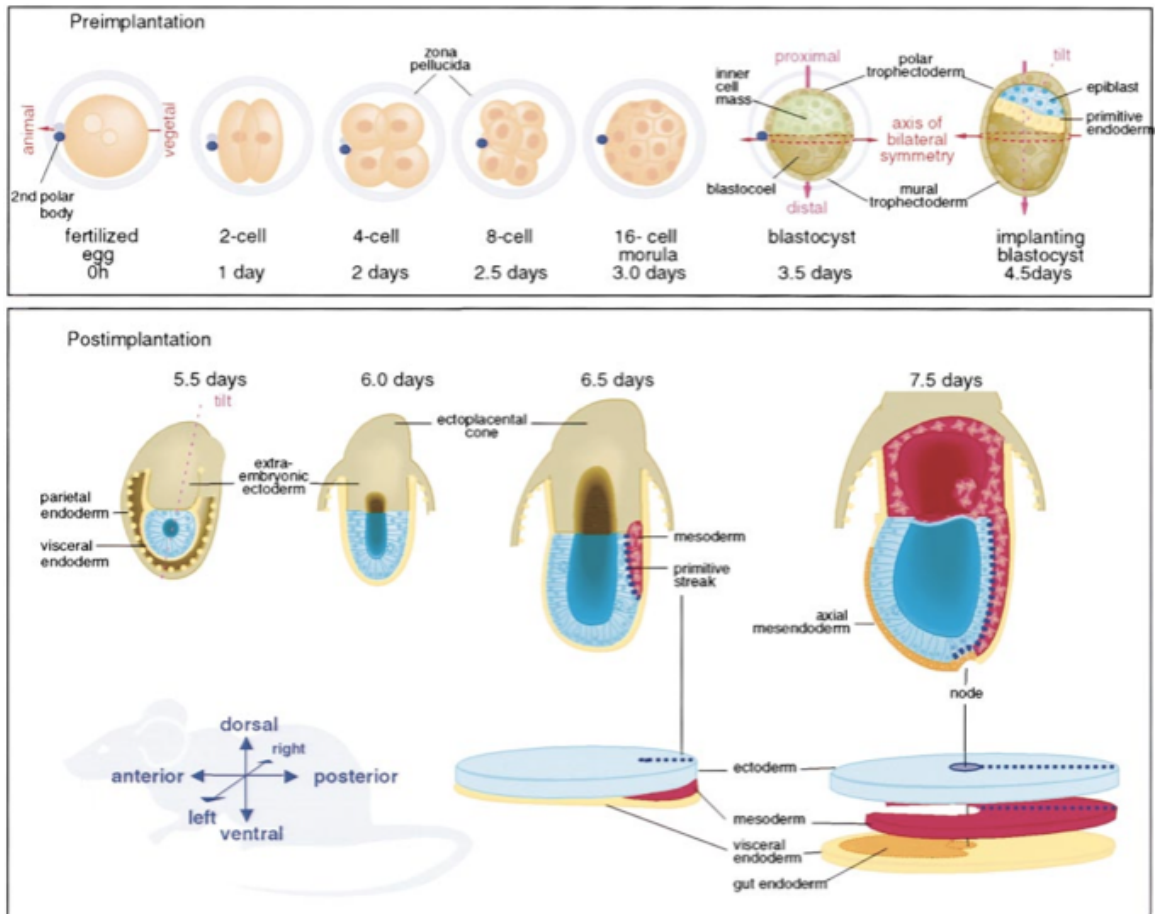


Fig 1.1 Early mouse development

Embryonic development of the mouse from fertilization until 7.5dpc. Top panel shows developmental stages before implantation into the uterus, bottom panel shows stages after implantation. Taken from Beddington and Robertson, 1999

these molecules appears to be the attenuation of Nodal signalling in the underlying epiblast so that it is able to differentiate into anterior neural plate (Brennan et al. 2001). Meanwhile Nodal signalling at the proximal end of the epiblast autoinduces its own activity by activating Nodal pro-protein processing enzymes FURIN and PACE4 and by an autoregulatory Nodal/Bmp4/Wnt loop to promote more Nodal transcript (Ben-Haim et al. 2006). The combination of these activities reinforces a proximal-distal signalling gradient, which will be converted to anterior-posterior. Antagonists secreted by the DVE also stop the formation of ectopic primitive streak. Visualization of DVE-AVE migration has been achieved through cell labelling experiments and the use of reporter mouse lines such as Hex-GFP. Time lapse imaging of embryos derived from the Hex-GFP mice show that Hex expressing cells are observed to actively migrate in this direction (Srinivas et al. 2004) The attractive or repulsive signals controlling direction are not well understood however a Wnt gradient may be important. OTX2 activates the Wnt inhibitor *Dickopf* and loss of OTX2 prevents AVE migration. This can be rescued by *Dickopf* transcribed from the *Otx2* locus suggesting Wnt repression through *Dickopf* is the necessary signal (Perea-Gomez et al. 2001; Kimura-Yoshida et al. 2005). The importance of Wnt signalling in axis formation will be discussed in more detail below. The Nodal antagonists *Cerberus* and *Lefty* can also influence AVE migration. Ectopic expression of either/both on one side of the embryo causes AVE to move preferentially towards that side (Yamamoto et al. 2004).

The AVE is responsible for patterning the future anterior side of the embryo although does not significantly contribute to it. Many signalling molecules expressed later in the Anterior Definitive Endoderm (ADE) that emerges from the primitive streak are also produced here. AVE expresses *Hesx1* and also induces this gene's expression in underlying anterior ectoderm. This population corresponds to future forebrain precursors (Thomas and Beddington. 1996). Interestingly, the gastrulation defect in the *Nodal* mutants is caused by loss of Nodal signalling in extraembryonic lineages. It can be rescued by wild type ES cell contribution to the epiblast but still results in anterior axis truncations (Varlet et al. 1997). OTX2 expressed from AVE is also necessary for head induction although loss of OTX2 leads to a much further caudal truncation (Acampora et al. 1997). Somewhat surprisingly, loss of AVE by mechanical ablation does not disrupt patterning of the entire anterior region but still causes forebrain

truncation. In addition, explants of AVE do not ectopically induce anterior markers like *Otx2* or *Engrailed1* in epiblast. Interestingly, axis duplication experiments with both the node and the EGO, fail to generate a complete axis with anterior structures. However when the AVE and the EGO are used in combination they induce anterior neural tissue in naïve epiblast (Tam and Steiner. 1999). These studies indicate AVE is necessary, but not sufficient to correctly pattern the early head region. As development proceeds the AVE is replaced by axial mesendoderm derived from the node. The anterior most population of these cells, the anterior definitive endoderm expresses an overlapping set of markers to that of the AVE. It is thought that the AVE induces anterior identity and that when the AVE is displaced proximally as a result of the forwarded movement of the ADE, the ADE will take over its role helping to sustain the anterior neural identity initiated by the AVE.

An important function of AVE is local suppression of Wnt, Nodal and BMP posteriorizing signals from the extraembryonic region and posterior proximal epiblast in the head region. OTX2 is a transcription factor important for induction of some of these antagonists (Perea-Gomez et al. 2001). The multifunctional antagonist CERBERUS has been shown in *Xenopus* to antagonize Wnt/Nodal/BMP signals and block the induction of *Brachyury* by a Nodal signal specifically (Piccolo et al. 1999). However in mice, Cerberus (*Cer11*) mutants develop normally. Mouse CERL1 does not repress Wnt signals suggesting that additional factors are involved (Belo et al. 2000; Shawlot et al. 2000). Double null mutations in both Lefty and Cerberus however, cause ectopic expression of primitive streak markers in the anterior region. Interestingly this defect can be rescued or suppressed by a *Nodal* loss of function allele (Perea-Gomez et al. 2002). In addition, mouse embryos null for the Nodal coreceptor *Cripto* fail to rotate AVE and distally express neural markers, but lack trunk mesoderm (Ding et al. 1998). These studies suggest that antagonism of posteriorizing signals by AVE, especially NODAL, is needed for head induction in the correct place.

The Wnt pathway is also important in anterior-posterior axis specification. Wnt3a is one of the first markers of primitive streak formation in the posterior epiblast and loss of Wnt pathway components affects this polarity. Proximal-distal patterning and specification of DVE is also perturbed by loss of Wnt regulation throughout the

epiblast. In *Xenopus*, Wnt signalling is classically thought of as a dorsal determinant of cell fate. To further understand early embryonic development, this pathway needs to be examined in more detail.

1.2 Wnt Signalling

The Wnt pathway is one of the most important signalling pathways in animals (schematic in Fig 1.2a,b). It was first identified in *Drosophila* as a mutation in a gene (*wingless*) that causes a defect in denticle belt segmentation. A mouse oncogene was later identified as a homolog (*int1*), leading to the general name, Wnt. Wnts are secreted glycoproteins that are able to bind to the FRIZZLED cell surface receptor family in conjunction with LRP coreceptors. In the absence of Wnt, the protein β CATENIN can be found at the membrane complexed with ECADHERIN to mediate cell adhesion. Free cytoplasmic β catenin is phosphorylated and rapidly degraded. A complex with the protein Adenomatous Polyposis Coli (APC) at its core and the active kinase, GSK3, mediates this. When Wnt is bound to receptors however, GSK3 becomes inactivated. β CATENIN is then free to translocate to the nucleus where it can interact with DNA binding proteins of the TCF/LEF family. TCF/LEF binds to specific sequences in Wnt responsive promoters and when it is bound by β CATENIN it activates downstream target genes (Reya and Clevers. 2005). TCF does not have any activating or repressive ability of its own. It relies on β catenin to activate, and cofactors such as Groucho proteins to repress transcription. Binding of β catenin and GROUCHO occur in the same physical space on TCF proteins and the two complexes have been shown to be mutually exclusive (Daniels and Weis. 2005). This helps to tightly regulate Wnt target genes. TCF can also interact with the closely related proteins CBP and p300. In *Drosophila*, these can repress transcription by acetylating TCF, and lowering its affinity for β CATENIN (Waltzer and Bienz. 1998). However they also have histone acetyl transferase activity and can help activate transcription by opening the chromatin structure. This appears to be dependent on the cellular context or regulation by other factors (Li et al. 2007).

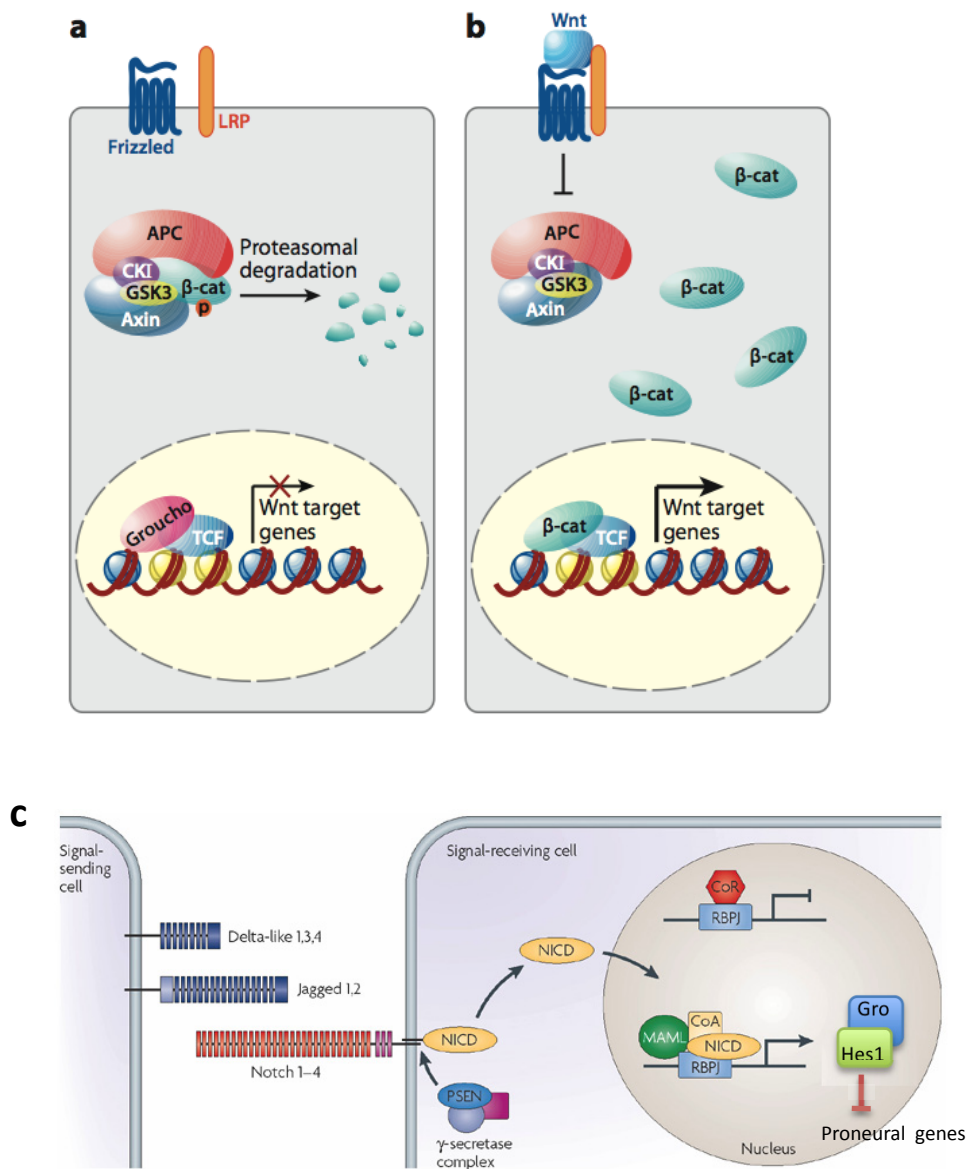


Fig 1.2 Involvement of TLEs in major signaling pathways

The Wnt pathway. In the absence of wnt ligand, β catenin is phosphorylated and targeted for degradation by the proteasome. TCF is bound by corepressors such as Groucho/TLEs and wnt targets are repressed **(a)**. When wnt ligand is bound by the receptor, Gsk3 is inactivated and β catenin is free to translocate to the nucleus. It can bind TCF and activate transcription of wnt targets **(b)** (Figure taken from Flier and Clevers, 2009).

(c) The Notch pathway. Notch ligands such as Delta and Jagged on signaling cells bind the notch receptor and cause cleavage of its intracellular domain. This translocates to the nucleus and binds CSL/RBPJ with cofactors to activate target genes. In the developing nervous system, these include bHLH Hes proteins which use Groucho/TLEs as corepressors to repress proneural genes (Figure adapted from High and Epstein, 2008)

Wnt signalling is involved in many different processes including embryonic development and embryonic and adult stem cell regulation. Misregulation of the developmental processes associated with the pathway can lead to cancer. Indeed around 60% of colorectal cancer cases have a mutation in the APC gene (Powell et al. 1992). One of the first and best known roles for Wnt signalling in development is axis specification as studied in the in the amphibian and zebrafish embryo. In *Xenopus*, the organizer is induced by an early signalling centre known as the Nieuwkoop centre. Because the organizers descendents mostly populate the Dorsal axis, in *Xenopus* this initial axis has interchangeably been referred to as Dorsal and anterior – dorso-anterior. The location of this group of cells is determined maternally and provides the first symmetry breaking event to establish anterior-posterior axis polarity (Heasman 2006). Organisms that develop with yolky eggs (such as fish and amphibians but not mammals) also have an early animal-vegetal axis that affects later development. Fertilization and polar body extrusion happens at the animal pole while the yolk tends to concentrate at the vegetal axis. In *Xenopus* after fertilization, the egg undergoes a major cytoplasmic rearrangement known as cortical rotation. Maternal determinants are concentrated by cortical rotation, to a vegetal part of the fertilized oocyte opposite the sperm entry site. The concentration of these elements is a result of mRNA transport by cytoskeletal motor proteins. Blocking this, for example using low temperature, stops axis formation and causes a ventralized embryo to develop instead (Gerhart et al. 1989). It was later found that depleting β CATENIN in *Xenopus* embryos using antisense deoxyoligonuclotides had a similar effect. Embryos develop ventralized and this can be rescued by β *catenin* mRNA injection (Heasman et al. 1994). Lithium chloride acts as a GSK inhibitor. Treating *Xenopus* embryos with LiCl has the opposite effect as β CATENIN depletion, eliciting a dorsalized phenotype. This is due to stabilized β CATENIN and increased Wnt signalling through the entire embryo (Klein and Melton. 1996) causing an expansion of dorsal (dorso-anterior) and loss of ventral fate. LiCl has a similar effect on sea urchin embryos. The sea urchin embryo also develops with animal-vegetal polarity, where the animal macromeres are fated towards ectoderm and the vegetal micromeres become mesoderm and endoderm. These vegetal micromeres are also the site of initiation of gastrulation and contribute to the primitive gut (archenteron) and skeleton. Micromeres can induce a secondary axis with archenteron

in the animal poles of earlier embryos if transplanted. Treating embryos with LiCl causes an expansion of vegetal cell identity. Depleting β CATENIN also had the opposite effect and transplantation of the organizer equivalent cells from β CATENIN deficient embryos failed to induce a secondary axis (Logan et al. 1999).

What Wnt targets lying downstream of TCF are the effectors of these processes? In the animal pole of *Xenopus* embryos where it is not normally expressed, *Siamois* is induced by injection of *Wnt8* mRNA. Several TCF/LEF binding sites were also found in the *Siamois* promoter (Brannon et al. 1997). *Siamois* is a homeobox transcription factor that can induce a secondary axis, including Spemann's organizer. Organizer genes such as *Gooseoid* and *Cerberus* are transcriptionally activated by SIAMOIS suggesting that this protein mediates Nieuwkoop centre activity (Carnac et al. 1996; Kessler 1997). A gene product with similar expression and function, *Dharma*, has also been discovered in zebrafish and is essential for axis formation. *Dharma* mutants have severe anterior truncations and lack a proper organizer, the embryonic shield. This protein can also ectopically induce organizer gene expression such as *Gooseoid*. Interestingly, *Dharma* mRNA expression in the yolk syncytial layer (YSL), which has been proposed to be the teleost equivalent of the mammalian visceral endoderm, is sufficient to at least partially rescue *Dharma* mutants (Yamanaka et al. 1998; Fekany et al. 1999). The TGF β nodal family is important in both the *Xenopus* organizer and its mouse equivalent, the node. *Xenopus Nodal Related 3 (Xnr3)* is one of the *Xenopus* homologues of *Nodal*. Its expression is regulated in part by TCF/LEF, which have been shown to bind and positively regulate the promoter. Both XNR3 and SIAMOIS directly induce *Gooseoid* expression which acts to repress ventral gene expression in the dorsal region of the embryo (McKendry et al. 1997).

While no Nieuwkoop Centre has been discovered in mammals and neither *Siamois* nor *Dharma* appear conserved, later Wnt responses appear the same as in lower vertebrates. Thus *β catenin* appears essential for early axis specification. *β catenin* null embryos express only some DVE markers (*Cer11*, but not *Hex*) and never initiate rotation of DVE. There is also a complete failure of primitive streak formation and no evidence of mesoderm induction (Huelsken et al. 2000). *Wnt3a* is first expressed in the proximal posterior epiblast and later in the primitive streak and is one of the earliest predictors of

primitive streak formation. *Wnt3a* null embryos fail to form a primitive streak, node or mesoderm. They subsequently die before reaching 10.5dpc (Liu et al. 1999). Mutations in the APC complex have also been shown to have reciprocal phenotypes. APC^{min} mice have a mutation in APC that decreases the activity of the GSK3 containing complex. Heterozygous mice have a predisposition to intestinal tumours but $APC^{min/min}$ mice do not form a normal axis and die by 5.5dpc. In fact, the primitive streak marker *Brachyury* becomes expressed throughout the epiblast creating a proximalized embryo and eventually leading to the ubiquitous expression of posterior mesodermal markers. Embryos also lost their ability to specify DVE. This study also found some evidence of asymmetrically expressed nuclear β CATENIN in the trophoblast of wild type 4.5dpc embryos. Moreover chimeras show evidence of distalization of the primitive endoderm suggestive a role in early AP specification (Chazaud and Rossant. 2006). MESD is a chaperone protein involved in the biosynthesis of the Wnt coreceptors LRP5/LRP6. *Mesd* mutant embryos have a milder but still significant defect in axis specification. They begin to express *Brachyury* and *Wnt3a* in proximal epiblast but fail to form a later primitive streak (Hsieh et al. 2003).

β catenin has been shown to be involved in aspects of endoderm specification. It can bind *Sox17* and in doing so promote endoderm formation. *Sox17* target genes can be upregulated by β CATENIN in *Xenopus* although this requires overexpression of *Sox17* too, suggesting that both proteins are required for synergistic stimulation of transcription (Sinner et al. 2004). One *Sox17* target shown to be upregulated by β CATENIN was *Foxa2*, which is a key regulator of endoderm formation. Loss of *Foxa2* in mice prevents definitive endoderm maintenance (Ang et al. 1993). When *β catenin* is deleted conditionally in cells normally fated to become endoderm, these cells in mutant embryos instead become precardiac mesoderm and fail to express endoderm markers (Lickert et al. 2002).

Another Wnt related factor to play a role in development is the TCF corepressor *TLE4*. This is a mammalian homologue of *Drosophila* Groucho, which keeps Wnt target genes, repressed in the absence of Wnt ligand. *TLE4* was found to be a repressed target of the homeobox transcription factor *Hex*. This repression was found to play an

important role in the regulation of anterior-posterior patterning in both *Xenopus* and mouse.

1.3 *Hex* and *TLE4*

The proline-rich homeodomain containing protein *Hex* was first identified as a marker of haematopoietic precursors. While it is expressed in the developing blood during embryogenesis, it is also expressed in the endoderm and its derivatives, like the liver and thyroid. *Hex* is first expressed during mouse development at 4.5dpc throughout the primitive endoderm as it first forms beneath the ICM. By 5.5dpc *Hex* expression becomes restricted to the distal tip visceral endoderm. As discussed above, these cells have anterior inducing capacity. Embryos in which *Hex* has been removed genetically exhibit evidence of an anterior truncation and loss of rostral forebrain markers. Chimeras of wild type embryonic cells contributing to the epiblast and *Hex* null extraembryonic tissues also show this phenotype, indicating this is a result of loss of HEX in the ADE specifically (Thomas and Beddington. 1998; Martinez Barbera et al. 2000). HEX has been shown to act as a transcriptional repressor and experiments in *Xenopus* suggest its role in anterior patterning is related to its capacity to suppress mesoderm induction. However, ectopic *Hex* expression in non-anterior cells also appeared to induce a non-autonomous activity that promotes Dorso-anterior identity in nearby cells, indicating that repression by HEX is important for the induction of anteriorizing signals. Fusion of HEX to reiterated modules of the VP16 activation domain (λ VP2) converts it to an activator of *Hex* target gene expression and injection of *Hex* λ VP2 in *Xenopus* embryos resulted in embryos with ectopic mesoderm and anterior truncations. Ectopic expression of wild type *Hex* repressed dorsal mesoderm gene expression, acting on genes such as *Gooseoid*, and *Chordin*. *Hex* therefore promotes anterior identity in the head region by suppressing dorsal mesodermal organizer identity (Brickman et al. 2000) promoting the establishment of an anterior endoderm domain that expresses *Cerberus* and helps to insulate the anterior neural plate from posteriorizing influences.

Recent experiments in our lab have also tied the inductive role for *Hex* to Wnt signalling. Ventral vegetal misexpression of modest levels of β CATENIN can induce a posterior secondary axis in *Xenopus* embryos. However coinjection of *β catenin* mRNA alongside *Hex* produced ectopic heads (Zamparini et al. 2006). Moreover, as previously shown, misexpression of *β catenin* or Wnts can dorsalize the ventral marginal zone of frog embryos (Glinka et al. 1996). This activity appears somewhat context independent as HEX can also promote β catenin activity in Ventral marginal zone explants, where the combination of the two RNAs mimics the phenotypes observed in response to high β CATENIN levels, the induction of heads in these explants (Zamparini et al. 2006). Taken together, these lines of evidence suggest that *Hex* is cooperating with *β catenin* to specify anterior identity in *Xenopus* embryos. The ability of *Hex* to potentiate Wnt activity was also observed in transient cell culture assays and found to be dependent on TCF. Moreover, a genome wide screen for *Hex* targets in mouse ES cells lead to the identification of *TLE4* as a Wnt repressor directly repressed by *Hex*, and experiments in *Xenopus* also support the notion that *TLE4* is a direct target. Taken together, these data suggest that the amplification of Wnt signalling by *Hex* is at least in part due to the regulation of *TLE4* expression and that this activity maybe be important for the specification of the anterior axis (Zamparini et al. 2006).

While, *TLE4* maybe an important component involved in regulating early Wnt signalling, the suppression of Wnt and Nodal signalling is necessary for anterior specification (see above). CERBERUS has Wnt antagonistic activity and is expressed in the same anterior domain as *Hex* (Brickman et al. 2000). The secreted Wnt repressor *Dickopf* is expressed in frog foregut endoderm underlying the head and in mouse headfold mesoderm and AVE. This gene also has head inducing ability and loss of *Dickopf* leads to anterior truncations, a phenotype similar to *Hex* mutants or AVE ablation (Glinka et al. 1998; Mukhopadhyay et al. 2001). FRITZ, FRZD8 AND FRZDB-1 are all soluble extracellular antagonists of Wnt ligand binding. These too are expressed in the anterior head region of the mouse embryo (Leysn et al. 1997; Mayr et al. 1997; Lu et al. 2004) and have homologues expressed in the anterior endodermal domain in frog. Clearly Wnt modulation in the anterior prospective head region and underlying cells is important. In Zamparini et al, *Hex* was shown to regulate two sets of targets, the first, including *TLE4*, were involved in the initial specification of the

anterior axis and involved the amplification of Wnt signalling. The second were a class of genes suppressed by Hex once the anterior territory in the endoderm was already induced and these include factors that suppress wnt signalling. This two-stage model is summarized in Fig 1.3. In addition, the zebrafish YSL also expresses *Hex* and this has been shown to suppress *Wnt8* and other axial mesoderm markers such as *Chordin*, which suggests a similar role in insulating the anterior region from posterior signals during gastrulation (Ho et al. 1999).

TLE4 is a member of a larger family of highly related proteins with overlapping functions and expression patterns. These may also play a role in patterning processes and indeed *TLE3* was also identified as a Hex target in our microarray screen. Their expression patterns in early embryos of any species have not been well characterized but *TLE3* and *TLE4* are expressed in the anterior regions of mouse and chick embryos at mid gastrulation and in the primitive streak. Mouse *TLE3* at least seems excluded from the headfold region and restricted to underlying gut endoderm emerging from the PS (Leon and Lobe. 1997; Vanhateren et al. 2005). The suppression of TLEs may be involved in initial anterior specification but as transcripts are seen later in the anterior region and overlap with regions Hex is known to be expressed, TLEs may also play additional roles. Further investigation of the *TLE4* Wnt antagonist and related members of its family is therefore an important part of understanding anterior patterning.

1.4.1 Groucho/TLE corepressors

TLE proteins are a family of vertebrate corepressors that do not bind DNA on their own, but are recruited to DNA by sequence specific DNA binding proteins. They are all related structurally and evolutionarily to the *Drosophila Groucho*. *Groucho* was first identified in flies as a spontaneous mutation that caused defects including extra bristles above the eyes, giving the impression of the famous bushy eyebrows of Groucho Marx (Lindsley and Grell. 1968). This phenotype and genetic evidence linked it to the *Enhancer of Split (ESpl)* group of mutants, leading to its alternative name, *Transducin Like Enhancer of split (TLE)*. *ESpl* mutants are typically linked to ectopic neural induction. Human and mouse homologues of the fly gene *Groucho*, were later cloned

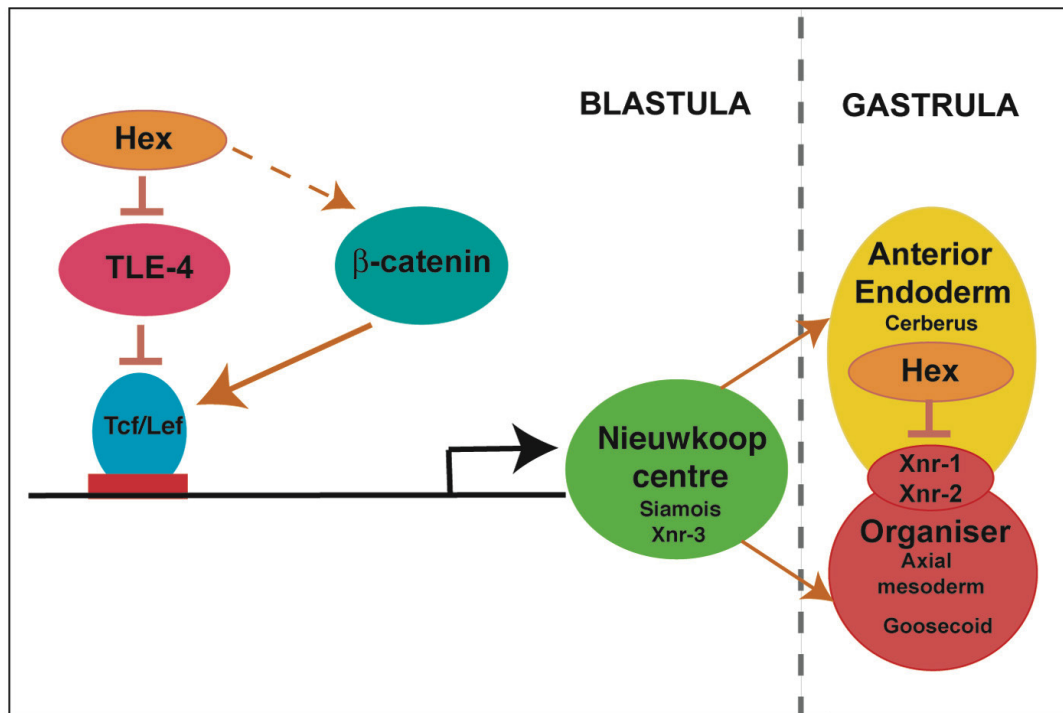


Fig 1.3 Schematic representation of Hex interactions with the Wnt and Nodal-related pathways

At blastula stage, Hex amplifies Wnt signaling through the repression of the Wnt antagonist Tle4. The Nieuwkoop centre genes *Siamois* and *Xnr3* are markers of this process and this signaling centre is responsible for the induction of both anterior endoderm and axial mesoderm. Following mesendoderm induction, Hex is expressed in the anterior endoderm where it antagonizes the propagation of the Nodal signal to prevent mesoderm formation in the head field. Broken lines indicate the induction of defined domains in the mesendoderm.

(Figure and legend taken from Zamparini et al, 2006)

and termed *Grg* (Mallo et al. 1993; Miyasaka et al. 1993). However for consistency in the literature, *TLE* has become standard nomenclature for all vertebrate *Groucho* homologues. The sequence and domain structure of full length *TLEs* is highly similar to *Groucho*. However the yeast *Tup1* repressor is also highly structurally and functionally similar and perhaps represents evidence of an even earlier evolutionary ancestor (Flores-Saaib and Courey. 2000). *TLE* proteins do not have specific DNA binding ability or much innate repressive ability and rely on interactions with other proteins to carry out their role as corepressors. Their domain structure and biochemistry give some information about their mechanism of action.

1.4.2 Biochemistry of TLE proteins

There are six known *TLE* genes in mammals. Four are full length; similar to *Drosophila Groucho* in structure, and two are short truncated versions with different activity and roles (Gasperowicz and Otto. 2005; Buscarlet and Stifani. 2007; Jennings et al. 2008). Full length *TLEs* (*TLE1-4*) are purely repressive. *TLE5*, also known as *AES* is a separate gene that resembles a truncated, N-terminal only *TLE*. *TLE6/Grg6* resembles a C-terminal only truncation. *TLE6* is unique to mammals while orthologs of the others are found in all vertebrate lineages. To understand the functional differences between the family members and their mechanism of action, we must look at the domain structure. This is summarized in Fig 1.4.

The N terminal Q domain interacts with other *TLEs* using two leucine zipper-like motifs and mediates tetramerization. Tetramerization has been shown to be important for the mechanism of action of *TLEs*. Overexpression of a tetramerization deficient mutant *Groucho* construct in *Drosophila* does not lead to the wing disk abnormalities that overexpression of wild type *Groucho* does (Song et al. 2004). Deleting the Q domain of *Groucho* negates the ability of the protein to repress transcription in a reporter assay. However, this domain does not seem to play a direct role in repression. Replacement by the tetramerization domain of p53 restores most of the repressive ability lost by deletion. This leads to a model where *TLE* proteins can mediate long-range repression from DNA recruitment sites by polymerizing via their Q domains and

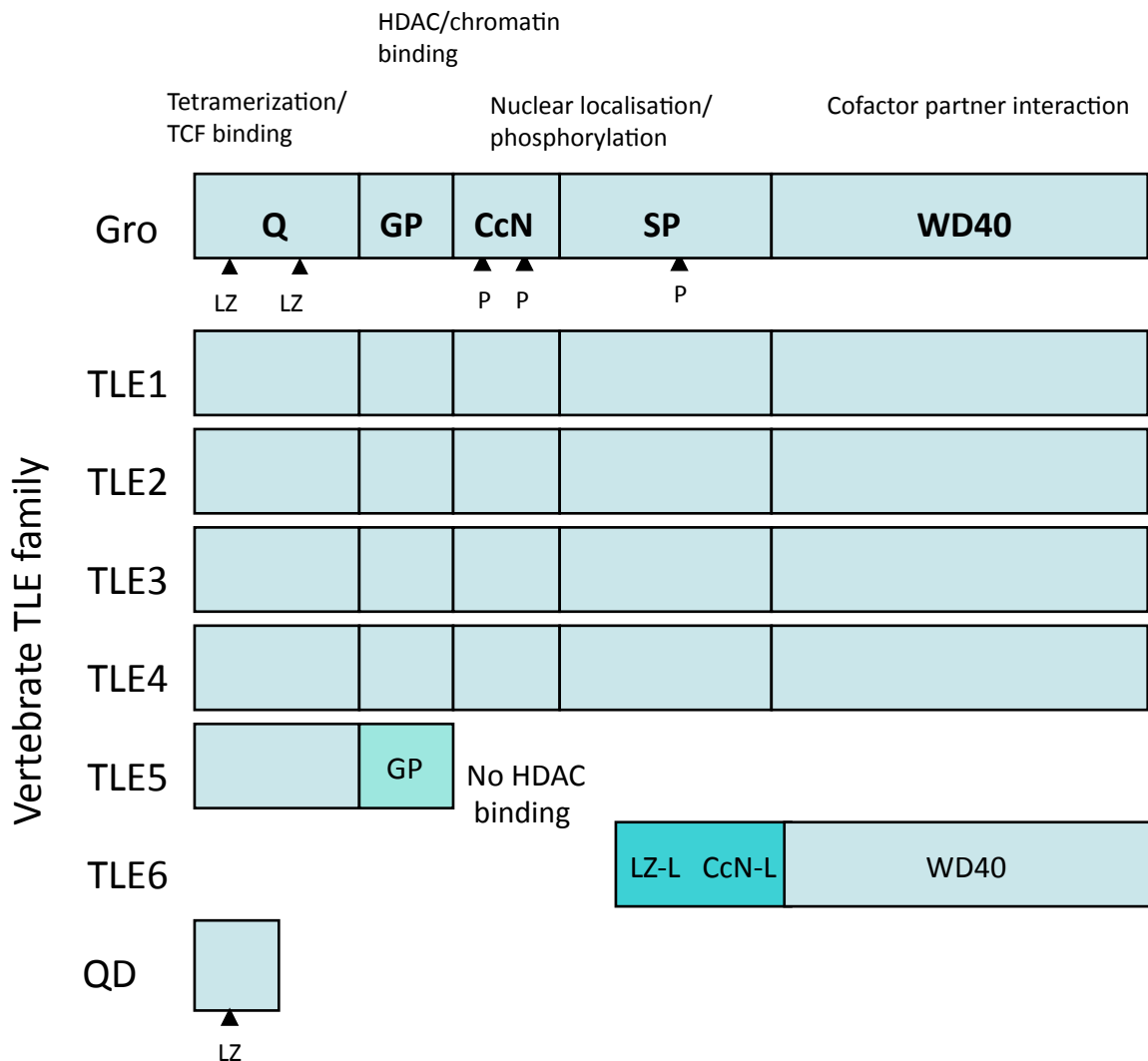


Fig 1.4 Structure of Groucho/TLE proteins

Schematic of the general structure of drosophila Groucho (top) and the vertebrate TLE homologues. General domain functions are indicated above. LZ marks coiled-coil leucine zipper like structural features used for tetramerization. P indicates CK2 phosphorylation sites in the CcN domain and MAPK phosphorylation site in the SP domain. These features are conserved in vertebrates. TLE5 has an altered GP domain that does not bind HDACS. TLE6 only has a WD40 domain with significant sequence homology to other TLEs but has a novel N terminal region with LZ-like and CcN-like features. QD is a splice variant consisting of only the N terminal half of the TLE4 Q domain.

spreading along the chromatin fibre (Chen et al. 1998; Flores-Saaib and Courey. 2000). However more recent evidence has contradicted this. Both wild type TLE3 and TLE3 Δ QD were able to condense synthetic chromatin arrays, suggesting single separate TLE molecules could interact with two histones. Chromatin condensation is one way TLEs have been proposed to mediate transcriptional repression. The QD was necessary to aggregate separate chromatin arrays however, suggesting it could play a part in mediating long range repression or higher order chromatin compaction (Sekiya and Zaret. 2007). The Q domain also interacts with transcription factors including the TCF/LEF family and binds these as native tetramers (Brantjes et al. 2001; Daniels and Weis. 2005). In summary, the Q domain has multiple functions and different requirements for tetramerization suggest more than one mechanism of action for TLEs. Moreover, while this data suggests aggregation along DNA is a component of Groucho mediated repression it is not the entire story.

Adjacent to the Q domain lies the glycine/proline rich GP domain. This has been shown to interact with histone deacetylases (HDACs) such as *Drosophila Rpd3*. Yeast TUP1 also interacts with the class III HDAC protein, SIR2. HDAC inhibitors such as TSA inhibit TLE mediated repression suggesting HDAC mediated chromatin silencing is also utilized by TLE family members to repress gene transcription (Chen et al. 1999; Flores-Saaib and Courey. 2000).

The central CcN domain has been implicated in the regulation of TLEs. It contains a nuclear localisation sequence and two serine residues, which can be phosphorylated by CK2 kinase. This phosphorylation is necessary for TLEs to be retained in the nucleus (Nuthall et al. 2004). Also involved in regulation is the adjacent SP domain. This was thought mainly to be a spacer region but contains phosphorylation sites, for example for MAPK. MAPK phosphorylation has been shown to reduce the repressive activity of GROUCHO. This may be to allow the derepression of genes that are targets of both GROUCHO and the receptor tyrosine kinase signalling (RTK) pathway, for example by EGFR (Hasson et al. 2004; Cinnamon et al. 2008). In *Xenopus*, RTK signalling through FGF4 also inhibits TLE mediated repression of Wnt targets. These include mesodermal markers such as *MyoD*, in agreement with the role of Wnt signalling in dorsal

mesoderm specification. This mechanism is an interesting example of crosstalk between signalling pathways through TLEs (Burks et al. 2008).

At the N terminus of full length TLEs lies the WD40 domain, which is the only part of a TLE protein to have its structure solved by x-ray crystallography. This has a seven bladed β propeller structure similar to the G protein receptor β subunit. The central pore of the propeller is the site of many interactions with DNA binding proteins. Two motifs known to interact with this region are found in a wide array of DNA binding proteins. These motifs, WRPW and eh1 (FxIxxIL) are found in a variety of transcription factors (Jennings et al. 2006). WRPW motif containing proteins include HES1 and the somitogenesis factor RIPPLY2 (Fisher and Caudy. 1998; Morimoto et al. 2007). Moreover the eh1 family is extremely large and includes at least three factors known to pattern anterior endoderm: HEX, GOOSECOID and HESX1. There are also many other homeodomain and Fox proteins in this family (Swingler et al. 2004; Yaklichkin et al. 2007). The full list of Eh1 and WRPW containing proteins found to interact with TLEs is extensive and ever growing (Buscarlet and Stifani. 2007). The C terminal of yeast TUP1 also has β propeller structure, with residues exposed around the central pore that are vital for its repressive ability (Green and Johnson. 2005). A mutation in the TLE like gene of *C.elegans*, *unc-37*, also maps to this region and causes an effective null phenotype (Pflugrad et al. 1997). These studies show functional conservation and emphasize the importance of the WD40 domain for TLE function, specifically for protein interactions.

Although the TLEs are dynamically regulated throughout gastrulation (Koop et al. 1996; Vanhateren et al. 2005) at the RNA level, surprisingly little is known about transcriptional regulation of TLEs. Regulation by HEX is one of the only instances of direct control by a known transcription factor found so far. Stat3 and the oncoprotein E2A-HLF have also been shown to directly regulate TLE5 and TLE6 respectively (Dang et al. 2001; Sekkai et al. 2005).

1.4.3 Non full-length TLE proteins

The vertebrate TLE family probably arose through tandem duplications of a single TLE ancestral gene. Based on phylogenetic analysis of different species TLEs, several independent duplications occurred to give the four full length TLEs we see in vertebrates today. Teleost fish underwent specific genome duplication in evolutionary history, creating extra copies of both *TLE2* and *TLE3*. Retention of these duplications and sequence and expression pattern divergence suggests adaptation to different roles. This would allow for greater control over TLE dependant transcriptional regulation than that provided by a single TLE like Groucho (Aghaallaei et al. 2005; Bajoghli 2007). *TLE2* also underwent a duplication event creating a new TLE without the exons after the GP domain, *TLE5*. In mammals, the remaining C-terminal encoding exons from the duplication event appear retained as part of an independently expressed gene, *TLE6*. *TLE2*, 5 and 6 cluster together on chromosome 10 in mouse.

C-terminal truncated forms of TLE such as *TLE5* also have a GP domain. However these proteins do not appear to bind HDACs, possibly due to sequence differences (Brantjes et al. 2001; Yu et al. 2001). They often also act as positive regulators of genes normally repressed by full length TLEs (Wang et al. 2000; Swingler et al. 2004). Because of this, they are often considered as dominant negative TLEs. Thus they are thought to bind full length TLEs via their intact Q domain and sequester them into inactive complexes, a form of anti-repression like squelching. Dominant negative proteins also appear to be generated by alternative splicing. A naturally occurring splice variant of *TLE4* in B cells, QD, contains just the first section of the Q domain with a single LzL motif. This was shown to block the interaction between TLE4 and PAX5 (Milili et al. 2002). Another C-terminal truncated TLE1 splice variant with an intact GP domain has some repressive activity with respect to TCF, but would be predicted to function as a dominant negative with respect to co-factors (Lepourcelet 2002).

It is becoming increasingly apparent that the regulation of transcription by TLE is becoming more complex. Short TLEs can behave as repressors or activators in a context dependant manner. Much of the evidence pointing towards short forms as dominant negatives relies on strong, non-physiological overexpression or use of the GAL4 DNA binding domain to bring TLE5 binding partners to DNA reporter constructs. In sea

urchins, endomesoderm specification downstream of TCF is suppressed by injection of the TLE homologue *LvGro* through the inhibition of wnt signalling in the vegetal pole producing a severely animalized phenotype. However, a truncated *LvGro* consisting of just the Q domain had the same effect, suggesting that in this context it too could behave as a repressor. Further molecular analysis confirmed this repression, although differences in the range of genes affected by long and short *LvGro* were observed (Range et al. 2005). TLE4 is able to bind PAX5 and repress the target gene *CD19*. However TLE5 was unable to interfere with this repression, even at high levels (Eberhard et al. 2000). TLE5 was also shown to be a corepressor of the androgen receptor. Here it could repress transcription when recruited to naked chromatin free DNA by the receptor. The HDAC inhibitor TSA also had no effect on this repression. It could be mediated by interactions with the basal transcription machinery, such as TFIIE, which AES associates with specifically (Yu et al. 2001). In a similar way, the *C.elegans* *TLE1* homologue *unc-37* can interact with members of the mediator complex (Zhang and Emmons. 2002). These studies also highlight the fact the HDAC recruitment is not the only way that TLE proteins can mediate repression.

The mammalian specific *TLE6* has been discovered fairly recently and remains relatively uncharacterized. Roles have been identified for it in mouse morula development, cancer progression and neurogenesis (Dang et al. 2001; Marçal et al. 2005; Li et al. 2008). *TLE6* consists of the WD40 domain and a separate divergent N terminal half with a CcN like domain and coiled-coil like structures similar to the LzL tetramerization sequence in TLEs. *TLE6* does not behave as an inherent transcriptional repressor as it does not repress when recruited to DNA by the GAL4 domain. This is consistent with its lack of repression domains. However it does antagonize repression by FOXG1 and TLE1, possibly competing with TLE1 for the FOXG1 eh1 motif. Interestingly, TLE6 does not bind HES1, which contains a WRPW motif, suggesting structural differences in the WD40 domains. TLE6 could be acting as a modulator of certain specific full-length TLE dependent processes (Marçal et al. 2005).

1.4.4 TLEs in development

Because of their role as corepressors with a wide range of important transcription factors, TLEs are involved in many developmental processes. They were first identified in *Drosophila* as mutations in the *Groucho* locus which enhanced the phenotype of other Enhancer of split mutants, some leading to the lethal commitment of most ectodermal cells to the neural lineage (Ziemer et al. 1988). *ESpl* mutants tend to be homozygous lethal due to the loss of epidermal tissue caused by the increased ectodermal to neural conversion. This was later found to be due to their involvement in the Notch signalling pathway (this pathway is summarized in Fig 1.2c). Notch signalling is a major pathway involved in cell – cell signalling and was initially described based on its regulation of neurogenesis. The induction of ligands such as JAGGED AND DELTA-LIKE activates NOTCH receptors in neighbouring cells. This causes lateral inhibition of downstream targets, a process by which the DELTA/JAGGED expressing cell blocks the cells around them from adopting their fate. In neural induction, the stimulation of Notch signalling shuts down neurogenesis in the neighbouring cells. The activation of the pathway proceeds as activated cell surface NOTCH receptors undergo cleavage and the intracellular domain (ICD) internalizes and enters the nucleus and binds the sequence specific DNA binding protein, CSL to activate transcription target gene transcription. The complex of CSL and NOTCH ICD is known to induce an assortment of bHLH proteins including key negative regulators of neural transcription, the Hes family. bHLH proteins control neural commitment and can either be positive, such as NEUROD proteins, or negative such as HES (Hairy enhancer of Split) related proteins. HES1, one of the mammalian HES homologues can repress neural fate as has been shown by its overexpression. Mutation of these genes allows ectopic activation of this fate (Knust et al. 1987; Lai 2004). Interestingly, Notch signalling also appears to have a positive role early in neural specification. Thus, constitutive expression of the NOTCH ICD in ES cells leads to increased specification of neural progenitors during neural differentiation (Lowell et al. 2006). NOTCH activation also had differing effects in the chick inner ear where it could both repress sensory hair cell formation as expected but also promote ectopic hair cells (Daudet and Lewis. 2005).

Further genetic evidence explaining Groucho's role in neurogenesis came from the interaction found between GROUCHO and HAIRY related basic helix-loop-helix (bHLH) proteins. These bind CSL with GROUCHO in the absence of pro-neural signals, leading to the repression of target genes such as the neural marker *Hunchback* (Paroush and Finley, 1994). The capacity of TLE to suppress neurogenesis in mammals has also been demonstrated. Early evidence of this came from the identification of an interaction between TLE1 and the mammalian bHLH protein (Grbavec and Stifani, 1996). In the developing nervous system, both *Hes1* and *TLE1* RNA are expressed in similar domains supporting the notion that they act in concert to suppress neurogenesis. Moreover, mutations of either gene gave a similar phenotype in which mutants display an over proliferation of neurons. Postmitotic neuronal specific expression of TLE1 is also tied to the loss of neurons, especially in the dorsal and ventral telencephalon. This was probably due to apoptosis caused by blockage of terminal neural differentiation (Yao et al. 2000). Forced expression of TLE1 in primary cultures of neural progenitors led to decreased terminal differentiation and an expansion of mitotic progenitors. The WRPW motif found in HES1, but not the eh1 motif was found to be essential for this (Nuthall et al. 2004; Buscarlet et al. 2008). These studies lead to the model that NOTCH induced lateral inhibition causes TLE mediated repression by HES1, and allows a pool of undifferentiated neural progenitors to survive in the developing nervous system to give rise to later neural lineages. While TLE appears the primary regulator of *Hes1*, HES1 also regulates the phosphorylation of TLE1 by the kinase CK2 leading to its increased nuclear localisation.

In addition to neural development, TLEs are also involved in many other developmental processes. TLE3 and TLE4 are expressed in the primitive streak in both mouse and chick, along with other structures undergoing epithelial to mesenchymal transition. This suggests they may play a role in mesoderm and endoderm specification (Koop et al. 1996; Leon and Lobe, 1997; Vanhateren et al. 2005). Mesoderm can be ectopically specified in *Xenopus* animal caps by the injection of *FoxD3* mRNA. This was found to be dependant on an eh1 motif in FOXD3, which is required to recruit TLE4 as a corepressor. Mutation of the eh1 motif destroyed both the binding and mesoderm specifying ability (Yaklichkin et al. 2007). *FoxD3* null mouse ES cells have an increased propensity to differentiate, especially towards mesoderm and endoderm.

Markers such as *Brachyury* and *Gooseoid* are increased, although increases in trophoblast markers are also seen (Liu and Labosky. 2008). TLEs are predicted to bind many other Fox genes in various species including the FoxA family, which is vital for endoderm specification (Friedman and Kaestner. 2006; Yaklichkin et al. 2007). FOXH1 may also recruit a TLE via *Gooseoid* to regulate axial mesendoderm development. FOXH1, which is normally a transcriptional activator, was shown to bind GOOSECOID as a corepressor and repress *Mixl1* in mouse embryos (Izzi et al. 2007). Repression of *Mixl1* was HDAC dependant and GROUCHO has been previously shown to bind GOOSECOID to mediate its repressive ability (Jiménez et al. 1999).

TLE is also involved in somitogenesis. Presomitic mesoderm (PSM) segments into individual units and these must transition from mesenchyme into epithelial somites. Termination of PSM specific genes in zebrafish is dependant on a protein RIPPLY1, which contains a WRPW motif and bound TLE2. RIPPLY1 without WRPW failed to downregulate PSM genes such as *Mesp-b* suggesting a TLE is the effector of RIPPLY1 action (Kawamura et al. 2005). A similar gene in mice, *Ripply2* also downregulates the *Mesp-b* homologue *Mesp2*, suggesting conservation of TLE involvement. The down regulation of Mesps is necessary for generating rostral-caudal polarity in somites (Morimoto et al. 2007). In *Xenopus*, TLE4 interacts with a protein, BOWLINE, which is part of a Ripply family. The Ripply family antagonizes the activator ability of *Tbx* genes in frog and zebrafish in conjunction with TLEs, which are vital for both paraxial mesoderm specification and somite segmentation. Interestingly, RIPPLY1 can repress transcription of the zebrafish *Brachyury* homologue *No Tail*, although it is not known if this is mediated by TLEs (Kondow et al. 2007; Kawamura et al. 2008).

TLEs also play a role in organogenesis. TLE3 is expressed in foregut endoderm at the 6-7 somite stage. However it is downregulated rapidly at the time of liver gene induction. In addition, forced lentiviral expression of TLE3 in foregut explants blocked the induction of liver markers such as *Alb* and *Ttr* (Santisteban et al. 2010). Full length and short TLEs are also found in the developing pancreas with TLE2 and TLE3 strongest in endocrine tissue. The transcription factor *Arx* can convert α cells into β cells and repression of insulin promoter activity in a β cell line could be improved by

interaction of TLE2 with *Arx* mRNA (Hoffman et al. 2008). These studies suggest TLEs are involved in the regulation of genetic programs controlling both pancreatic and liver differentiation.

The effects of loss of TLE activity on embryonic development have not been well studied. Making a cell or mouse line with complete loss of TLE activity is complicated by redundancy between family members, although individual TLEs have been mutated. *TLE5* homozygous null mice are viable and fertile although a growth defect is observed shortly after birth in all embryos. This becomes severe in about 20% of animals leading to a ~40% reduction in weight (Mallo et al. 1995). *TLE3* null mice die *in utero* around 13.5dpc. Death is apparently due to a placental insufficiency because of incomplete trophoblast giant cell differentiation caused by lack of TLE3 (Morrish et al. 2007). No early embryonic phenotype for loss of a TLE has been described to date. In this thesis, I explore the roles of TLEs in lineage specification through the generation of a set of both gain and loss of function tools.

1.5 Embryonic stem cells

Embryonic stem cells (ESCs) are generally defined as cells that are derived from the ICM of a blastocyst and have the potential to contribute to every somatic lineage of an animal. They can also be maintained and propagated in an undifferentiated state in *in vitro* culture with appropriate conditions. Whether they represent a true biological cell type or simply a functional state of being able to be maintained in these artificial conditions is unclear. However they are useful both as a model for developmental processes on a cellular level, and potentially as a source of cells for clinical applications. ES cells from mice were first isolated by Evans and Kaufman (Evans and Kaufman. 1981). These cells could contribute to chimaeric mice and also, as was subsequently shown, to the germline. Germline contribution still remains the most stringent test of the functionality of ES cells.

An important feature of ESCs is their ability to divide and grow while remaining in an undifferentiated pluripotent state. This is facilitated by a complex network of transcription and regulation and a number of key extrinsic cues. At the centre of this network are three master regulators: *Oct4*, *Sox2* and *Nanog* (Chambers and Tomlinson. 2009). OCT4 and SOX2 bind cooperatively to DNA on the promoters of many pluripotency genes such as *Fgf4* to activate transcription (Ambrosetti et al. 2000). A specific level of OCT4 is necessary for ES cells to maintain pluripotency. Reduction to 50% levels causes differentiation towards trophoblast, while doubling the levels causes ES cells to differentiate towards primitive endoderm and mesoderm (Niwa et al. 2000; Morrison and Brickman. 2006). Part of this function seems to be evolutionarily conserved as a *Xenopus Oct4* homologue *PouV* can compensate for loss of *Oct4* in mouse ES cells. Although amphibians do not have stem cells in the classical sense, POUV can repress commitment markers such as *Goosecoid* and *Cerberus* in frog embryos suggesting an earlier evolutionary role (Morrison and Brickman. 2006). In addition, *Oct4* null mouse embryos fail to develop beyond the blastocyst stage. Null embryos fail to develop ICM cells, instead upregulating trophoblast markers in all cells (Nichols et al. 1998). *Sox2* null ES cells also differentiate towards trophoblast although the phenotype is not as severe as loss of *Oct4*. Forced expression of OCT4 can in fact compensate for loss of *Sox2* to some extent, suggesting SOX2 may help stabilize *Oct4* transcriptional complexes (Masui et al. 2007). *Nanog* is a homeodomain protein that increases ES cells capacity for self-renewal, even in the absence of LIF (Chambers et al. 2003; Mitsui et al. 2003). *Nanog* null ES cells can still self renew indefinitely, although they have an increased propensity to differentiate (Chambers et al. 2007). In fact, levels of NANOG fluctuate naturally in normal culture conditions from low to high. High NANOG correlates with low levels of the primitive endoderm marker *Gata6* (Takahashi and Yamanaka. 2006; Chambers et al. 2007; Singh et al. 2007). HEX is also expressed at low, fluctuating levels in ES cells and its expression is mutually exclusive with NANOG. Based on gene expression including increased *Gata6*, these HEX positive cells appear to be a primitive endoderm intermediate precursor. In chimaeras they also show a bias towards extraembryonic endoderm (Canham et al. 2010). These studies suggest NANOG is marking a sub population of ICM like ES cells at the furthest point away from commitment, on a scale of pluripotent self renewal to differentiation.

Recently, it was discovered that terminally differentiated adult cells could be induced to revert to an ES cell like state, termed induced pluripotent stem cells (iPS). This was achieved by transgenically expressing four factors in adult fibroblasts: OCT4, SOX2, C-MYC and KLF4 (Takahashi and Yamanaka. 2006). It was later found that this list could be varied or factors omitted (Nakagawa et al. 2007; Yu et al. 2007). Constitutive activation of reprogramming factors was found not to be necessary either as the transgenes could be removed or recombinant membrane-penetrating proteins used instead (Kaji et al. 2009; Zhou et al. 2009). Although NANOG was not needed for iPS induction, selection of NANOG expressing colonies improved reprogramming efficiency and predicted germline competency (Okita et al. 2007). These findings suggest the self-renewal/pluripotency program is itself self-stabilising once established, given the correct exogenous factors.

These extrinsic factors are vital for maintaining ESCs, which were first grown *in vitro* on mitogenically inactivated fibroblasts. They appeared to provide both a substrate that was amenable for ES cell attachment and secreted factors that regulated the intrinsic pluripotency network and kept ES cells in an undifferentiated state. It was subsequently discovered that the factor responsible for this was a protein, DNA or Leukaemia Inhibitory Factor (LIF). ES cells could be maintained without feeders on gelatin coated plastic in media supplemented with LIF and fetal calf serum (Smith et al. 1988). LIF binds the gp130 receptor and causes it to dimerize. This activates the downstream transcription factor STAT3, which inputs into the pluripotency network (Niwa et al. 1998; Nichols et al. 2001). It was later found that BMP4 could replace fetal calf serum in media. BMP4 activates Id proteins, which act to inhibit neural differentiation (Ying et al. 2003). Although mouse ES cells can be maintained using the simple combination of LIF and BMP4, a wide range of signalling pathways including TGF β , Wnt and Map kinase/ERK have been shown to feed into the pluripotency network (Pera and Tam. 2010). Moreover, the ability of LIF and BMP4 to support ES cells maybe unique to the mouse system.

Primate ES cells do not respond to LIF induced Stat3 induction and require TGF β activation by ACTIVIN plus BMP4 and FGF2 to maintain pluripotency (Thomson et al. 1998). This may be because they are derived from a later developmental equivalent

stage to mouse ESCs. Interestingly, a later multipotent cell type known as epiblast stem cells (EpiSCs) can be derived from 5.5dpc mouse embryos. These share some of the characteristics of human ESCs both in their gene expression patterns and their requirement for ACTIVIN, BMP4 and FGF2 rather than LIF (Tesar et al. 2007). Interestingly, gp130 null embryos can survive and develop normally. However if implantation is delayed, gp130 null embryos show increased apoptosis in the ICM and fail to resume development (Nichols et al. 2001). Thus the *in vitro* culture environment used to culture mouse embryos may be similar to diapause-delayed implantation, in that they are slowed through normal development so both contexts require this additional signal to maintain pluripotency.

Another pathway feeding into the pluripotency network is Map kinase/ERK. FGF factors bind cell surface receptors and activate the downstream Ras-Erk signalling cascade. This in turn activates differentiation related genes and allows cells to transit to lineage commitment (Burdon et al. 1999). Mutation of *Fgf4* in cells or treatment with an FGF receptor inhibitor blocks differentiation to neural or mesodermal lineages (Kunath et al. 2007). ESCs naturally secrete FGF4, which would be expected to induce differentiation (Rathjen et al. 1999). This is an example of the delicate balance between signals to maintain self-renewal and those to allow differentiation that exist together in ESCs. Interestingly, inhibition of MAPK activity appears to enhance mouse ES cell culture, while its activation appears required for human cells.

The Wnt pathway has also been suggested to contribute to self-renewal. Overexpression of WNT5A and WNT6 in fibroblast feeders increases their ability to support ESC self-renewal (Hao et al. 2006). This appears due to the secreted Wnts as conditioned media has the same effect without feeders. *Stat3* transcript levels are increased following Wnt induction suggesting Wnt signalling synergises with LIF. However not all Wnt proteins are able to maintain self-renewal. Media conditioned by NIH3T3 cells expressing WNT3A supports self-renewal while WNT11 conditioned media does not (Singla et al. 2006). GSK3 inhibition also affects cells in a similar manner. GSK3 degrades β catenin so inhibition of this protein leads to more transcriptionally active β catenin-TCF complexes. The inhibitor 6-bromoindirubin-3'-oxime (BIO) is able to maintain human ESCs in an undifferentiated state in the absence of feeders. This effect also seems to be

synergistic with LIF (Sato et al. 2004). Transcript levels of GSK3 itself increase upon differentiation (Adjaye et al. 2005). The mechanism for this may be to increase expression of pluripotency transcription factors in addition to STAT3. *Oct4* and *Nanog* both have TCF binding sites in their promoters. Mutation of *TCF3* in ESCs causes delayed differentiation upon LIF withdrawal (Pereira et al. 2006; Tam et al. 2008). Additionally, inhibition of Wnt signalling is necessary to allow neural differentiation of ESCs. Addition of the Wnt inhibitor SFRP2 increases this while the GSK3 inhibitor lithium chloride inhibits differentiation to neural precursors (Aubert et al. 2002). Other downstream components of the Wnt pathway have been implicated in ESC regulation. TCF/CBP mediated transcription appears to contribute to self-renewal while TCF/p300 activates differentiation related genes. Altering the balance towards TCF/CBP dependant transcription by inhibiting p300 phosphorylation with the small molecule inhibitor IQ-1 helps inhibit differentiation of mouse ESCs (Miyabayashi et al. 2007).

This information has led to the development of a new culture system for ESCs, 2i culture. It uses two small molecule inhibitors instead of inductive signalling to maintain self-renewal (Ying et al. 2008). PD0325901 inhibits the Mek/ERK signalling cascade, which as discussed earlier, leads to inability of the cells to commit to differentiation in the mesoderm and neural lineage. CHIRON99021 is another GSK3 inhibitor that has been shown to help maintain self-renewal. CHIRON is more specific than BIO and provides more evidence that GSK3 inhibition is the important mechanism rather than any off target pharmacological effects (Murray et al. 2004). However, it is still unclear whether the canonical Wnt/TCF pathway is downstream of GSK3, or whether GSK3 is acting through another downstream pathway. Both inhibitors act together to maintain ESCs in an undifferentiated state. LIF is unnecessary although it still provides a beneficial effect to the system. 2i has also been used to grow naïve human ESCs that appear to represent a similar developmental stage as the mouse and to derive rat ES cells, suggesting that the mechanism of action is not species specific, unlike LIF induction in mice (Buehr et al. 2008).

1.6 TLEs in ES cells

As will be discussed later, TLE proteins are expressed in mouse ES cells. However the roles they play in these cells are so far unclear. The importance of the Wnt pathway in regulating ES cell self-renewal might be expected to involve TLEs as TCF corepressors. Indeed, the effects of altering TCF-TLE binding motifs on pluripotency described above seem to confirm this. TLE5 is also expressed in ESCs and its expression decreases upon differentiation, directly controlled by reducing STAT3 (Sekkai et al. 2005). FOXD3 inhibits differentiation in ES cells and has been shown to use TLE3 as a corepressor (Liu and Labosky. 2008). TLE/TCF can recruit HDACs and bind pluripotency associated genes; acetylation of these is associated with pluripotency (Spivakov and Fisher. 2007; Huangfu et al. 2008). Of course, this is all circumstantial evidence and the role of TLEs in ESC self-renewal has not been directly investigated before. In addition, the roles of TLEs in embryonic development would implicate TLEs in control of ESC differentiation as well.

In this thesis, I attempt to identify roles of TLE proteins in ES self-renewal. Consequences of loss of function and forced expression are examined to this end. I have also used ES cell differentiation as a model for embryonic development to investigate TLE involvement in early lineage specification.

Introduction to experimental strategies and results

The *Drosophila Groucho* gene was initially identified through genetic studies as a corepressor of Notch mediated transcription. *Groucho* and its homologues in other species have been shown to be involved in the regulation of diverse states of development and differentiation including neurogenesis, somitogenesis and haematopoiesis. They have also been shown to be involved in early lineage specification in vertebrates but a direct role in this has not been identified to date in the mouse. TLEs have no sequence specific DNA binding ability. They act as corepressors for other DNA binding proteins. Many transcription factors use TLEs as corepressors and the known motifs WRPW or eh1 are often found in TLE binding proteins. Throughout development, TLE proteins are also expressed in cells alongside the factors with which they interact such as HES1, RUNX1 and HEX. Therefore any effect seen may be due to affecting more than one TLE-corepressor interaction.

In this thesis I use an ES cell model to try to isolate specific lineage decisions regulated by TLE family proteins.

A role for TLE proteins in early development has been described in *Xenopus*, sea urchin and other organisms. Our laboratory recently implicated the transcriptional regulation of TLE3 and TLE4 by the homeobox transcription factor HEX as essential for early anterior axis specification. HEX acts to promote anterior identity by amplifying Wnt signalling, in part, by suppressing the expression of TLE proteins. This high level stimulation of the Wnt pathway leads to the induction and expansion of the anterior endodermal domain known to promote the establishment of the anterior neural axis. We wanted to investigate this in more detail by asking whether altering TLE activity also has an effect on anterior identity specification.

At the present time, relatively little is known about the role TLE proteins play in the earliest stages of mammalian embryonic development. While TLE knockout mouse lines have been made, no phenotype before peri-natal stages has been observed. This is likely due to redundancy as the family contains four members, of which three appeared expressed in early development. Previous studies have characterized the expression pattern of members of this family from 7.5dpc, which are expressed in all germ layer

derivatives and multiple developing organs. However, based on *in silico* analysis they appear to be expressed as far back as the zygote.

TLE1, TLE3 and TLE4 are also expressed at high levels in ES cells and have been implicated in the regulation of pluripotency. TCF is believed to regulate *Nanog* via a TLE mediated repression mechanisms and they could also act on *Oct4*. They have been indirectly implicated in the control of self-renewal and differentiation as corepressors for other proteins. TLEs also have direct roles in lineage specification in the neural and possibly mesendodermal lineage. As factors that promote differentiation will be inhibitors of ES cell self-renewal and vice versa, the role of the TLEs in early lineage specification may provide clues as to their function in ES cells.

In this thesis I have taken two complementary approaches to delineating specific roles for TLE family members in ES cells and early developmental decisions. I describe these approaches and the reagents generated for them in Chapter 3. The first was to use overexpression of a wild type full length TLE1 and TLE1 point mutations with defined loss or gain of activity with respect to specific interactors or signalling pathways. This approach allowed me to analyse the molecular basis for TLE phenotypes. One mutation had loss of WRPW and eh1 motif binding and an enhanced ability to suppress wnt signalling. The other had loss of WRPW binding specifically but the mutation did not affect other interactions. The second strategy was to assess whether the lack of an early phenotype in development is due to redundancy by generating compound TLE3 and TLE4 mutations in ES cells. Analysis of *in-silico* expression data and mRNA levels in ES cells showed that these were the most expressed TLEs in this context. In Chapter 4, I show that TLE family members act in early differentiation. In ES cells, they repressed self-renewal associated genes and enabled initial differentiation to proceed.

Complementary evidence from the gain and loss of function approaches also showed both positive and negative effects of TLEs on later lineage specific differentiation. TLEs both promote differentiation towards neural progenitors while restricting neural differentiation through the Notch pathway. In addition, in an *in vitro* mesendodermal differentiation assay, PS/mesoderm markers are increased by loss of TLE. Reduction though not complete loss of TLE activity allows more efficient anterior endoderm

differentiation suggesting a later role for TLE mediated corepression by homeobox proteins in anterior patterning.

Summary of thesis main aims

- Construction of a range of tools to analyse the role of TLEs in ES cell self renewal and differentiation, namely ES cell lines both overexpressing and mutant for TLE proteins
- Analysis of the role of TLE proteins in ES cell self renewal; to identify TLE proteins effects and the mechanism for these
- Analysis of the role of TLE proteins in ES cell neural and mesendodermal differentiation

Chapter 2

Materials and Methods

2.1 Cloning

2.1.1 Restriction Digests

1 μ g of DNA was put in a 20 μ l digest mix containing 2 μ l of reaction buffer and 10 units of the appropriate enzyme. All restriction enzymes were from New England Biolabs or Roche Diagnostics.

2.1.2 Modification of DNA ends

Vector backbones for cloning were sometimes dephosphorylated to prevent recircularization with cohesive ends. This was done using Antarctic Phosphatase (NEB) in the supplied buffer for 15m at r.t. The enzyme was then inactivated by heating at 65°C for 10m. Synthetic oligonucleotide linker was phosphorylated with T4 polynucleotide kinase (NEB) in T4 buffer with 100mM dATP. The reaction was carried out at 37°C for 30m and enzyme then inactivated at 65°C for 20m.

2.1.3 Ligation of DNA fragments

Ligations were normally performed with a 3:1 ratio of insert to vector DNA. For synthetic linkers, 2pmol of linker was ligated with 0.2pmol vector. DNA was mixed in a 20 μ l total reaction with 2 μ l Quick ligase buffer and 1 μ l Quick ligase (NEB). Reactions were performed for 5m at r.t. before being chilled on ice for transformation.

2.1.4 DNA transformation

DNA for subcloning (1ng) or from ligations (2 μ l of the reaction) was added to chemically competent *Escherichia coli* (*E.Coli*) and transformed according to the suppliers instructions. DH5alpha cells were used for subcloning and MAX Efficiency TOP10 for subcloning (Invitrogen). Bacteria were plated after recovery onto LB agar

plates containing ampicillin (100mg/ml) or kanamycin (50mg/ml). X-gal was also spread onto plates if necessary for indicating recircularized vector in TOPO cloning. Plates were incubated at 37°C overnight to allow growth of colonies.

2.1.5 Preparation of Plasmid DNA

For small-scale minipreps, single bacterial colonies were picked and inoculated into 5ml LB media with ampicillin (100mg/ml) or Kanamycin (50mg/ml). Cultures were incubated with shaking overnight at 37°C. 1.5ml of this culture was centrifuged and DNA prepared from the cells with the Quiagen Miniprep Kit (Quiagen) according to the manufacturers instructions. Large-scale plasmid preparations were performed in the same way using 250ml of LB and the Quiagen Maxiprep Kit (Quiagen).

2.2 General Molecular Biology

2.2.1 Preparation of genomic DNA

Cells or mouse tissue samples were lysed in TE-SDS with 5mg ProteinaseK (Sigma) at 50°C for 4hrs. KAc was added to 1.5M and DNA was separated from cell debris by the addition of 1 volume of chloroform followed by centrifugation. The aqueous phase was extracted and precipitated by adding 2 volumes cold EtOH and incubation at -20°C for 20m. DNA was pelleted by centrifugation at 13000rpm for 20m followed by a wash with 70% EtOH. DNA was dried and resuspended in RNase free water (Ambion)

2.2.2 Agarose gel electrophoresis of DNA

DNA was generally separated in 1% agarose gels containing 0.5mg/ml Ethidium bromide in TAE buffer. DNA was loaded with 1X loading buffer into the wells and 1kb ladder (Invitrogen) was also added to a well to mark fragment size. Electrophoresis was performed in TAE at 100V until loading buffer dye had migrated an appropriate distance. DNA was visualised on a UV lightbox.

2.2.3 Preparation of DNA from agarose gels

DNA fragments of interest were cut from agarose gels with a scalpel under UV light. The DNA was extracted and purified using the Quiagen gel extraction kit (Quiagen) following the manufacturers instructions.

2.2.4 Preparation of RNA

RNA was extracted from cells using the RNAEasy kit (Quiagen) following the manufacturers instructions. During the protocol, RNA was subjected to a 15m on-column digestion by RNase free DNase1 (Quiagen) to remove any contaminating genomic DNA.

2.2.5 cDNA synthesis

cDNA was synthesized using SuperscriptIII reverse transcriptase (Invitrogen) according to the manufacturers instructions. Briefly, 500ng RNA was incubated with 1 μ l of 1 μ M random primers (Promega) and 1 μ l of 10mM dNTPs at 65 $^{\circ}$ C for 5m in a total volume of 14 μ l. 6 μ l of transcription mix containing 4 μ l First Strand buffer, 1 μ l 0.1M DTT and 1 μ l of SuperscriptIII enzyme was then added. This was incubated at 50 $^{\circ}$ C for 1h and inactivated at 75 $^{\circ}$ C for 15m. The total reaction was diluted with nuclease free water 1:6 and aliquoted for future PCR analysis.

2.2.6 Quantitation of nucleic acids

DNA or RNA was quantitated using a Nanodrop spectrophotometer (Fisher Scientific) to measure concentration. An A260/280 ratio of >1.8 was used to judge purity.

2.2.7 Polymerase Chain Reaction

General PCR was carried out using *Taq* DNA polymerase (Quiagen) according to the manufacturers instructions. Briefly, DNA (1ng of plasmid, 100ng genomic or 3 μ l diluted cDNA) was added to a reaction containing 1X CL and Q PCR buffers, 200 μ M dNTPs, 0.5 μ M each of forward and reverse primers and 0.01 μ l *Taq* per 1 μ l reaction volume. Amplification was carried out in a thermal cycler according to the manufacturers recommended conditions. Annealing temperature was according to the T_m of primers (generally 58°C) and amplification time was 30s per Kb. For long range genomic PCR the amplification time was extended by 20s per cycle for the final 20 cycles.

For the amplification of construct components for cloning, Phusion High fidelity DNA polymerase (Finnzymes) was used to minimize sequence errors introduced during amplification. The reaction conditions used were similar to those for *Taq*. Two step fusion PCR was used to generate fused amplicons from two separate templates, A and B. This used standard PCR to generate A and B products with a short overlapping extension at the 3' end of A and the 5' end of B. The second step uses both products in a single reaction as first strand primers for each other, annealing using the overlapping sequence at the intended AB sequence junction. Second strand synthesis is from oligonucleotide primers annealing at the 5' end of A and the 3' end of B to give the product AB.

2.2.8 TOPO cloning of PCR products

TOPO cloning of PCR fragments was used for some construct building steps of for making DNA standard templates of rtPCR primer amplicons. TOPO TA (for *taq*) or ZeroBlunt (for Phusion) vectors were used (Invitrogen). 5 μ l of gel purified DNA was used per reaction, which were performed according to manufacturers instructions.

2.2.9 Quantitative real time PCR

Quantitative PCR was performed on reverse transcriptase synthesised cDNA to analyse gene expression. The SybrGreen (Roche Diagnostics) system, which uses fluorescence integration into the product, was used in most cases except for Nanog. This was quantified with the Roche UPL system due to problematic amplification with SybrGreen. UPL probe 25 was used. For each gene, 3 μ L of cDNA synthesized and diluted as above was used. This was added to a mastermix containing 5 μ L SybrGreen Mix1 and 1 μ L of each primer (0.5mM). For UPL system, 5 μ L of Probe Mix was used with 0.95 μ L each primer and 0.1 μ L probe. All samples were analysed in either duplicate or triplicate in 364-well plates using a Light Cycler 480 real time PCR machine (Roche Diagnostics). To normalize for the amount of mRNA in each sample, the housekeeping gene TBP was used as a reference. The relative expression levels for each gene were expressed as a ratio between those of a single reference point (plotted as 1) and the experimental condition of interest in each dataset. This ratio was calculated from measured raw Ct threshold values by the delta Ct (Pfaffl) method using the equation shown:

$$\text{Ratio} = \frac{(\text{Efficiency}_G)^{Ct_{G(\text{reference point})} - Ct_{G(\text{experimental condition})}}}{(\text{Efficiency}_{\text{TBP}})^{Ct_{\text{TBP}(\text{reference point})} - Ct_{\text{TBP}(\text{experimental condition})}}$$

Where G=gene of interest. Amplification efficiency was assumed to be 100% (i.e. 2) where this was unable to be determined experimentally.

An average value was calculated from the triplicate wells, discarding any single value that severely deviated from the mean. Primers used for qPCR in this thesis are listed in the table below:

Gene	Forward primer	Reverse primer
Klf4	CGGGAAGGGAGAAGACACT	GAGTTCCTCACGCCAACG
Dppa3	GATGCACAACGATCCAGATTT	TGGAAATTAGAACGTACATACTCCA
Nr0b1	ACCGTGCTCTTTAACCCAGA	CCGGATGTGCTCAGTAAGG

Rex1	TCTTCTCTCAATAGAGTGAGTGTGC	CCAGGACAGCTCAGGATACAG
Gata4	GCCTGCGGCCTCTACATGAA	CAGGACCTGCTGGCGTCTTA
Gata6	GGTCTCTACAGCAAGATGAATGG	TGGCACAGGACAGTCCAAG
Oct4	GTTGGAGAAGGTGGAACCAA	CTCCTTCTGCAGGGCTTTC
Nanog	CCTCCAGCAGATGCAAGAA	GCTTGCACTTCATCCTTTGG
Sox2	GTGTTTGCAAAAAGGGAAAAGT	TCTTTCTCCCAGCCCTAGTCT
Ecadherin	AGACTTTGGTGTGGGTCAGG	CATGCTCAGCGTCTTCTCTG
Fgf5	GTTTCCAGTGGAGCCCTTC	GAGACACAGCAAATATTTCCAAAA
Brachyury	GTGACTGCCTACCAGAATGA	ATTGTCCGCATAGGTTGGAG
Wnt3a	CGCTCAGCTATGAACAAGCA	GGTGTTCCTCCACCACCATC
Nestin	CTGCAGGCCACTGAAAAGT	TTCCAGGATCTGAGCGATCT
Sox1	GTGACATCTGCCCCATC	GAGGCCAGTCTGGTGTGAG
Six3	CCTTCCCCTCCTCTTCGTAA	CGGTTTGTTCTAGGGATGGA
BLBP	AACCAGCATAGATGACAGAACTG	ACTTCTGCACATGAATGAGCTT
NeuroD1	CGCAGAAGGCAAGGTGTC	TTTGGTCATGTTTCCAATTCC
Tuj1	GCGCATCAGCGTATACTACAA	TTCCAAGTCCACCAGAATGG
Cerberus	GACTGTGCCCTTCAACCAG	AGXAGTGGGAGCAGAACC
FoxA2	CATCCGACTGGAGCAGCTA	GCGCCCACATAGGATGAC
Hex	CTACACGCACGCCCTACTC	CAGAGGTCGCTGGAGGAA
Cxcr4	TTTCAGCCAGCAGTTTXXXX	TCAGTGGCTGACCTCCTCTT
Sox17	CTCGGGGATTAAGGTGAA	CTTAGCTCTGCGTTGTGAG
Mixl1	AGTTGCTGGAGCTCGTCTTC	AGGGCAATGGAGGAAAAGT
Frzd5	CAGCACTCAGTTCCACACCA	CAGCAGGATCCTCCGAGA
Goosecoid	GAGACGAAGTACCCAGACGTG	GGCGGTTCTTAAACCAGACC
h/mTLE1	ACGGAGCCAGCTGTATTGAC	TCGAGCTGGTACTTGTGAGG
mTLE1	AGAGGCACAGATAAGCG	TCTTGTCCTCCATCACTGTCA
TLE3	AGACAGCCTCAGCAGATACG	TTTGTCCAGCCCATTTTCAG
TLE4	CCATGACAATGATCACCAAAG	TCTGCTTTTTGCTCTCTGAGG

2.2.10 Sequencing of DNA

The functionally important segments of the targeting vector were sequenced before use to confirm their integrity. This was performed using appropriate sequencing primers by the University of Edinburgh sequencing service (The Gene Pool, Ashworth, University of Edinburgh).

2.2.11 Southern Blotting

DNA was extracted from targetted cell lines identified by PCR screening and from control cells. After purification, 5 μ g was digested with BclII restriction enzyme. Digests were separated by agarose gel electrophoresis as above. A 1% agarose gel was used and electrophoresed at 4V/cm overnight. Migration distance of digested DNA and reference ladder was recorded. The separated DNA strands in the gel were nicked by exposure to UV light and denatured with 0.5M NaOH, 1M NaCl which was afterwards neutralised with 0.5M Tris, 3M NaCl (pH 7.4). Transfer of the DNA onto a Hybond N+ nitrocellulose membrane (GE Healthcare) was performed as standard using the upward transfer blotting technique in 20XSSC (0.3M tri sodium citrate, 3M NaCl). The membrane was baked at 80°C for 2hrs to crosslink the DNA and stored for analysis.

Analysis of digestion patterns produced from the lines was with a 3' external probe downstream of the TLE4 targeting vector 3' arm. The template was amplified from genomic DNA by PCR and gel purified. A radioactive probe was made from it using the Megaprime DNA labelling kit (GE Healthcare) according to the manufacturers instructions. The blot was blocked in QuikHyb (Stratagene) and the purified probe added and incubated at 65°C overnight. Washes in 0.5XSSC 0.1%SDS were performed until no increased background levels of radiation were detectable on the blot using a Geiger counter. The blot was then exposed to X-ray film to produce a hybridisation pattern for analysis.

The following primers were used to generate a 3' probe:

TLE3 3' BclI probe F	CCTTGGTGTTTTGCCCTTTA
TLE3 3' BclI probe R	GCCCTCTGAAGTCTCACCAG

2.2.12 Western Blotting

Western blotting was used to measure the protein expression from TLE1 expression constructs in HEK293 cells. Protein was extracted from the cells by harvesting cells from plates at equal plating densities and boiling in Lameli Sample Buffer (BioRad) for 10 minutes followed by vortexing to denature. Samples were then centrifuged to remove insoluble debris and loaded onto precast Novex 10% BisTris acrylamide gel (Invitrogen), which was electrophoresed at 200V for 40m. Separated protein was transferred onto nitrocellulose membrane by Western transfer at 360mA for 1hr. The membrane was blocked in TBST (25mM Tris, pH 7.4, 3mM KCl, 140mM NaCl, 0.1 % TWEEN 20) with 5% dried milk powder (Marvel). The blot was stained overnight with rabbit anti-FLAG antibody (1:1000)(Cambridge Biosciences). It was then washed in TBST and stained with HRP conjugated anti-rabbit secondary (Sigma). After further washing, the blot was developed using Pierce Reagent (Pierce) and visualised by exposure to X-ray film.

2.2.13 Constructs

The following constructs were used in this thesis for experiments and as cloning components:

pFLAG CMV2 containing TLE1wt, TLE1 S239A/S253A, TLE1 S239E/S253E, TLE1 V488S, TLE1 C488R, TLE1 R534A, TLE1 E550K and TLE1 L743F; pVP16-TLE1; pEGFP-Grg6 (gifted by Stefano Stifani, McGill University); pMIR QD (a gift from Amanda Fisher, Imperial College London); pYX AES (Geneservice); pCS2 xTCF3; pCS2 TCF3 Δ catBD VP2; pTOPflash (Upstate Biotechnology); pKO901 (NEB); pRSET-B mORANGE and mCHERRY (gifts from Roger Tsein's lab); pCAGIPfloxGFP (by Adam Yates); pBSK Flox CMV-HygroTK; pBSK C2MAZSPA (Andrew Smith's lab); pTTO TLE3 (gift from Susan McConnell).

2.3 Cell culture and experiments

2.3.1 Cell lines

All ES cell lines used for overexpression were based on E14tg2a (Austin Smith lab). TLE4^{+LacZ} and TLE4^{LacZ/LacZ} ES cells were derived from the ICM of 3.5dpc blastocysts from timed matings between TLE4^{+LacZ} mice. Derivations were performed by Jan Ure (Transgenics Facility, ISCR, University of Edinburgh). Blastocyst outgrowths were genotyped and expanded. Before use, cells were screened for mycoplasma and checked for normal karyotype (Jonathan Rans, ISCR, University of Edinburgh). HEK293 cells were also provided by Austin Smith's lab.

2.3.2 Maintenance of Cells

For routine culture, ES cells were maintained on 0.1% gelatin coated TC plasticware (IWAKI) in Glasgow Modified Eagle's Medium (Gibco) containing 10% fetal calf serum, non-essential amino acids, L-Glutamine, Sodium Pyruvate, 0.1mM β mercaptoethanol and 1000U/ml LIF. Cells were incubated at 37°C in a humidified 6% atmosphere. HEK 293 cells were cultured in the same way but without LIF.

Cells were passaged when judged nearly confluent (generally every 2-3 days). They were dissociated from the substrate using brief incubation with 0.1% trypsin before the trypsin was neutralized with an excess of serum containing media. Cell were centrifuged at 1300rpm, resuspended in fresh medium and around 1/7 replated.

For freezing, cells were trypsinised and neutralized as before and resuspended in media containing 20% FCS and 10% DMSO. They were frozen in cryovials at -80°C and transferred to liquid nitrogen for long term storage

2.3.3 Transient transfection of HEK293 cells and TOPflash assays

For testing of overexpression vector fluorescence reporters, DNA was transiently transfected into HEK293 cells using Lipofectamine2000 (Invitrogen) according to the manufacturers instructions. Cells were examined 48hrs later by fluorescence microscopy.

For TOPflash luciferase assays, HEK293 cells were plated in 24 well plates at an initial density of 10^5 per well. When cells had reached 80% confluency they were transfected in triplicate using Lipofectamine2000 with DNA mixtures containing 10ng TOPflash luciferase reporter plasmid, 10ng pRL-SV40 renilla luciferase and 100ng of each expression vector required per condition. All expression vectors used the CMV promoter and levels of CMV were kept constant across conditions using empty pCDNA3 vector to make up any differences. Total DNA transfected into each well was 800ng and pBSK was used to make up any remaining differences between amounts used in each condition. Cells were collected and analysed with the Dual Luciferase assay reporter system (Promega) using the manufacturers instructions. Samples were analysed on a Mediators PHL luminometer (Mediators Diagnostika) and firefly luciferase values normalised to the constitutively active SV40 renilla luciferase for each well. All transfections were carried out in triplicate and the average luciferase value for each set calculated.

2.3.4 Stable transfection of ES cells

DNA for electroporations ($50\mu\text{g}$ as standard) was prepared by restriction digest overnight followed by ethanol precipitation as described before and resuspension in $100\mu\text{l}$ of sterile pH8 Tris buffer. For non-integrative Cre vector transfections, plasmid DNA was used uncut.

For overexpression lines and gene targeting, ES cultures were grown to approximately $2-10 \times 10^7$ cells per electroporation. Cells were dissociated from the substrate by trypsinisation and neutralization as standard. They were washed twice with PBS and the concentration counted using a haemocytometer. 10^7 cells in PBS were placed in a disposable electroporation cuvette with the DNA. Electroporation was carried out on a

Gene Pulser at 800V and 3 μ Farad capacitance (BioRad). Electroporated cells were then diluted in media and plated at 5X10⁵ and 1X10⁶ cells per 10cm dish. Selective agents were added after 24hrs as required. Concentrations were as follows: 2 μ g/ml puromycin, 150 μ g/ml hygromycin, 10 μ M gancyclovir. Surviving colonies were selected and expanded by picking from the plate by pipette followed by dissociation and replating in individual wells of a 96 well plate. Lines were further expanded by sequential passaging.

2.3.5 Antibody staining of cells

Cells were washed with PBS and fixed in PBS 4%paraformaldehyde for 20m. They were then washed and permeablized with PBS 0.1% TritonX-100 (PBST). Non-specific antibody binding was blocked with 1%BSA, 3% secondary antibody species serum in PBST. Primary antibody staining was performed overnight at 4°C with the antibody diluted in the above blocking solution. Cells were then washed with PBST and stained with an appropriate secondary antibody conjugated to an Alexa fluorophore in the dark for 2hrs at r.t. The plates were washed again and DAPI was used as a counterstain to mark total cells. Staining patterns were visualised using fluorescence microscopy.

Antibodies used in this thesis were as follows:

Rabbit anti Nanog (R&D systems), mouse anti Oct3/4 (Santa Cruz), goat anti Sox2 (Santa Cruz) mouse anti nestin (gift from Sally Lowell), mouse anti β III-tubulin (Covance)

2.3.6 2i culture of ES cells

Cells were grown in 2i media according to the conditions developed by Qi-Long Ying and coworkers (Ying, Wray et al. 2008). This is a mixture of N2B27 media (Stem Cell Sciences), 3 μ M CHIRON99021, 1 μ M PD0325901 (Stemgent) and LIF. CHIRON concentrations were reduced for some experiments as described. Cells were plated at

approximately 2×10^4 /cm² and passaged 1:10 after 3 days. TrypLE Express cell dissociation buffer (Invitrogen) was used for this and cells were washed with PBS to remove dissociation buffer.

2.3.7 Neural Differentiation

Monolayer neural differentiation was performed according to the protocol developed by Qi-Long Ying and co-workers (Ying, Stavridis et al. 2003). ES cells were plated at a density of 10^4 /cm² in N2B27 neurobasal media (Stem Cell Sciences) with LIF on gelatin coated plastic. Cells were left to attach overnight and the media was replaced with N2B27 minus LIF. Cultures were left to differentiate and grow and the media changed as necessary with fresh N2B27 when the pH indicator in the media started to indicate increased acidity (between 1-3 days). Full neural differentiation, with cultures containing significant numbers of neurons with elongated TujI positive axons, took 7d of culture.

2.3.8 Mesendoderm differentiation

ES cells were differentiated towards the mesendoderm lineage using the protocol developed by Gillian Morrison and co-workers (Morrison, Oikonomopoulou et al. 2008). Cells were plated at a density of 6×10^3 /cm² in gelatinized 6 well plates in N2B27 media containing 20ng/ml Activin A and 10ng/ml BMP4 (R&D systems). They were left incubated to undergo the initial stage of differentiation for 48hrs. The media was then changed to SF03 (Iwai Chemicals Company) supplemented with 0.1%BSA and 20ng/ml Activin A, 20ng/ml EGF and 10ng/ml FGF4 (R&D systems). Cells were left to differentiate for a further 5d with the supplemented SF03 being refreshed after 2d.

2.3.9 Flow cytometry

Cells were dissociated from the substrate using trypsin as standard and pipetted to single cell suspension. They were then centrifuged and resuspended in FACS buffer (PBS, 10%FCS, DAPI to mark dead cells) and chilled on ice. Flow cytometry was performed with a Fortessa flow cytometer (BD Biosciences) using laser and filter combinations optimized for the 487nm excitation and 410nm emission maximums of mCHERRY and data analysed and plotted using Flowjo (Treestar Software)

2.3.10 Colony forming assays

Cells were plated in normal media in the presence or absence of LIF in 6 well plates at a density of $50/\text{cm}^2$. They were left to grow into colonies for 5d to allow potential differentiation. Alkaline phosphatase staining was performed using the Alkaline Phosphatase Kit (Sigma) according to the manufacturers instructions. Briefly, plates were washed with PBS to remove residual media and debris and fixed with AP fixative (25% Citrate solution, 65% acetone, 8% of 37% Formaldehyde). Plates were then washed with water and stained with freshly made AP stain containing Fast Red Violet in the dark for 15m at r.t. Stained plates were washed with water again and dried before colonies were counted, scored and photographed under a dissecting microscope. Colony type percentages in the figures are an average of four biological replicates.

2.4 Mouse experiments

2.4.1 TLE4^{+LacZ} mice

TLE4^{+LacZ} mice were obtained by kind donation from Susan McConnell (Stanford University, USA). Mice were shipped following Home Office approval and the line was transferred to the ISCR animal facility from a local intermediary quarantine facility by embryo transfer into B16 females followed by successive inbreeding. For ES cell

derivation, mice were outcrossed onto a 129/SV background to increase the processes efficiency. Routine genotyping was performed using the following primers:

PLAP F (mutant)	GTGCAGGAGCAGACCTTCAT
Grg4 5' intron F (wt)	CCTTGCCTCCCTGTCTTTC
Grg4 3' intron R	CCCATCAGGTGAGACCACTT

All animal husbandry was carried out by Carol Manson (Animal unit, ISCR, University of Edinburgh).

2.4.2 β galactosidase staining of embryos

Embryos were dissected in M2 media using a dissecting microscope. For 3.5-4.5dpc stages, preimplantation stage embryos were flushed from the uterus at 2.5dpc and cultured for a further 1-2 days in K2 embryo culture media at 37°C. Dissected embryos were washed in PBS and fixed with X-gal Fix (PBS, 0.1M phosphate, 5mM EGTA, 2mM MgCl₂, 0.2% gluteraldehyde) for 20m. Fixed embryos were washed in rinse buffer (100mM sodium phosphate, 2mM MgCl₂, 0.01% sodium deoxycholate, 0.2% NP-40) and stained (5mM potassium ferricyanide, 5mM potassium ferrocyanide, 1mg/ml X-gal (Promega) in rinse buffer) at r.t. overnight. Embryos were then refixed with 4% PFA and transferred to PBS for visualisation by brightfield microscopy.

β galactosidase staining of ES cells was carried out using the same reagents and same general method although incubation was only for around 2h at 37°C.

Chapter 3

TLE family expression in ES cells and early development and the generation of reagents to investigate their roles

3.1 Expression of TLEs in ES cells

To determine which TLE family members to focus on I examined the expression of different TLE transcripts as they appear in public domain databases. *In silico* expression information on TLE family members was collated from available databases. EST profiles from the NCBI Unigene database are summarized in Fig 3.1a. The TLE family contains four full-length functional proteins and a number of shorter peptides (see Figure 1.3). Of the four full length TLEs (*TLE1-4*), only TLE3 and TLE4 are expressed at the blastocyst stage from which ES cells are derived and only TLE4 appears expressed around the onset of gastrulation (egg cylinder stage, 6.5dpc)(Fig 3.1a). Gene trapping is a technique for the simultaneous identification and mutation of genes (Gossler et al. 1989). The majority of gene trap insertions have been generated with promoterless vectors and therefore the likelihood of gene trap insertions occurring is directly proportional to their expression level (Nord et al. 2007). As a result the number of gene trap insertions in a particular loci can be seen as proportional to its expression level in ES cells. Figure 3.1b shows the number of traps observed and documented in the database for the in the International Gene Trap Consortium (IGTC). Three full-length TLE family members, *TLE1*, *TLE3* and *TLE4* have all been trapped in ES cells. However, based on both in silico blastocyst expression and the numbers of gene trap events, *TLE3* and particularly *TLE4*, appear the most significant family members. Although TLE1 was not observed as expressed in blastocysts, in the EST databases it does appear expressed in ES cells based on the gene trap database. Of the truncated TLEs, TLE6 appears expressed throughout early development and produced a significant number of gene trap insertions. *TLE5*, like *TLE1*, appears in the gene trap database, but appears relatively rarely in ESTs derived from pre and peri implantation stages of development.

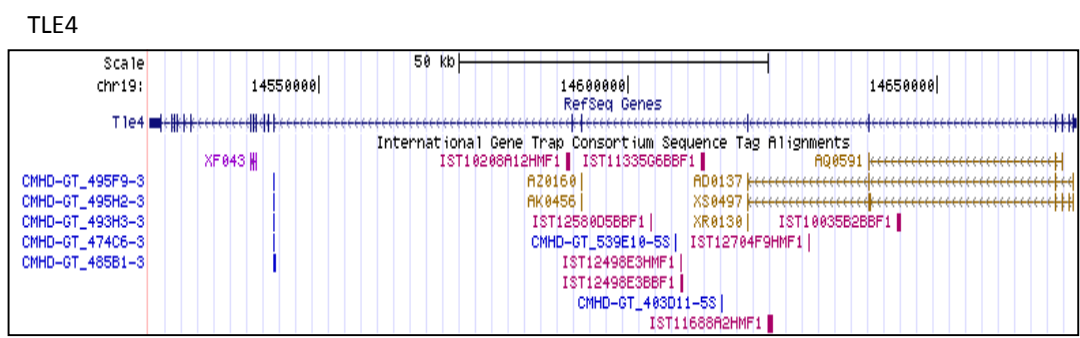
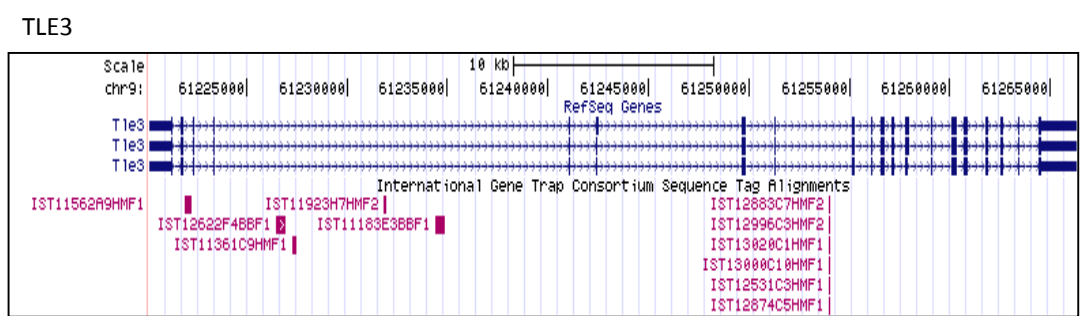
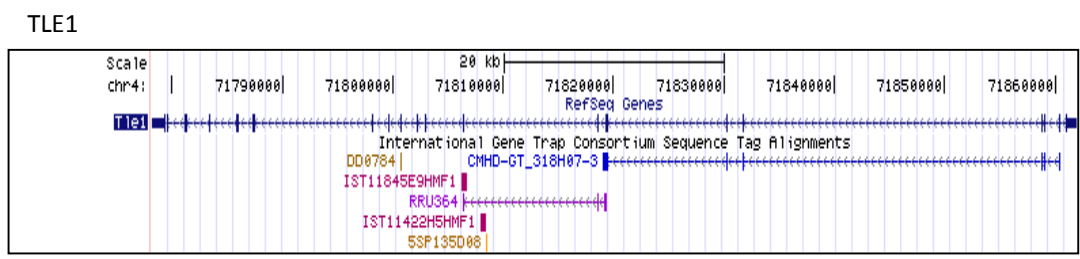
As I was interested in the activity of full-length TLE proteins, I sought to quantitate the expression of these four transcripts in E14tg2a ES cells. Quantitative RT PCR was used to analyse TLE1, TLE3 and TLE4 in these cells as maintained under standard culture conditions and during differentiation in response to LIF withdrawal and in neural differentiation (Fig 3.1c). While, TLE2 was undetectable despite multiple PCR primer pairs tried, all three TLEs were expressed at broadly similar levels in normal culture

a

	Gene expression (transcripts per million)			
	Zygote	Morula	Blastocyst	Egg cylinder
TLE1	0	0	0	0
TLE2	0	0	0	0
TLE3	0	262	14	0
TLE4	35	180	78	157
TLE5	0	0	14	0
TLE6	140	36	104	14

b

	Number of gene insertions recorded
TLE1	5
TLE2	0
TLE3	14
TLE4	26
TLE5	5
TLE6	17



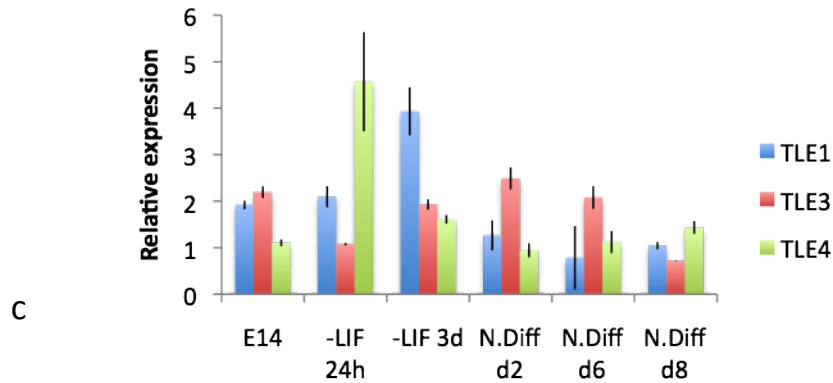


Fig 3.1 Expression of the TLE gene family in embryonic stem cells

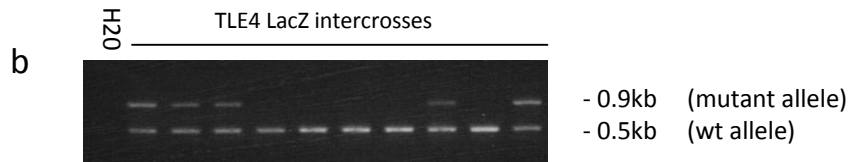
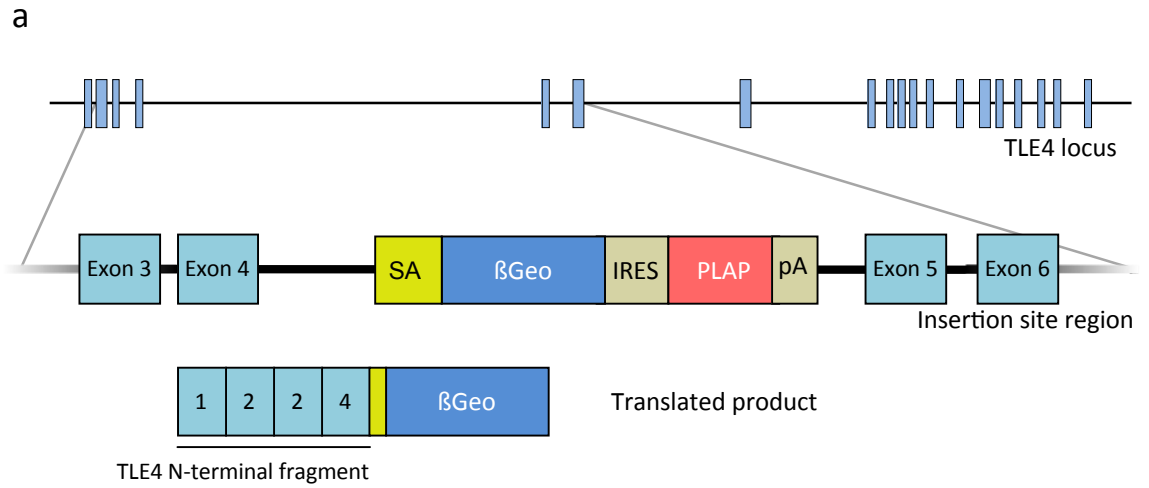
(a) EST expression profiles in mouse early embryonic stages. Data shown is taken from the Unigene EST database (<http://www.ncbi.nlm.nih.gov/UniGene>). **(b)** Trapping of TLE family loci by the International Gene Trapping Consortium. Genome tracks showing vector insertion sites are from the USC genome browser (<http://genome.ucsc.edu>) TLE1, TLE3 and TLE4 have been trapped multiple times by promoterless traps showing significant expression in ES cells. **(c)** Expression of TLE genes in E14 ES cells. Samples were taken for RNA extraction in normal growth conditions with serum and LIF, after LIF withdrawal for 1 and 3 days and at days 2,6 and 8 of a monolayer neural differentiation protocol. cDNA was synthesized and used for qPCR analysis of TLE1, TLE3 and TLE4. PCR was performed in technical triplicate and levels are shown normalized to TBP and relative to TLE4 level in E14 cells. TLE2 was undetectable by multiple primer pairs.

conditions in the presence of LIF. Upon LIF withdrawal, the expression level of all three TLEs was increased, although with differing kinetics. Interestingly, TLE4 was expressed at dramatically higher levels following LIF withdrawal in these cultures and TLE3 was most significant upregulated in the early stages of neural differentiation. As ES cells are known to contain a heterogeneous mix of partially differentiated and undifferentiated cells, these levels might explain the frequency with which these transcripts comes out in *in silico* datasets. However, all three genes are expressed at quite high levels in all these cultures and in the absence of data on additional cell lines it is difficult to make any definitive statements about their relative levels.

While the RT-PCR suggests three TLE transcripts are expressed in ES cells, *TLE1*, *TLE3* and *TLE4*, only *TLE3* and *TLE4* were identified as Hex targets (Zamparini et al. 2006) Moreover, TLE3 and TLE4 both appear to be more ubiquitously expressed based on in silico analysis therefore my loss of function studies began with these two genes. However there is a clear possibility that redundancy with TLE1 may still be an issue.

3.2 Expression of TLE4 in early stage mouse embryos

Based on the in silico analysis in Figure 3.1, *TLE4* appears the most likely transcript to be expressed at peri implantation stages. I also was able to exploit a previously generated gene trap line for *TLE4*. *TLE3* and *TLE4* mutant mouse lines had been generated by the McConnell laboratory, but they have only been able to maintain the *TLE4* line, based on a behavioural phenotype in the TLE3 heterozygotes (S. McConnell personal communication). The TLE3 and TLE4 mutants were generated from targeted insertions of the pTTO gene trap into intron 4 of the TLE4 locus (Friedel et al. 2005). This vector inserts a β -geo neomycin resistance/LacZ reporter and polyadenylation sequence into the *TLE4* transcript after exon 4 of 20 exons. It leaves only the first section of the Q domain so is predicted to be an effective null mutation (Fig 3.2a). We obtained these mice (Kind gift of Susan McConnell). Mice were genotyped and found to be heterozygous for *TLE4*. Despite extensive inbreeding, we were unable to obtain live pups homozygous for the *TLE4* mutation. Observed frequencies of heterozygotes and homozygotes were close to the expected Mendelian ratios assuming homozygous



c

	wt	LacZ
wt	+/+	+/-
LacZ	+/-	-/-

	Expected (homozygous viable)	Expected (homozygous lethal)	Observed
wild type	25%	33%	39% (n=81)
heterozygous	50%	66%	61% (n=127)
homozygous	25%	0%	0% (n=0)

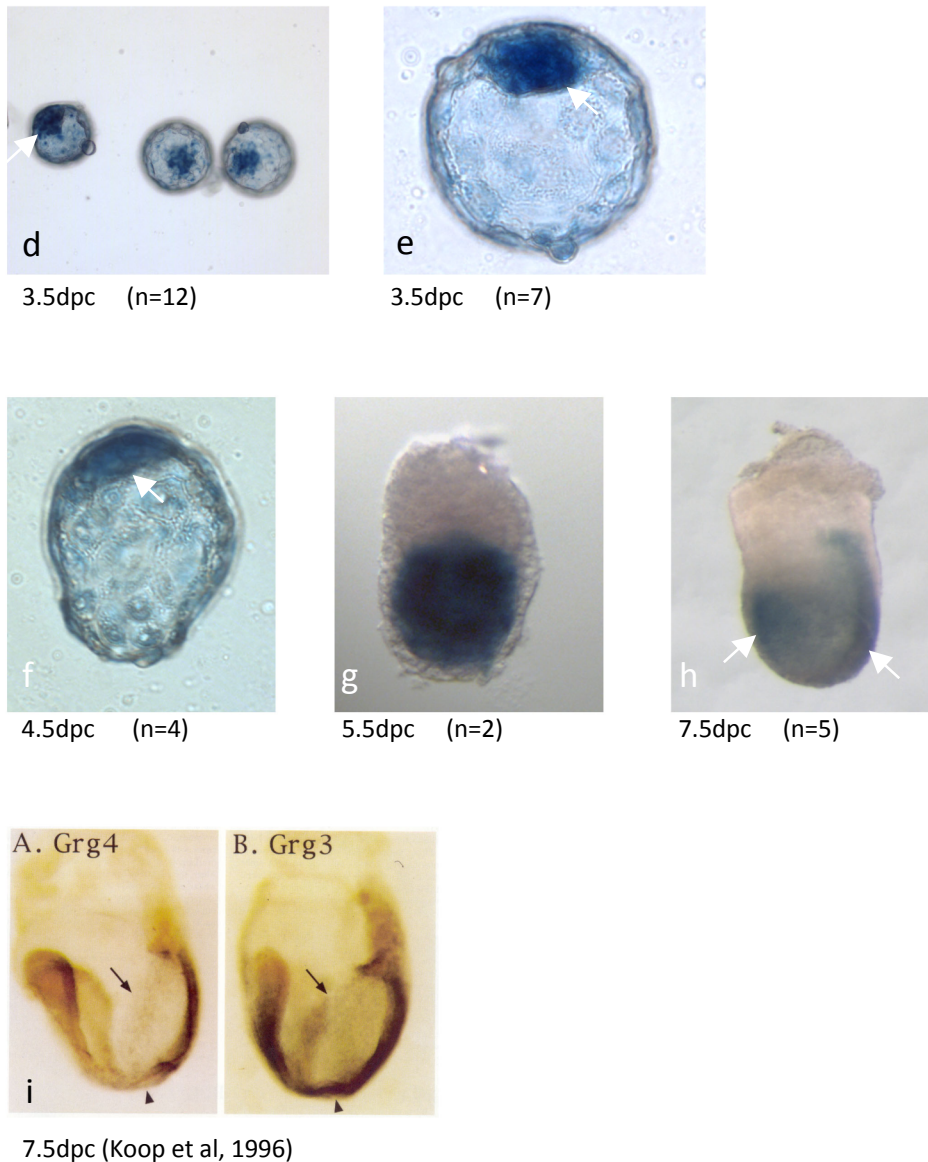


Fig 3.2 Expression pattern of TLE4 in early development

(a) Schematic of targeting in the TLE4 locus (As performed by Friedel et al, 2005). The targeted trap contained β geo to mark TLE4 expressing cells, a placental alkaline phosphatase (PLAP) gene used to stain neuronal axons in the original reference and a polyadenylation sequence to terminate transcription. The vector was targeted to intron 4/20 and leaves only an N-terminal fragment of TLE4 fused to β geo translated. **(b)** TLE4^{+/LacZ} mice were interbred and genotyped by PCR for the presence of wt and mutant alleles (representative litter shown). **(c)** Table shows expected Mendelian ratios and the observed results. β galactosidase staining was carried out on early stage TLE4^{+/LacZ} embryos. Day 3.5 (**d,e**), 4.5 (**f**), 5.5 (**g**) and 7.5 (**h**) embryos were dissected and stained. Arrows indicate expression mentioned in the main text. n represents the number of embryos examined for each stage. **(i)** The observed LacZ staining at 7.5dpc conforms quite well with previous in situ data published by Koop et al, 1996.

lethality (Fig 3.2b,c). Genotyping of embryos up to 16dpc showed that homozygous null embryos were still developing. It was concluded that there must be a lethal phenotype that affects the pups before or shortly after birth. However there were no easily identifiable morphological differences between mutant and wild type embryos. This would be interesting to investigate at a later time, as there is no published phenotype for *TLE4* null mice. However detailed analysis lies outside the scope of this thesis.

Expression patterns for TLE3 and TLE4 in mouse embryos have previously been published from 7.5dpc onwards. It was therefore interesting to look at expression at earlier stages. To this end I used the *TLE4 LacZ* reporter gene trap mice. Pre and post implantation stage embryos from 3.5-7.5dpc were obtained from *TLE4 LacZ* mice. These were dissected, fixed and stained for β galactosidase activity using X-gal. The TLE4 reporter was expressed as early as 3.5dpc (Fig 3.2a,b) and although most strongly in the inner cell mass (arrows), faint blue staining was also observed in the trophoctoderm. The pattern was also observed at 4.5dpc, where expression is seen in both the epiblast and primitive endoderm (Fig 3.2c), although by 5.5dpc, the expression of LacZ was restricted to the epiblast (Fig 3.2d). By 7.5dpc TLE4 started to become restricted towards the early headfold region and most strongly in the primitive streak (Fig 3.2e, arrows). This expression pattern was consistent with published RNA in-situ hybridisation at the same stage (Fig 3.2f, Koop et al, 1996).

3.3.1 The generation of TLE mutants with altered binding and corepression activity

As TLE proteins are known to act as a co-repressor on diverse classes of transcription, over expression experiments are very difficult to interpret. To circumvent this problem we began a collaboration with Stefano Stifani's laboratory (see appendix 1) to test the activity of point mutations predicted to alter TLE activity. These point mutations were introduced in the context of the human cDNA sequence to allow me to differentiate between the endogenous allele and any molecules over expressed.

The TLE variants we generated in collaboration with the Stifani group were obtained from a variety of sources. Human TLE1 L743F, E550K, R534A, C488R and V486F are

point mutations affecting the central binding pore of the WD40 domain of TLE1. This site interacts with WRPW and eh1 motifs in TLE binding partners and so could affect binding to either or both these classes of sequence specific transcription factors. TLE1 S239E/S253E and S239A/S253A affect residues implicated in phosphorylation and have been shown to regulate nuclear retention of TLE1 (Nuthall et al. 2004). Mutation of serine to glutamic acid mimics constitutively active phosphorylation and hence increased activity. Mutation to alanine makes the residue unphosphorylatable and hence less able to remain in the nucleus. TLE1 VP16 is a fusion of TLE1 to an HSV protein transactivator domain, which has been shown to increase transcription factor activity as a fusion (Sadowski et al. 1988). Grg6 GFP is a truncated TLE that has been shown to have partial repression activity (Dang et al. 2001) fused to GFP. AES (TLE5) is a C-terminal truncated TLE that lacks a WD40 cofactor-binding domain and has been implicated as a dominant negative TLE (Brantjes et al. 2001). QD is an even shorter C-terminal truncation that has also been described as a dominant negative (Milili et al. 2002). This lacks both cofactor binding and repression mediating domains. However it still contains an LzL motif that can bind other TLEs and may sequester them into inactive complexes.

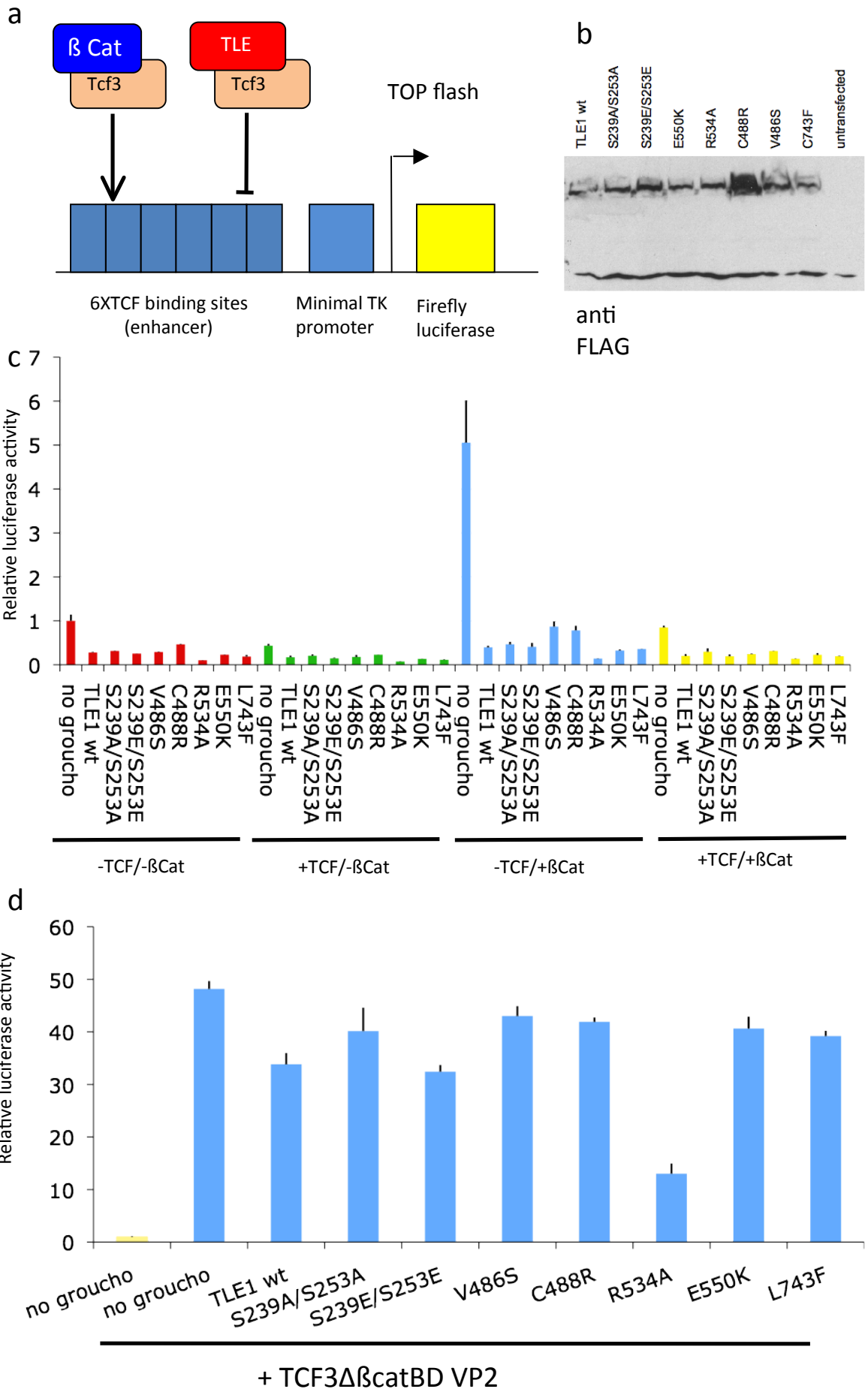
3.3.2 Activity of point mutants and fusion proteins with respect to Wnt signalling.

As our interests in TLEs were initially based on their role in Wnt signalling, we tested these fusions for their activity on a Wnt reporter gene in transient transfections. The aim of this was to identify possible mutants with altered ability to affect the pathway, either positively or negatively. These could then be overexpressed in ES cells as dominant negative/positive proteins to modulate the normal effect of TLEs. The Wnt pathway is normally activated by the binding of Wnt ligands to the Frizzled receptor, which suppresses the activity of the APC-GSK3 complex and allows β catenin to translocate to the nucleus and activate transcription of targets in conjunction with TCF/LEFs. In the absence of Wnt ligands, the APC-GSK3 complex causes degradation of β catenin and Wnt targets are kept fully repressed, in large part by TLEs bound to TCF/LEFs.

Plasmids expressing the different TLE variants and Wnt pathway components were co-transfected alongside a Wnt reporter and assayed for their ability to stimulate or repress transcription of this reporter. This experiment used a reporter plasmid containing

reiterated TCF binding sites acting upstream of a basal TK promoter driving luciferase. Activation of the reporter was achieved by cotransfecting plasmids expressing β catenin and TCF. When TCF binds TLE, it competes with the capacity of the TCF- β catenin complex to bind these sites and activate transcription (Fig 3.3.2a). The assay was performed in HEK293 cells and TLE point mutations FLAG tagged so that their levels could be monitored by western blot. All proteins were expressed from the CMV promoter. The expression level of these proteins appeared broadly similar indicating that observed alterations in TLE activity were due to an intrinsic property of the mutation (Fig 3.3.2b). The TOPflash reporter assay was performed on all the point mutations (Fig 3.3.2c) and fusion proteins (Fig 3.3.2e) described above. All proteins were expressed from the original plasmids, which contained CMV promoters except for QD. This was subcloned from pMIR into the pCDNA expression vector using *KpnI* and *XhoI* restriction sites. All transfections were normalized to the level of luciferase activity obtained from TOPflash in the absence of exogenous factors. The endogenous activity of these promoter elements is presumably due to both the basal level activity of the TK promoter and to endogenous TCF and β -catenin. Thus TLE1 suppresses TOPflash activity in the absence of added exogenous β -catenin (Fig 3.3.2c, e) and interestingly TCF itself inhibits the activity of β -catenin, even in the absence of additional TLE. This observation has been reported by others who have shown that endogenous levels of TLEs and other co-repressors in HEK 293 cells can suppress TOPflash activity through an interaction with additional excess TCF (Brantjes et al. 2001). However, in all instances, the level of transcription from these reporters was repressed by the exogenous TLEs co-transfected in these assays and the behaviour of the different TLE point mutants with respect to each other was always the same.

While all TLE point mutations repressed transcription of this Wnt reporter, the behaviour of these mutations relative to each other was similar and observed in all contexts (presence or absence of β catenin and TCF). This made the interpretation of differences between individual mutations repression ability difficult. To circumvent this I employed a strong TOPflash activator, a fusion of TCF3 directly to a strong transcriptional activation domain, TCF3 Δ β catBD VP2 (Fig 3.3.2d). This fusion protein contains TCF3, but with the β catenin binding domain deleted and replaced with two copies of the VP16 transactivator (Zamparini et al. 2006). Cotransfection of plasmids



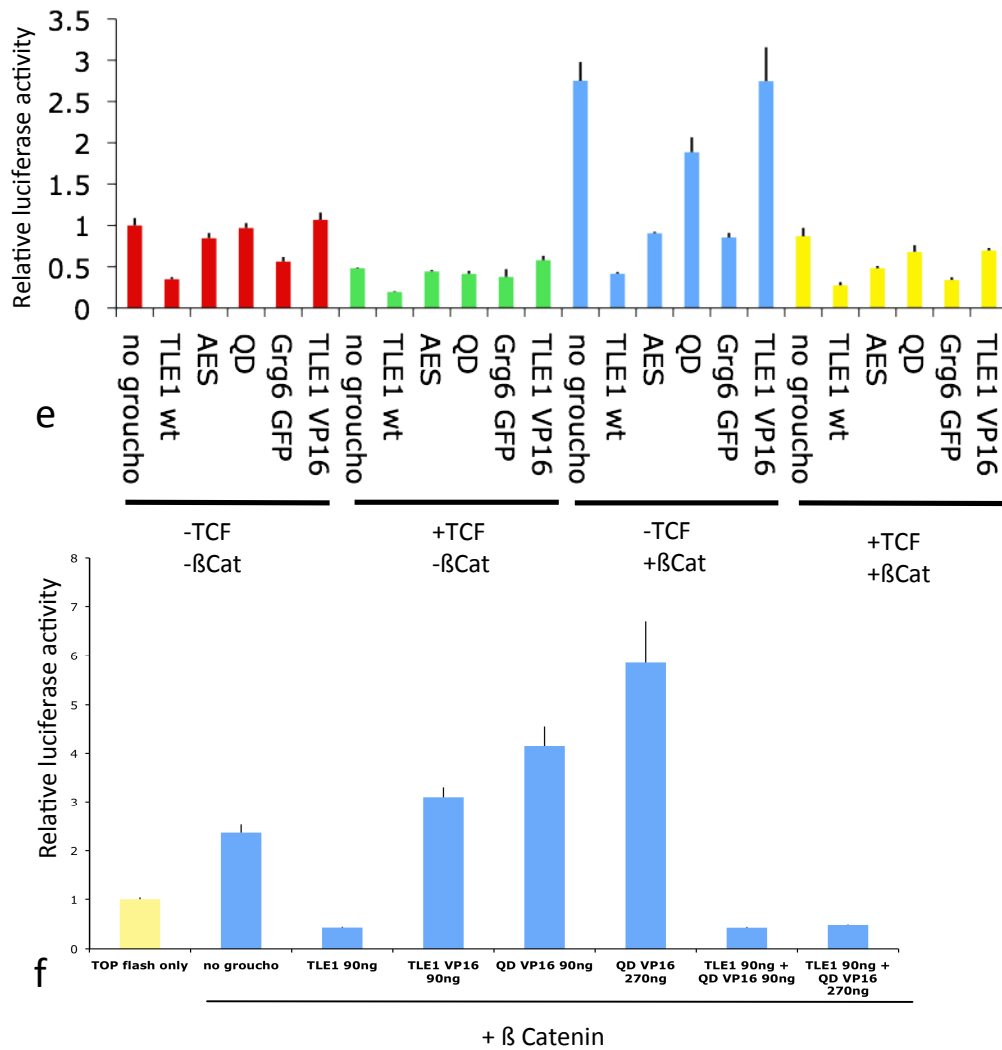


Fig 3.3.2 Analysis of TLE variants and point mutations for *wnt* modulating activity

The effect of a panel of TLE point mutations and other variants on *wnt* signaling activity in cells was investigated using the TOPflash luciferase reporter system. HEK293 cells were transfected with the TOPflash plasmid and constructs expressing these TLE proteins in biological triplicate. All expression vectors used the CMV promoter. Luciferase activity was measured on cell lysates after 24hrs using a luminometer. **(a)** Schematic of the TOPflash luciferase reporter construct used. **(b)** Western blot showing the expression of the FLAG-tagged proteins in HE293 cells. **(c)** Cells were transfected with vectors expressing the following hTLE1 proteins: wtTLE1, TLE1 S239A/S253A, TLE1 S239E/S253E, V488S, C488R, R534A, E550K and L743F. The experiment was performed with different combinations of cotransfected *xTfc3* and β catenin. **(d)** A TOPflash experiment was performed on the TLE1 point mutations, cotransfected with TCF3 Δ β catBD VP2 which greatly increases reporter activity. **(e)** The first experiment was repeated with TLE1wt and other groucho variants; AES, Grg6GFP, TLE1-VPI6 and QD. **(f)** QD-VPI6 was tested in the same assay in comparison with TLE1-VPI6 and in competition with wild type TLE1

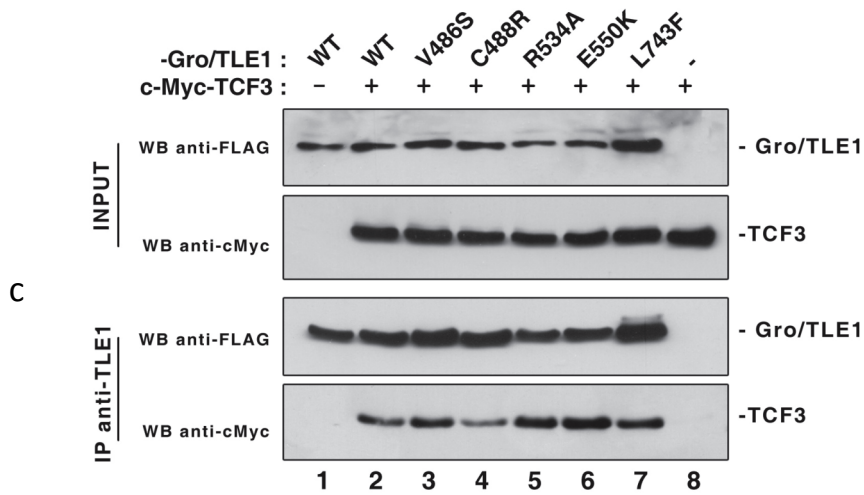
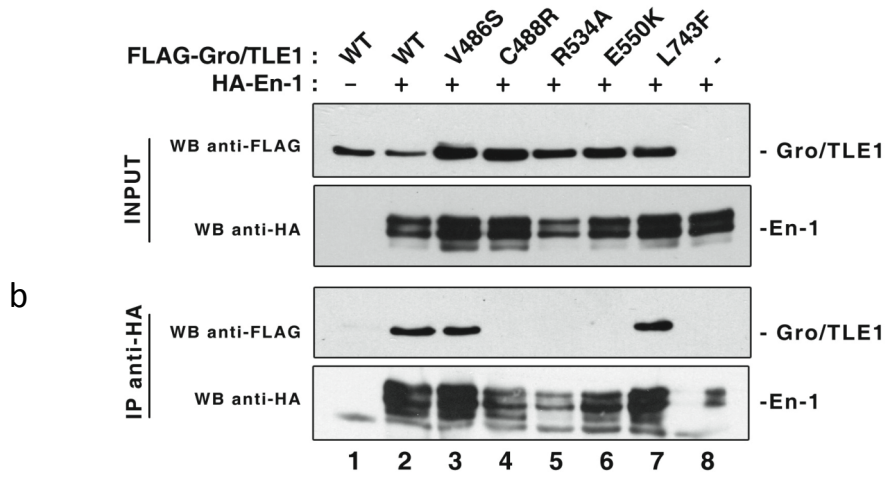
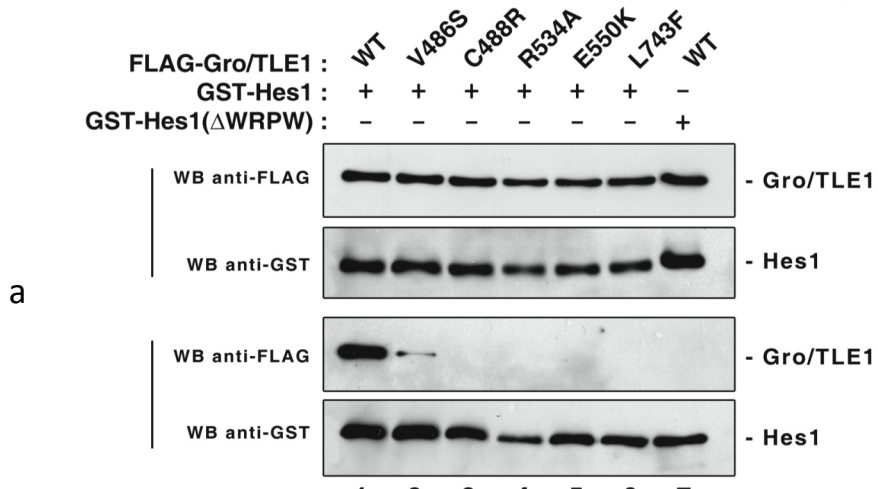
expressing this protein alongside the TOPflash reporter gene resulted in a ~50-fold stimulation in luciferase activity. In this context, wild type TLE1 has little repression activity and most of the point mutations have even less effect on TCF3 $\Delta\beta$ catBD VP2 activity. And while S239E/S253E had a similar activity to wild type TLE1, TLE1 R534A could repress the activity of TCF3 $\Delta\beta$ catBD VP2 some 4-fold. Thus TLE1 R534A appeared particularly effective at suppressing Wnt induced transcription.

The other TLE variants were also tested for their ability to modulate TOPflash activation (Fig 3.3.2e). None of the proteins displayed in this figure were able to activate TOPflash, indicating that they were unable to function as dominant negatives. Thus while the TLE1 VP16 transactivator fusion is unable to repress TCF activity, it appeared unable to activate TCF activity either, suggesting that VP16 was unable to function in the presence of the endogenous TLE repression domain. In an attempt to circumvent this, a QD VP16 fusion was also constructed which lacked the full length TLE repression domain. This was constructed by cloning the QD sequence into pTLE1 VP16 in place of the TLE1 sequence as a single ORF. QD VP16 behaved as a stronger transactivator than TLE1 VP16, but was still unable to compete with TLE1 (Fig 3.3.2f).

3.3.3 Altered cofactor binding activities of TLE1 point mutations

The ability of TLE1 point mutations to bind to common TLE interaction motifs was also studied. Biochemistry for this was performed by our collaborators, Stefano Stifani's lab (Buscarlet et al. 2008, see appendix). Immunoprecipitations for the FLAG tagged point mutations were performed with tagged versions of HES1, ENGRAILED1 (EN1) and TCF3. These proteins all typify classes of TLE interactions: HES1 with a WRPW interaction motif, En-1 containing the engrailed homology motif, and TCF3. We found that all these mutations, except TLE1 V486S, impaired the interaction of TLE1 with Hes1 and the WRPW motif (Fig 3.3.3a). Interestingly, while unable to bind WRPW, TLE1 V486S and TLE1 L743F, are able to bind both En-1 and TCF (Fig 3.3.3b, c), suggesting that these mutations are specifically defective in their interactions with Hes proteins. Moreover, TLE1 C488R, TLE1 R534A and TLE1 E550K bound only Tcf3 and not Hes or En proteins (Fig 3.3.3c). This is not surprising as Tcf proteins

(Buscarlet et al, 2008)



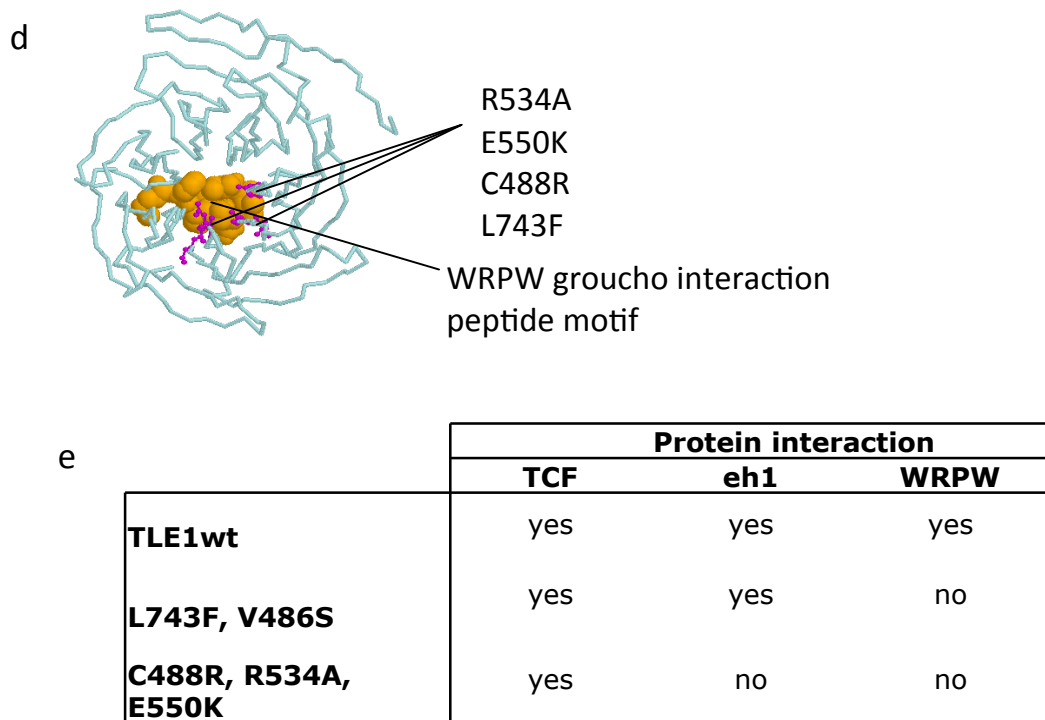


Fig 3.3.3 Interaction of different TLE1 point mutations with hes1, engrailed1 and TCF3

(Panels a, b and c and legends taken from Buscarlet et al, 2008)

(a) HEK293 cells were co-transfected with plasmids encoding FLAG epitope-tagged WT or mutated Gro/TLE1 and either a fusion protein of GST and full-length Hes1 (*lanes 1-6*) or truncated Hes1 lacking the WRPW motif required for Gro/TLE binding (Δ WRPW) (*lane 7*). Each cell lysate (*INPUT*) was incubated with glutathione-Sepharose beads and the precipitated material (*PD*, pull-down), together with 1:10 of each input lysate, was subjected to Western blotting (*WB*) analysis with anti-FLAG or anti-GST antibodies. *B* and *C*, HEK293 cells were co-transfected with plasmids encoding FLAG epitope-tagged wild-type or mutated Gro/TLE1 proteins, as indicated, and either HA epitope-tagged En1 **(b)** or Myc epitope-tagged *Xenopus*-Tcf3 **(c)**. Each cell lysate (*INPUT*) was subjected to immunoprecipitation (*IP*) with either anti-HA (*B*) or anti-Gro/TLE1 (*C*) antibodies. Immunoprecipitates, together with 1:10 of each input lysate, were analyzed by Western blotting with the indicated antibodies.

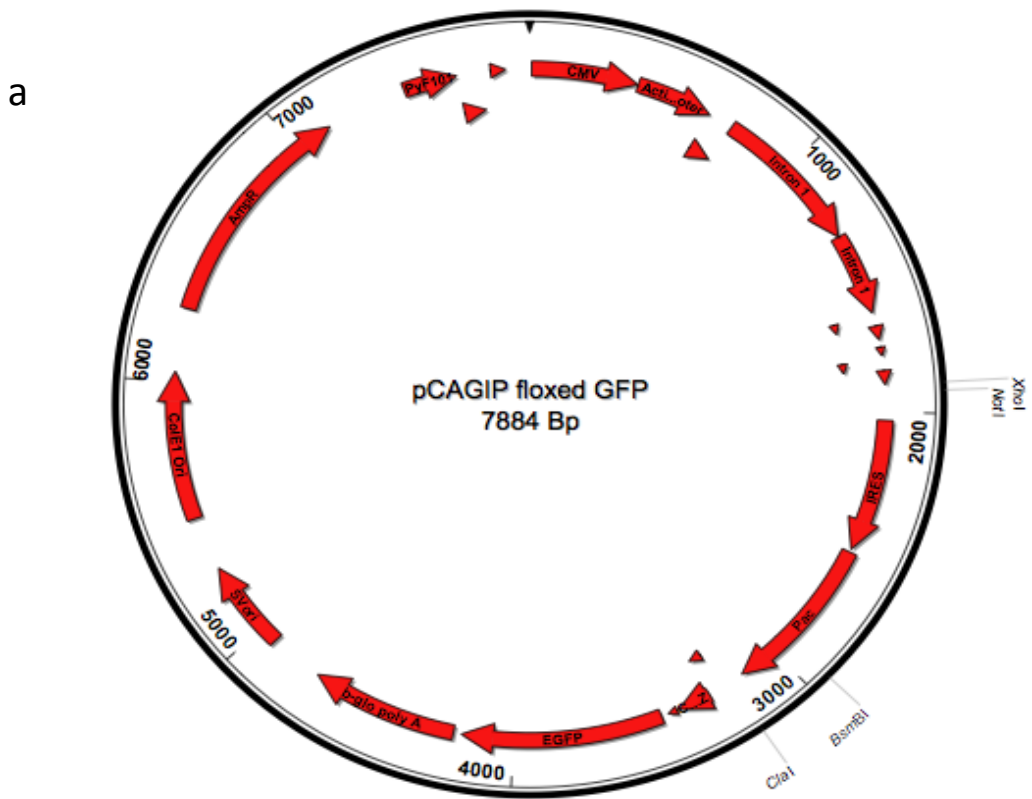
(d) Structure of the WRPW domain of human TLE1 interacting with a WRPW peptide. The residues mutated in the point mutants used in this study are highlighted. The structure was determined by Pickles et al (2002) and deposited in the Protein Database under 2CE9 (<http://www.ebi.ac.uk/pdbe/>). **(e)** The interactions exhibited by different point mutations are summarized here.

bind the N terminus of TLEs. The lack of interaction of R534A with either eh1 or WRPW could also explain why this C terminal mutation is particularly effective at suppressing Tcf mediated transcription. Transfected TLE1 R534A would not be titrated by endogenous WRPW or En homology domain containing proteins and the effective concentration free to bind TCF would therefore be higher. Analysis of the crystal structure of the TLE1 WD40 domain bound to peptide motifs has shown that all these residues mutated are situated in the central binding pore (Fig3.3.3d). However mutating R534 was predicted to have a more serious structural effect than L743 for example, consistent with the biochemistry (Jennings et al. 2006). The different interactions exhibited by each mutation are summarized (Fig 3.3.3e).

3.4 Generation of TLE1 overexpression constructs

From the immunoprecipitations and from the previous luciferase assays, two of the most interesting TLE1 point mutations were chosen for further study in overexpression experiments alongside the wild type protein. TLE1 R534A was chosen for its loss of function of Eh1 and WRPW motif interactions and its increased ability to antagonise wnt signalling. L743F was chosen for its specific loss of WRPW binding.

As ES cells in culture might be expected to adapt to the presence of high levels of a global co-repressor like TLE, I thought it important to be able to rescue phenotypes by removing TLE. A strategy that allowed the rescue of individual clonal lines also would control for non-TLE induced phenotypes as a result of clonal variation. To achieve this end I used a variation on the pCAGIPC vector. This contains the strong CAG promoter, which consists of a chicken β actin promoter, CMV enhancer, β actin intron and the β globin polyadenylation signal (Niwa et al. 1991). The specific vector engineered for this study allows for selection of cDNA expression by puromycin and monitoring of expression by a red fluorescent marker via a puromycin acetyl transferase (*Pac*)-mCHERRY fusion. The expressed cDNA can then be removed by recombination using Cre recombinase. Loss of the insert is monitored by GFP expression. It was modified from the pCAGIP flox GFP vector (Fig 3.4a). A *Pac*-mCHERRY fusion ORF was made using two step fusion PCR with a Cla1 site downstream of mCHERRY. This was TOPO



TCGAGTT**CGAA**GCTAGCAATT**GTCGACGAG**TTAATTA**ACCGGTGC**
CAAGCTTCGATCGTTAA**CAGCTGCTC** AATTAATT **TGGCCACGCCGG**

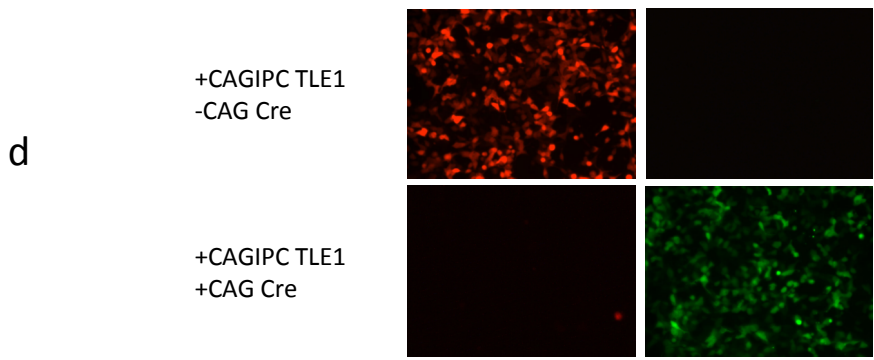
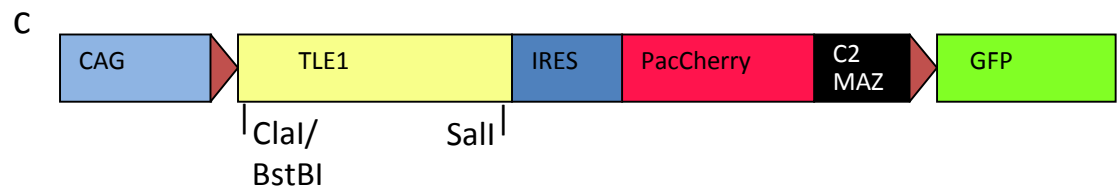
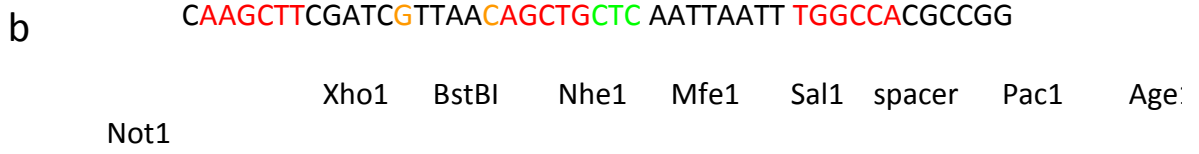


Fig 3.4 Overexpression strategy and construct design for TLEI and point mutations

(a) Map of the vector used as a basis (pCAGires-puro flox GFP) showing sites used for cloning. An in-frame fusion of mCHERRY and the puromycin-acetyl-transferase gene was synthesized by fusion PCR. This was cloned into the *Clal* and *BsmBI* sites. **(b)** A synthetic oligonucleotide linker containing restriction sites useful for cloning was inserted into the *XhoI-NotI* sites downstream of the CAG promoter. **(c)** Diagram of the finished construct containing TLEI. All TLEI inserts were cloned into the overexpression vector *BstBI* and *Sall* polylinker sites. **(d)** The constructs were tested for functionality by transient transfection into HEK293 cells alone or with a CAG-Cre expression construct. The expression of PacCherry and GFP after vector recombination was verified by fluorescence microscopy after 48h.

cloned and sequenced to check for any errors introduced during PCR. The C terminal portion of this was digested out and cloned into pCAGIP flox GFP in frame with the existing *Pac* ORF using the *BsmBI* site in *Pac* and *ClaI*. To facilitate the insertion of different TLE variants into this vector, a synthetic oligonucleotide polylinker containing useful restriction sites was cloned into the *XhoI* and *NotI* sites downstream of the CAG promoter (Fig 3.4b). TLE1wt, TLE1 R534A and TLE1 L743F were all introduced into this vector as depicted (Fig 3.4c).

The constructs tested for functionality by transient transfection into HEK293 cells. The PacCHERRY fusion protein was expressed and functional based on the red fluorescence observed in the cells. When Cre is co-expressed in these cells, the CHERRY fluorescence disappeared and was replaced by GFP (Fig 3.4d).

3.5 Generation and initial characterisation of TLE overexpressing ES cell lines

Once the expression constructs had been verified, they were introduced into ES cells. The constructs were linearized by digestion with *FspI* and purified DNA was electroporated into E14tg2a ES cells. They were subjected to selection in 2µg/ml puromycin for 10 days and surviving colonies were picked and expanded. It was hoped to use mCHERRY fluorescence as a reporter of TLE expression levels in different clones. However despite the fact the cells were able to survive relatively high concentrations of puromycin, demonstrating the expression of the PacCHERRY fusion, no visible fluorescence could be observed by microscopy. This could be due to differences in the levels of protein required to generate visible fluorescence as opposed to enzymatic inactivation of an antibiotic. Differences between the levels of expression required for antibiotic resistance and visible reporter activity in fusion proteins have previously been described (Tsakiridis et al. 2007). Verification of overexpression levels was therefore performed by quantitative PCR (Fig 3.5a). cDNA from selected clones was analysed using primers amplifying total TLE1 (endogenous mouse and overexpressed human). Levels were compared between two independent clones for each vector. In all cases TLE1 transcript levels were raised significantly above the endogenous levels in a control cell line with a stably integrated empty CAGIPC vector.

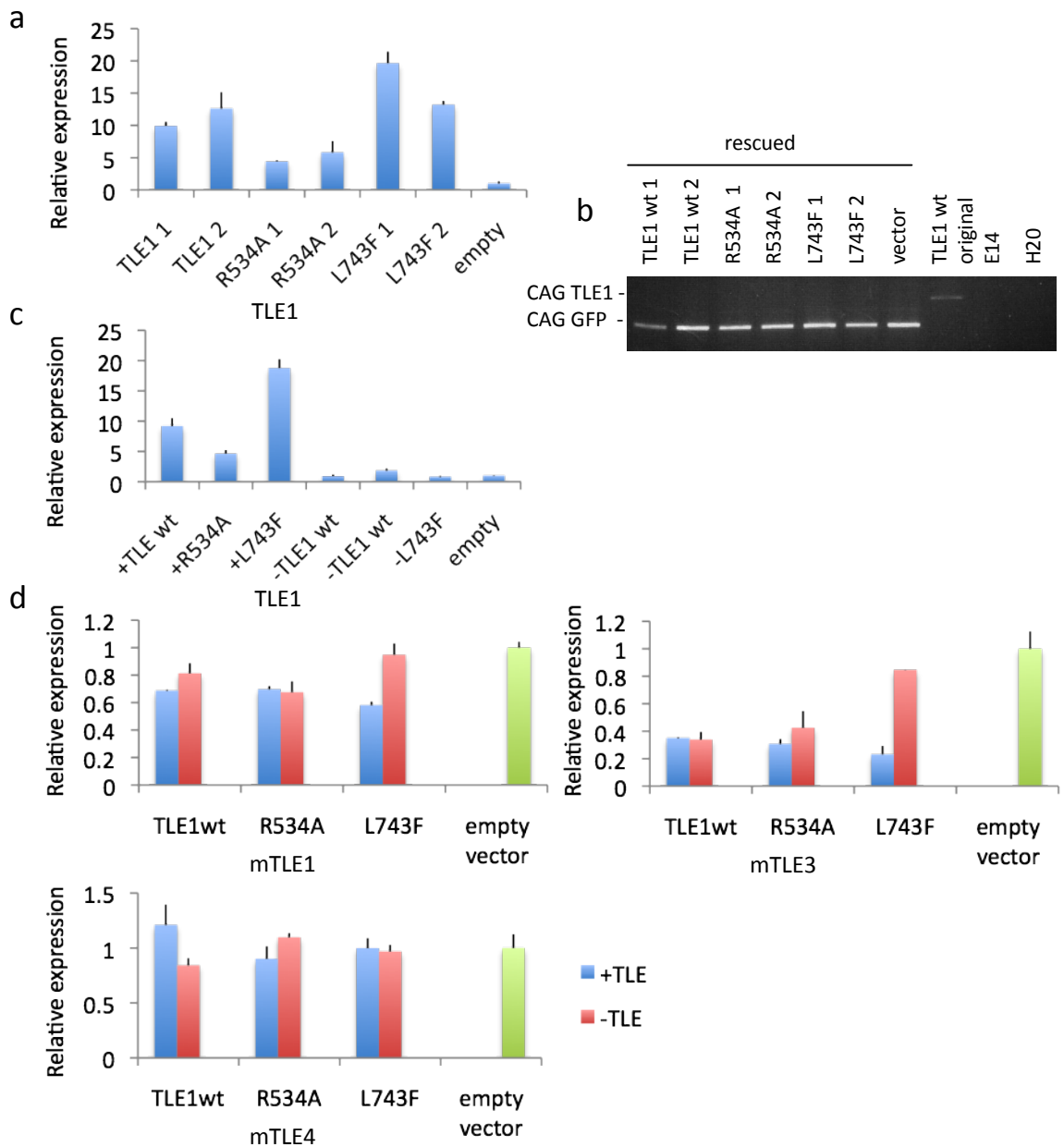


Fig 3.5 TLE expression levels in ES cell lines stably expressing CAG TLEI

(a) Transfected ES cell clones resistant to puromycin were subjected to RNA extraction and cDNA synthesis. Levels of total TLEI expression in the samples were analysed by real time qPCR. The data is plotted as fold increase over the vector alone control cells. Lines expressing the highest amounts of TLEI (TLE1 wt 2, R534A 2 and L743F 1) were chosen for further study. **(b)** The TLEI cassette was removed from these lines to generate -TLEI subclones. Vector recombination was confirmed by genomic PCR using a forward primer in the promoter and reverse primers in TLEI and GFP. **(c)** qPCR was performed as before to confirm the loss of TLE overexpression in these subclones. **(d)** Expression levels of endogenous TLEs was also analysed by qPCR in these lines. Mouse specific TLE1, TLE3 and TLE4 primers were used. Transcript levels are relative to TBP and plotted as fold change from empty vector levels

However, levels of TLE1 R534A were noticeably lower than TLE1wt or the other mutant. It is possible the stronger effects of this mutation described earlier cause ill effects in cells with high expression leading to negative selection. The strongest expressing clones were selected for further study (TLE1 2, TLE1 R534A 2 and TLE1 L743F 1).

To demonstrate that any phenotypic effects observed in the cells were not from mutation caused by insertion into endogenous genes or clonal variation, it was important to generate subclones with the TLE1 cassette removed. Overexpression lines were electroporated with an unlinearized CAG Cre recombinase vector and plated at colonial density to allow the growth of subclones with recombined expression vector. Colonies were picked and GFP positive subclones were expanded. GFP positive subclones selected for use were also replica plated in puromycin and were unable to survive demonstrating a loss of the floxed cassette. This was confirmed by PCR analysis of genomic DNA of the subclones (Fig 3.5b). Primers amplifying the region from the CAG promoter to GFP gave the expected band in recombined subclones. The band generated by amplification of CAG TLE1 was not observed. Loss of TLE1 mRNA overexpression was also demonstrated by quantitative rtPCR (Fig 3.5c). Levels of TLE1 transcript in recombined subclones have returned to the same as those in empty vector control cells.

As there is considerable redundancy in the TLE family, I thought it important to assess the overall levels of TLE in response to TLE1 over expression. Quantitative PCR was performed using primers specific for mouse TLE1, TLE3 and TLE4 (Fig 3.5d). Endogenous TLE1 levels may be slightly decreased while TLE4 is not significantly affected. TLE3 appears downregulated in all overexpression lines compared to the empty vector control. However TLE3 levels also remain low in the recombined subclones of both TLE1wt and R534A. It is unclear whether this is due to a permanent downregulation of TLE in these cells or just due to natural variations in expression between clones. However, the high levels of overexpressed TLE1 mutations mean that these proteins are likely to contribute most to overall TLE activity in the cells.

To check for CHERRY fluorescence by a more sensitive method and to examine on a population level the efficiency of over expression, I analyzed expression of mCHERRY

and GFP by flow cytometry (Fig 3.5.2). The TLE overexpression cell lines, those with the empty vector, and those transfected with Cre were analyzed alongside E14 control by flow cytometry. Cells were also grown for analysis in $2\mu\text{g/ml}$ puromycin in case selection for the PacCHERRY fusion increased fluorescence. Data is presented as dot plots with CHERRY (horizontal) and GFP (vertical) axes. Unfortunately, I was only able to detect a slight shift towards higher red fluorescence as a result of PacCHERRY expression. The highest percentage of cells lying within the mCHERRY+ gate is from the L743F line (10.2%). This is in agreement with this line having the highest level of TLE1 expression according to the previous rtPCR. In recombined lines (bottom three plots, right) GFP is expressed in all cells in agreement with their visible green fluorescence indicating that the excision of the TLE1 expression cassette was effective.

3.6 Derivation of TLE4 mutant ES cells

The generation of ES cells with increased TLE activity and the use of point mutations with defined interaction deficiencies provided a powerful and highly useful method of investigating TLE function in this context. However to investigate the role of TLEs in ES cell self-renewal and differentiation in more detail, we also decided to generate TLE mutant ES cells as a loss of function model. TLE3 and TLE4 were chosen for mutation as the primary members of the family in ES cells. We took advantage of the pre-existing TLE4 gene trap mouse line discussed in 3.2 for TLE4 null ES cells as the basis for this. To save time and unnecessary or potentially disruptive manipulations of wild type ES cells, we derived TLE4^{+/-} and TLE4^{-/-} ES cells from blastocyst stage embryos from crosses between TLE4^{+LacZ} mice. These were genotyped to identify heterozygous and homozygous null lines for TLE4 (Fig 3.6a). They were also karyotyped and found to be normal (data not shown). There was no apparent morphological difference between these cells and E14 ES cells in normal culture. To further investigate TLE4 expression in ES cells, TLE4^{+LacZ} cells in normal culture were stained for β galactosidase activity. Interestingly, the expression was heterogeneous, possibly reflecting levels of partial differentiation that are seen in ESC culture (Fig 3.6b).

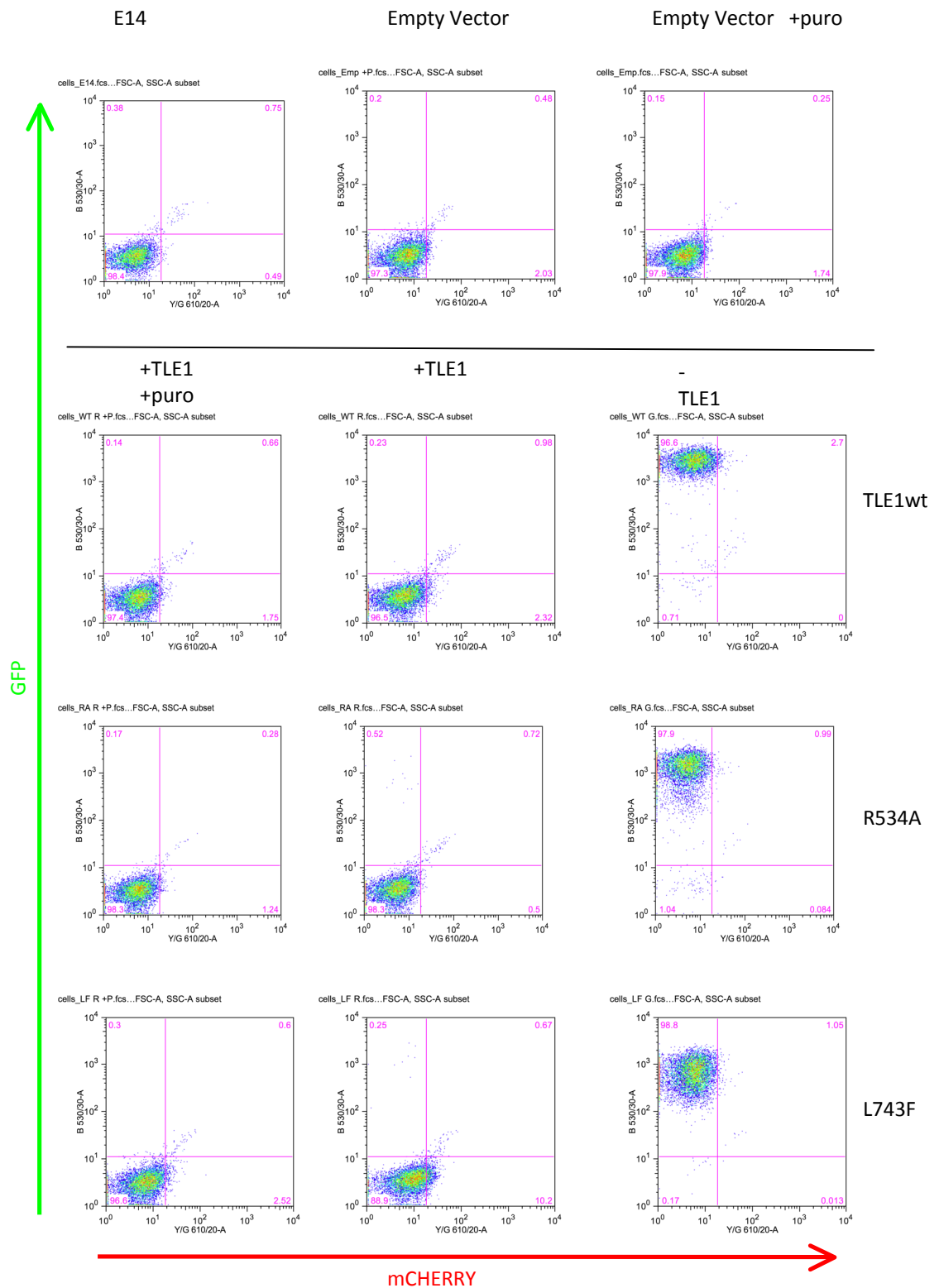


Fig 3.5.2 FACS analysis of mCHERRY and GFP expression in TLE1 overexpressing and recombined subclones. Cells were also grown for analysis in the presence of puromycin to ensure expression of the PuroCherry fusion and check whether selection could increase mCHERRY fluorescence.

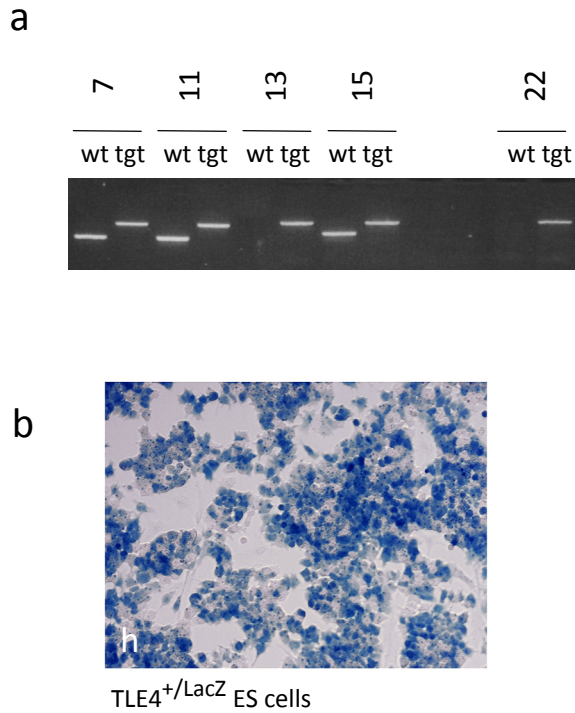


Fig 3.6 Derivation of TLE4 heterozygous and homozygous mutant ES cells

(a) PCR Genotyping of ES cell clones derived from TLE4⁺/LacZ intercross blastocysts. 500bp band indicates wild type alleles, 900bp band indicates targeted alleles. **(b)** β galactosidase staining of TLE4⁺/LacZ ES cells derived from this mouse line.

3.7 Construction of the TLE3 targeting vector

A targeting construct for TLE3 was generated and is depicted in Fig 3.7. The vector is promoterless and takes advantage of increased targeting efficiency that result from the requirement for an endogenous genes expression. The construct was targeted into the fourth intron in a gene containing 20 exons. Only the first section of the TLE3 Q domain was left which was predicted to be an effective null mutation. Targeting arms used were from pTTO TLE3 (Friedel et al. 2005).

The construct used an Engrailed2 splice acceptor to drive expression and an excisable HygroTK cassette that allowed both positive and negative selection. To avoid translating a fusion of TLE3 and HygroTK, a t2a peptide coding sequence was included before the ATG codon of HygroTK and in frame with the ORF of the spliced TLE3 transcript. This is a short peptide sequence (t2A, Gly-Asp-Val-Glu-Glu-Glu-Asn-Pro-Gly;2B-Pro) from the TaV virus (Szymczak et al. 2004) that causes the ribosome to skip between the glycine and proline without forming a peptide bond, thus generating two intact but separate polypeptides. After the selection cassette is removed, the mORANGE fluorescent marker will be expressed from the TLE3 locus, again using t2a to separate the protein. To reduce the chance of downstream exons of TLE3 splicing onto exon 4 without the gene trap, a C2MAZ sequence was added after the polyA of mORANGE. This sequence contains a binding site for the MAZ DNA binding protein. MAZ bends DNA which causes a severe obstacle to RNA PolII and efficiently terminates transcription (Ashfield et al. 1994). A version of the vector was also constructed which replaced HygroTK with a *Pac*-TK fusion and mORANGE with mCHERRY (Fig 3.7j). This was given TLE4 targeting arms and was designed for use in an alternative targeting strategy to target one allele each of TLE3 and TLE4 at the same time in wild type ES cells. This involved using Hygromycin and Puromycin selection in conjunction and would allow monitoring of TLE3 and TLE4 expression using the different fluorescent markers. However the double selection method proved problematic and when the TLE4^{+/*LacZ*} mice became available, I decided to use homozygous null ES cells derived from them as a more efficient strategy.

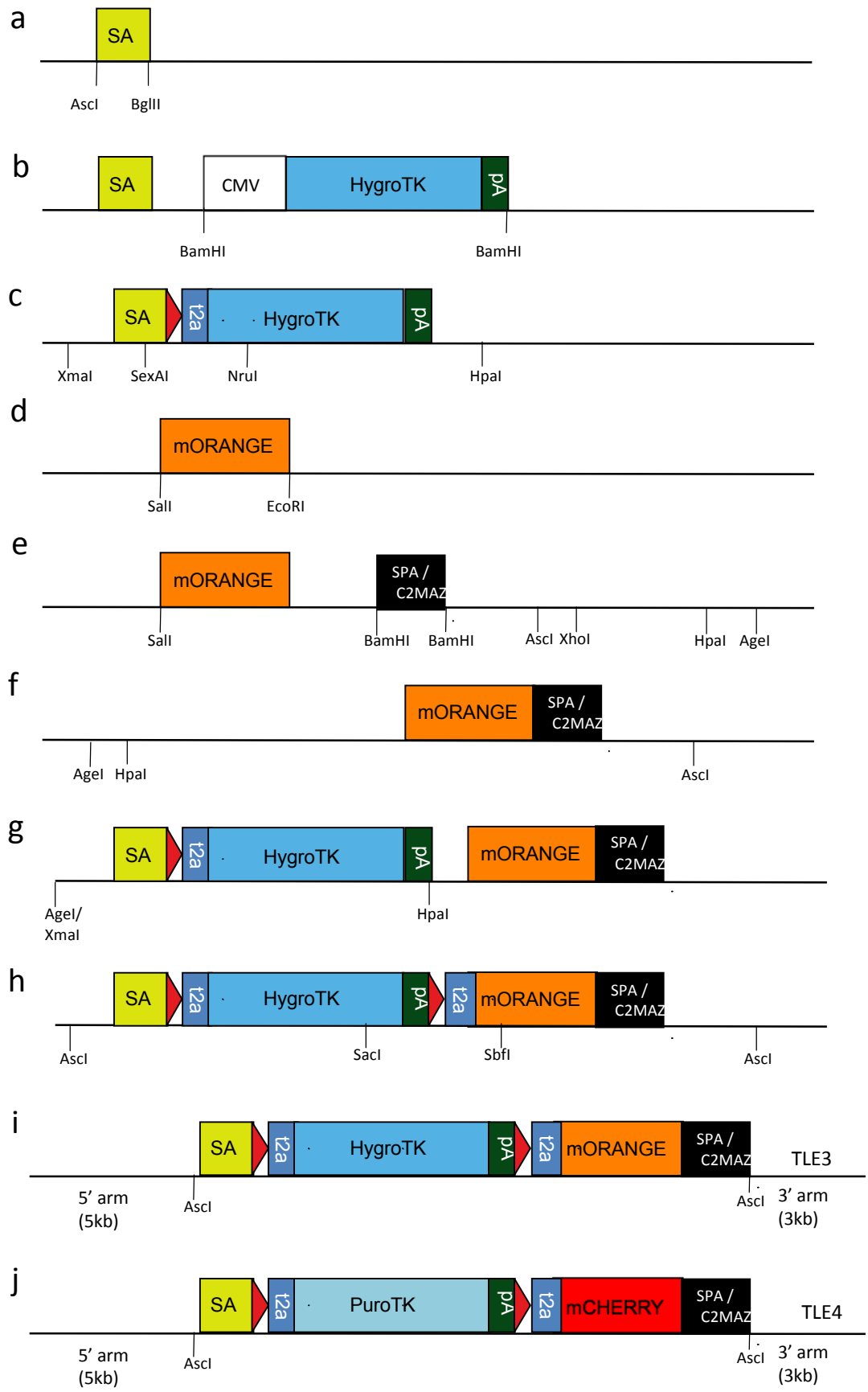


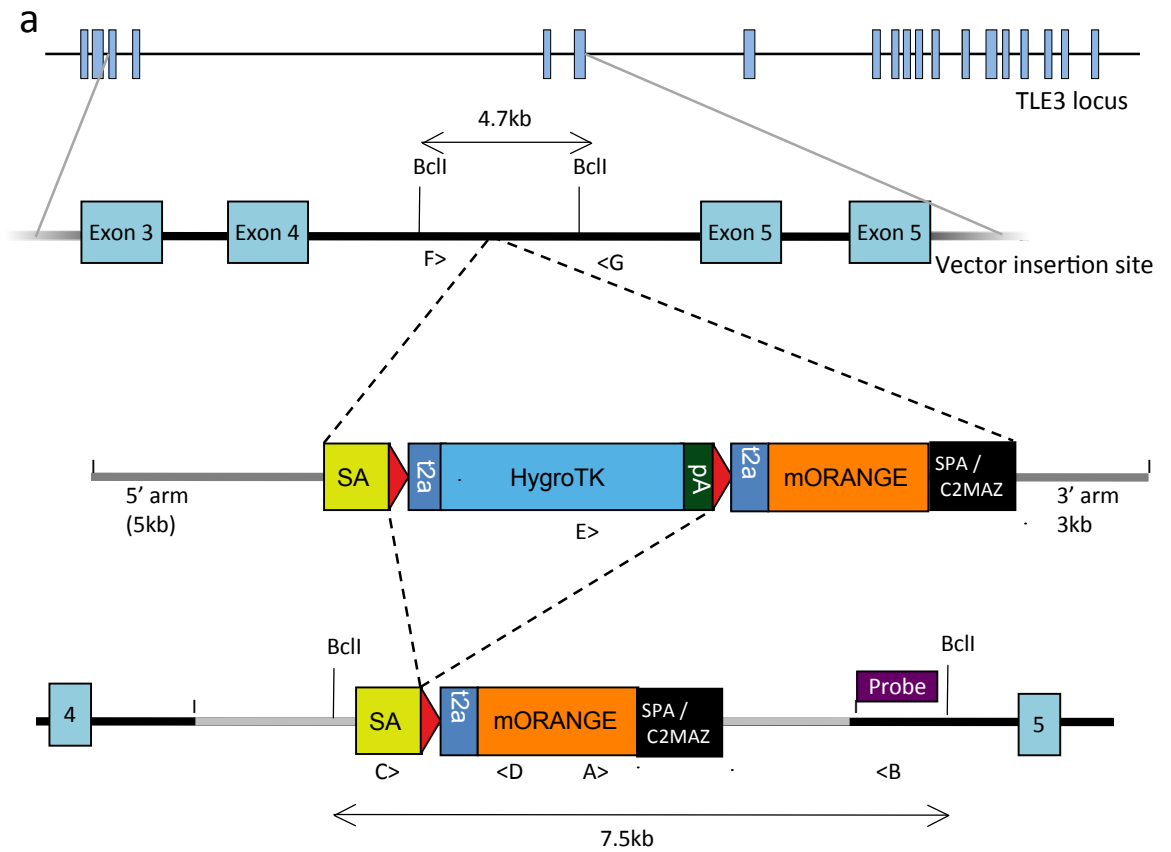
Fig 3.7 Cloning of the TLE3 targeting vector

(a) The En2 splice acceptor (SA) was digested and cloned into the pKO901 MCS vector using *Ascl* and *BglII*. **(b)** CMV HygroTK was cloned downstream of the SA into a *BamHI* site. **(c)** The SA and HTK were coupled by a sequence containing a *LoxP* site and *t2a* sequence. This was done by PCR amplifying the adjoining end sections of the SA and HTK using primers with overlapping extensions containing *t2a* and *LoxP*. These were then joined together using fusion PCR and TOPO cloned. An ORF was preserved between the SA exon and HTK. Part of this TOPO cloned component was cloned into the targeting construct using *SexAI* in the SA and *NruI* in HygroTK. **(d)** mORANGE was PCR amplified from the parental vector and cloned into pKO901 using *EcoRI* and *Sall*. **(e)** A fragment containing the C2MAZ sequence with synthetic-polyA was cloned in downstream of mORANGE. **(f)** The section of DNA containing mORANGE-C2MAZSPA was rotated in the vector using digestion with *XhoI* and *Sall* and religated after backbone dephosphorylation in the opposite orientation. This reoriented restriction sites to make the next step possible. **(g)** A fragment from pKO901 containing the SA-*LoxP*-selection cassette was digested using *HpaI* and *XmaI*. This was cloned into the *HpaI* and *AgeI* sites of the pKO901 backbone containing mORANGE-C2MAZSPA. **(h)** Sequences were amplified by PCR containing the ends of HygroTK-polyA and mORANGE using primers containing overlapping sequence with a *LoxP* site and *t2a* sequence. These were joined together using fusion PCR in a similar way to the first *t2a* fusion and TOPO cloned. Part of this was cloned into the targeting vector using *SacI* in TK and *SbfI* in mORANGE. **(i)** This construct was inserted into the *Ascl* site of the pTTO TLE3 targeted gene trap between the targeting arms to complete the new targeting vector. **(j)** A version of the vector was also constructed in a similar way for targeting TLE4. Briefly, mCHERRY was PCR amplified and inserted in the same way as mORANGE. PuroTK from pCMV PTK was inserted into pCMV HTK using *NdeI* and *NruI* site and this was cloned into the targeting vector as in step (b). In step (i), the finished construct was inserted into the *Ascl* site of pTTO TLE4 between the targeting arms to complete the TLE4 targeting vector.

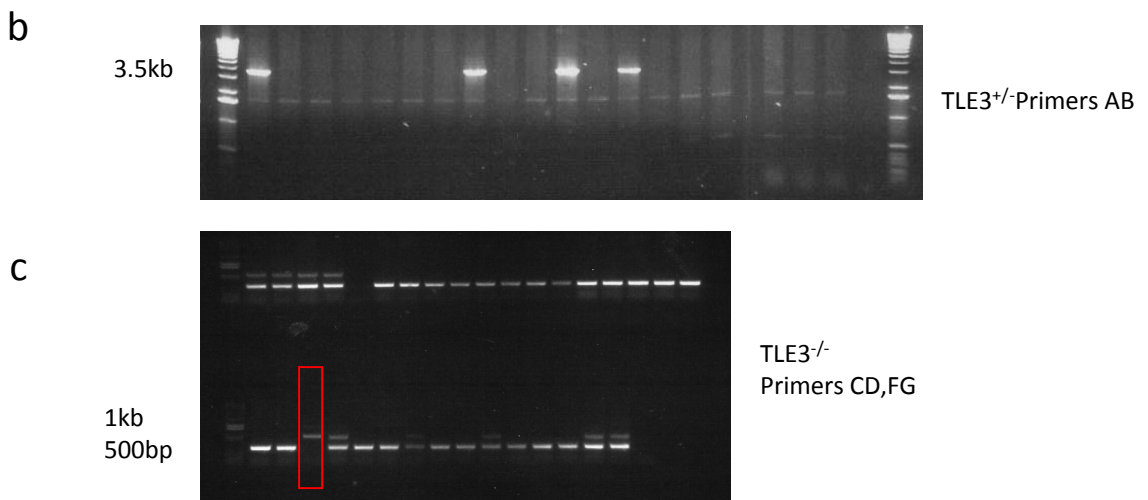
3.8.1 Generation of TLE3/TLE4 mutant ES cells

TLE3 was then targeted in TLE4^{-/-} cells to generate TLE3/TLE4 null ES cells. The targeting strategy is shown in schematic (Fig 3.8.1a). Targeting vector was linearized and electroporated into cells. These were incubated with selection in 150 μ g/ml hygromycin for 10 days. Surviving clones were picked and expanded and PCR genotyped. Fig 3.8.1b shows PCR in which genomic DNA was amplified using a forward primer in mORANGE and an external reverse primer in TLE3 exon 4, just 3' of the vector 3' targeting arm (primers AB). The expected band of ~3.5kb indicating a correctly targeted insertion was observed in 4/19 clones examined. This represents a targeting frequency of 21% and is lower than the published expected targeting frequency of 66% but still acceptable. The selection cassette was then removed from these clones by electroporating with a CAG Cre expression vector and selection in 10mM gancyclovir for 10 days. Surviving clones were then picked and expanded. Replica plated clones died in 150 μ g/ml hygromycin confirming a pure population of cells without the selection cassette. Vector recombination was also confirmed by genomic PCR using primers flanking the LoxP sites (primers CD).

A recombined subclone was expanded and electroporated once more with the TLE3 targeting vector. Selection in hygromycin and picking of colonies was performed as before. Genotyping of surviving clones was again performed by long range genomic PCR using a 3' external reverse primer and a forward primer in HygroTK that should only amplify in clones with new a new vector insertion in the correct place (primers BE). However, this time the expected 5kb band representing targeting was seen in 18/20 clones (data not shown). This was unexpected as the previous targeting frequency was only 21%. Further diagnostic PCR tests were performed on retargeted clones to confirm this. In all clones tested a 500bp band representing the untargeted TLE3 vector insertion site (primers FG) was seen. However a further test using primers flanking the LoxP sites in the vector (primers CD) revealed the recombined vector from the first targeting was missing in all 18 clones with the apparent retargeting. It was therefore concluded that the vector was able to retarget the 1^o targeted allele with extremely high frequency due



Primers	
AB	3.5kb=targeted, no band=untargeted
CD	1kb=targeting vector without selection cassette (1° targeting event unaffected) No band=1° targeted locus retargeted
FG	500bp=wild type TLE3 allele No band=both alleles targeted



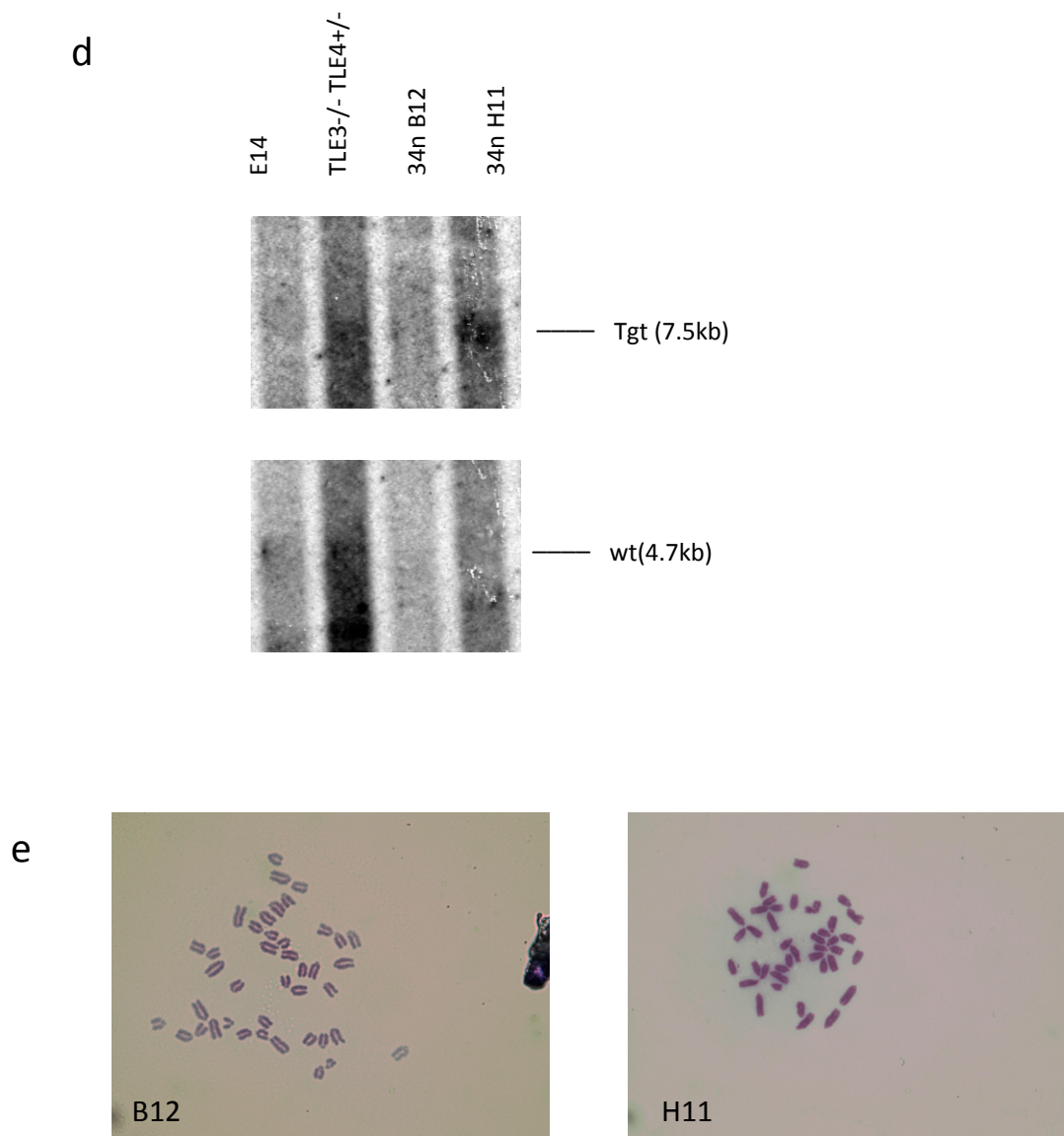


Fig 3.8.1 Targeting of the TLE3 loci in the TLE4^{lacZ/LacZ} cells

Schematic of the targeting strategy used to trap both loci of TLE3 in TLE4 null ES cells. **(a)** The targeting vector was directed into the middle of intron 4-5 of the TLE3 locus in TLE4^{lacZ/LacZ} ES cells. Following selection by hygromycin and confirmation of correctly targeted clones, the selection cassette was removed by Cre transfection and selection with gancyclovir. The second locus of TLE3 was targeted in these cells using the same method. Genomic PCR was used to initially screen resistant clones for the primary **(b)** and secondary **(c)** targeting stages. Primers indicated in the schematic are explained in the table. **(d)** Southern hybridization using a probe 3' of the TLE3 targeting arms (indicated in (a)). DNA was digested with BclI which cuts a 4.7kb fragment from the wild type locus and a 7.5kb fragment with the vector inserted. **(e)** Karyotypes of TLE3/TLE4 null clones B12 and H11

to greater sequence homology. To circumvent this problem the electroporation was repeated and a higher number of clones were picked for screening. A rapid PCR genotyping strategy was once again used to look for double targeting events (Fig 3.8.1c). 128 clones were screened in total. All but two produced a band representing untargeted TLE3 (primers FG) and lacked a band representing the first targeted allele (indicated by red box). These two potential TLE3/TLE4 nulls, H11 and B12 were expanded for further analysis.

Southern hybridisation was used to confirm the correct genotype of the mutant lines. This used a 0.8kb external probe, just 3' of the targeting arm homology that hybridised with a 7.5kb fragment from *BclI* digestion of genomic DNA from a targeted allele. This compared to a 4.5kb fragment from digestion of the wild type locus (restriction and probe sites indicated in Fig 3.7a). The expected bands were observed in each sample including loss of the wild type band in 34n cells, further confirming the targeting of both alleles (Fig 3.8d). They were also checked for karyotypic integrity. While H11 had the expected chromosomal spread, B12 had abnormalities in the chromosomal numbers and had to be discarded (fig 3.8.1e). This TLE3/TLE4 null cell line is hence referred to as 34n.

3.8.2 Generation of TLE1 rescued TLE3/TLE4 null cells

To confirm any observed phenotype in the mutant cells was specific to loss of TLE activity, it would be useful to have a subclone of the 34n cells with TLE added back to rescue them. For this purpose, 34n cells were electroporated with the CAGIPC TLE1wt vector. Selection and expansion of clones was performed as before. Once again no mCHERRY fluorescence could be seen as a reporter for TLE1 expression. Transcript levels were therefore analysed by quantitative rtPCR (Fig 3.8.2). Amplification of cDNA with TLE1 primers showed increased TLE1 levels in all candidate clones compared to the parental line. However clone (5) was picked for further analysis because of its much higher expression levels.

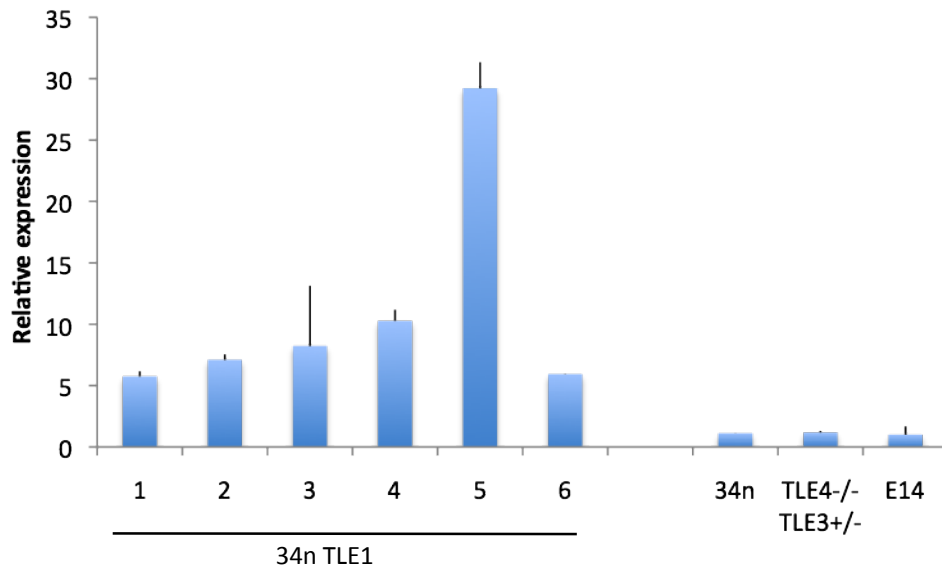


Fig 3.8.2 TLE1 expression in 34n TLE1 rescued lines

34n null cells were electroporated with CAG TLE1 and subjected to puromycin selection. Resultant clones were analysed by real time qPCR for TLE1 expression levels. Levels are shown relative to E14 and normalized to TBP for each sample. The highest expressing clone (5) was chosen for further study.

3.9 Altered TLE activity across a range of generated cell lines

A range of cell lines, both overexpressing and reduced in different TLE proteins, has been developed. Transcript levels of TLE1, TLE3 and TLE4 in the mutant cell lines were analysed by quantitative rtPCR. TLE levels in the overexpression lines are also included and are summarized here (Fig 3.9). CAGIPC TLE1 and point mutation lines and the 34n TLE rescued cells all had increased TLE1 levels. The mutant lines represent an allelic series of reducing TLE activity. There still appeared to be some residual TLE3 and TLE4 transcript in 34n cells though transcript is greatly reduced. The primers used for rtPCR are in exons downstream of the vector insertion site. It is possible that mRNA is being spliced around the vectors although the use of the C2MAZ sequence should prevent this for TLE3 at least. TLE1 loss of function would be also required for a true TLE null ES cell. However these significantly reduced levels of the most expressed TLE family proteins in 34n cells would be expected to produce a relevant phenotype. It is also interesting that TLE4 levels in TLE4^{+/-} cells are almost the same as wild type cells. TLE3 levels in TLE4^{-/-}/TLE3^{+/-} cells are also the same as those in TLE4^{-/-} only cells. This raises the possibility of feedback regulation of TLE3 and TLE4 where expression from one allele is raised in response to loss of the other.

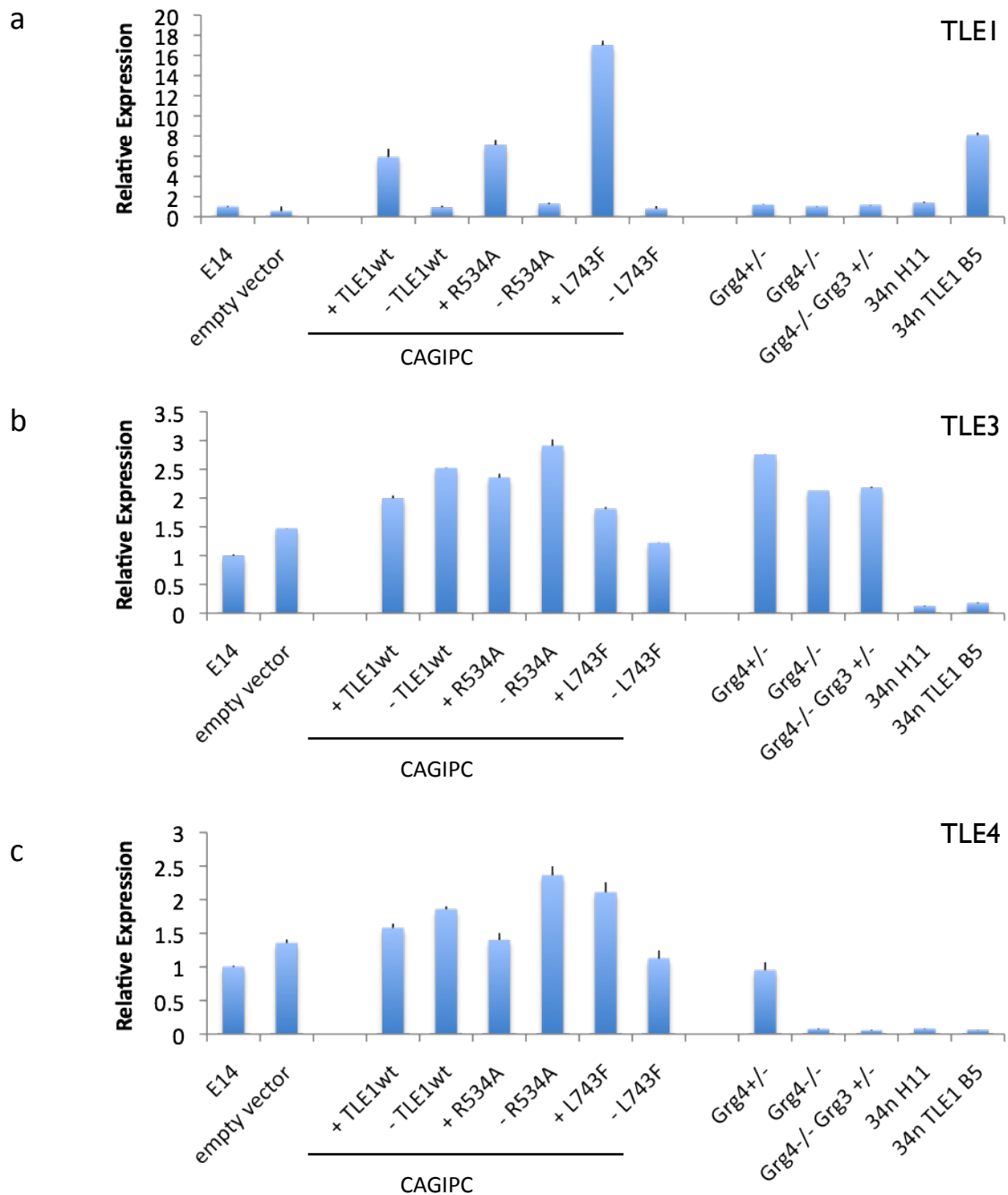


Fig 3.9 Expression of TLE genes in all experimental cell lines

The expression levels of TLE1, TLE3 and TLE4 was analysed in all cell lines generated for this thesis for comparison: overexpression lines CAG TLE1, CAG R534A, CAG L743F, and their recombined subclones, the allelic series of TLE3 and TLE4 mutants and the TLE1 rescued TLE3/4 null cells. cDNA was synthesized from all lines under normal maintenance and growth conditions. Real time qPCR was performed in technical triplicate on the samples for total TLE1 **(a)**, TLE3 **(b)** and TLE4 **(c)** Levels for each gene are shown relative to those for E14 cells. Note the different scale in **(a)** due to high TLE1 overexpressors; TLE1 copy numbers in E14 are actually ~50% of TLE4.

3.10 Discussion

In this chapter I have identified the key members of the TLE family in ES cells and early mouse embryonic development. I have also described the generation and initial characterisation of a range of molecular tools and cell lines that can be used to study the activity of this family of proteins. TLE3 and TLE4 are the highest expressed full length TLEs both in ES cells and early stage embryos as shown by EST data, gene trapping frequencies and quantitative PCR. Advantage was taken of a previously generated mouse line and ES cells derived from this to study the expression pattern of TLE4. In agreement with *in silico* data, TLE4 was expressed at latest from blastocyst stages through gastrulation and beyond. The expression pattern of the TLE4 reporter at mid gastrula was in agreement with previously published RNA *in situ* hybridisations. This data provides novel *in vivo* information about TLE4 expression patterns in pregastrulation mouse embryos. In addition, the TLE4 LacZ reporter was used to visualise the expression of this gene in ES cells. This confirmed its presence in these cells and showed heterogeneous expression, which is known in ESC cultures to often reflect different levels of undifferentiated and partially differentiated states. It would be interesting to combine this reporter with staining for a self-renewal marker such as *Nanog*, to see whether TLE expression coincides with a more or less ES like state.

From this data and because of our previous interest in TLE3 and TLE4 as Hex targets, we decided to mutate these genes to create a loss of function model. Mutation of more than one TLE was necessary, as single mutants do not have an early phenotype. TLE2 did not appear expressed in this context. Although TLE1 may provide some redundancy for loss of these, its absence in early embryos and reduced gene trapping frequency suggested it is not normally biologically relevant for regulation of pluripotency and early lineage specification. Also, the complete loss of 2 out of the 3 primary TLEs expressed in this context was expected to produce a strong phenotypic effect; this is confirmed in chapter 4. TLE4^{LacZ/LacZ} cells derived from TLE4^{+LacZ} mice were used as a basis to generate this model. Vectors were designed and engineered to target TLEs and terminate their expression plus provide a fluorescent reporter of normal expression. The TLE3 vector was successfully targeted to both *TLE3* alleles in ES cells. Including TLE4^{+LacZ} cells and intermediate targeted lines, this provides a complete allelic series

of TLE3 and TLE4 expression. Gradual loss of TLE expression along this series was confirmed. A further cell line was generated to allow partial rescue and confirmation of the specificity of any observed phenotype by TLE1 overexpression in the 34n cells.

To complement this loss of function model, I developed gain of function tools to overexpress a TLE1 and variants of this with defined losses of activity. We generated a range of TLE1 point mutations and TLE variants in collaboration with the Stefani lab and screened these for interaction with typical classes of sequence specific transcription factor and ability to modulate specific signalling pathways. Of particular interest were two of these TLE1 point mutations – R534A and L743F. TLE1 R534A did not interact with either of two classes of typical TLE cofactors. However it was able to bind TCF by a different site and strongly repress Wnt signalling induced transcription. This was possibly a consequence of its reduced ability to bind other factors and therefore increased effective concentration. TLE1 L743F showed a specific deficiency in binding the WRPW class of cofactor. The comparison of these two point mutations plus the wild type protein provided a useful tool to identify particular TLE interactions correlating with certain biological effects. TLE1wt, TLE1 R534A and TLE1 L743F were all transgenically expressed at relatively high levels in ES cells. The overexpression system used also provided a method of monitoring expression and an ability to later remove TLE1 to confirm specificity of any effect.

Both these strategies were used to investigate the roles of TLE proteins in ES cell pluripotency and early lineage specification, which will be discussed in the next chapter.

Chapter 4

The effects of altered TLE activity in ES cell self-renewal and lineage specification

4.1 TLE1 overexpression reduces the efficiency of self-renewal in ES cells

Upon establishing the TLE1 overexpressing cell lines I began to characterize their phenotypes in ES cells. The cells could be grown in normal ES cell culture conditions. They had no readily apparent growth defect when compared to either parental or rescued cell lines. However, overexpression lines do have a slightly different morphology in culture compared to those with just an empty vector (Fig 4.1a). Cells have a less rounded appearance, seem less adherent to each other and have more cytoplasmic projections. This morphology has also been observed in *Nanog* null ESCs (Chambers et al. 2007). Based on these observations, I tested whether TLE1 overexpressing cells have a deficiency in self-renewal.

To test the capacity of these cells to self-renew, I addressed the ability of single cells to form undifferentiated colonies at clonal density. Cells were plated at clonal density and grown for five or six days until colony morphology could readily be discerned. Plates were then fixed and stained for alkaline phosphatase (AP) activity. AP activity is present in undifferentiated ESCs and provides a rapid and easy way of identifying them. The plates were then examined under a microscope and colonies were counted and classed according to morphology and AP staining. Undifferentiated ES colonies have a tightly packed rounded appearance and stain strongly for AP. I also scored mixed and differentiated colonies based on the extent to which the colonies were composed of AP negative, morphologically differentiated cells (Fig 4.1b, insert). In this experiment, I found that cells overexpressing TLE1 had a higher percentage of differentiated and mixed colonies than empty vector control cells. When the TLE1 expression cassette is removed, percentages of undifferentiated cells increased (Fig 4.1b). The reduced self-renewal ability is similar for both wild type TLE1 and point mutations. This suggests that neither eh1 nor WRPW motif containing proteins are required for TLE1 to induce this phenotype and suggests that it may be in part triggered through the TLE1-TCF interaction.

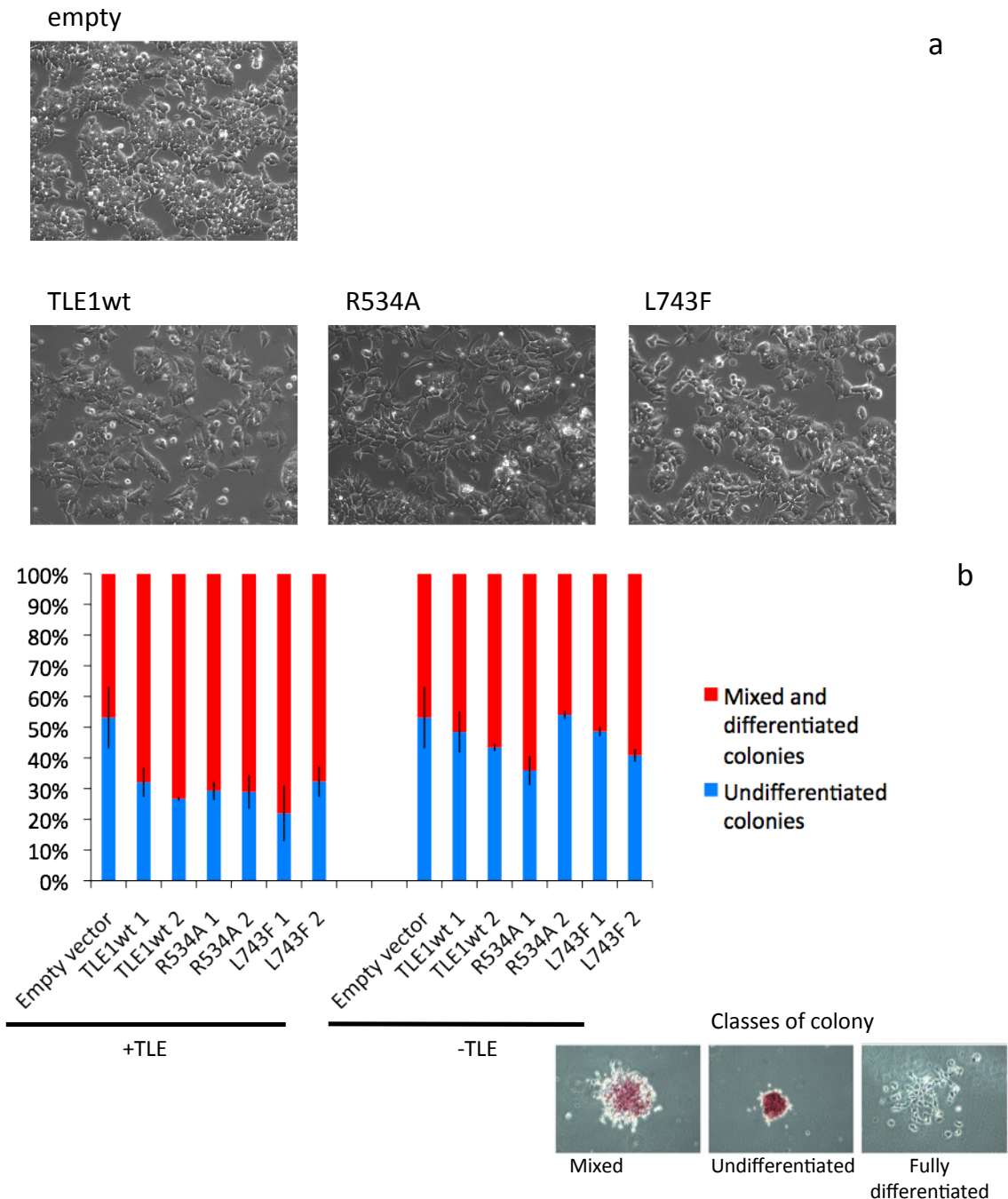


Fig 4.1 Self renewal ability of TLE overexpressing cells at colonial density

(a) Brightfield microscopy of TLE overexpressing and empty vector control cells showing representative fields. **(b)** TLE overexpressors and recombinant subclones were plated in normal media at a density of 50 cells /cm² and were left to grow into colonies for 5d. Plates were then fixed and stained for alkaline phosphatase activity and examined under a microscope. Colonies were counted and classed according to the apparent level of self renewal or differentiation as judged by AP staining and morphology. The figure represents the average percentage of each class per plate over 4 biological replicates. Differences shown between +TLE and -TLE samples were statistically significant ($p < 0.001$ using a Student's t-test) Examples of representative colonies for each class are shown below for reference.

4.2 TLE mutant ES cells exhibit enhanced self-renewal ability

Due to the self-renewal defects in TLE overexpressing ES cells, I then asked if cells with reduced TLE activity exhibited higher than normal levels of undifferentiated growth and clonal self-renewal. Typical AP stained colonies derived from clonal plating of the allelic series of TLE mutations alongside an E14 control are depicted in Fig (Fig 4.2a). The results showed that in normal culture conditions with LIF, reduction in TLE levels correlates with an enhanced self-renewal. Less than 6% of colonies formed by 34n cells showed significant signs of differentiation. Both control lines, TLE4 mutant cells and E14s behaved similarly, despite the differences in genetic background. Control lines exhibited approximately 40-50% wholly undifferentiated colonies. Morphology of 34n colonies was rounded and tightly adherent and they demonstrate no evidence of differentiated cells at the periphery of the colony (Fig 4.2b). The experiment was also carried out in the absence of LIF (Fig 4.2a, lower panels; Fig 4.2b, lanes 6-10). As is expected, E14 and TLE4^{+/-} cells differentiate in absence of LIF, however 34n cells still effectively generate undifferentiated colonies. Greater than 60% of colonies appeared as normal undifferentiated ES cell colonies in the absence of LIF. This is greater than the values obtained for wild type ES cells in normal culture conditions. TLE4^{-/-} TLE3^{+/-} cells were also able to self renew with almost the same efficiency as the 34n cells, suggesting that there may be a critical level of TLE in ES cells necessary for them to be able to differentiate.

That this phenotype is due to a reduction in global TLE levels was indicated by the rescue of the 34n phenotype by the ectopic expression of TLE1. Thus Figure 4.2a and b also show that TLE1 over expression both reduces the ability of these cells to adopt a hyper undifferentiated phenotype and increases the capacity of this line to differentiate in the absence of LIF.

E14 and TLE4^{-/-} TLE3^{+/-} cells were also grown in the absence of LIF for 3 days to cause loss of ES markers and enhance any observed differences between the lines. They were then fixed and stained for OCT4 and NANOG and observed by fluorescence

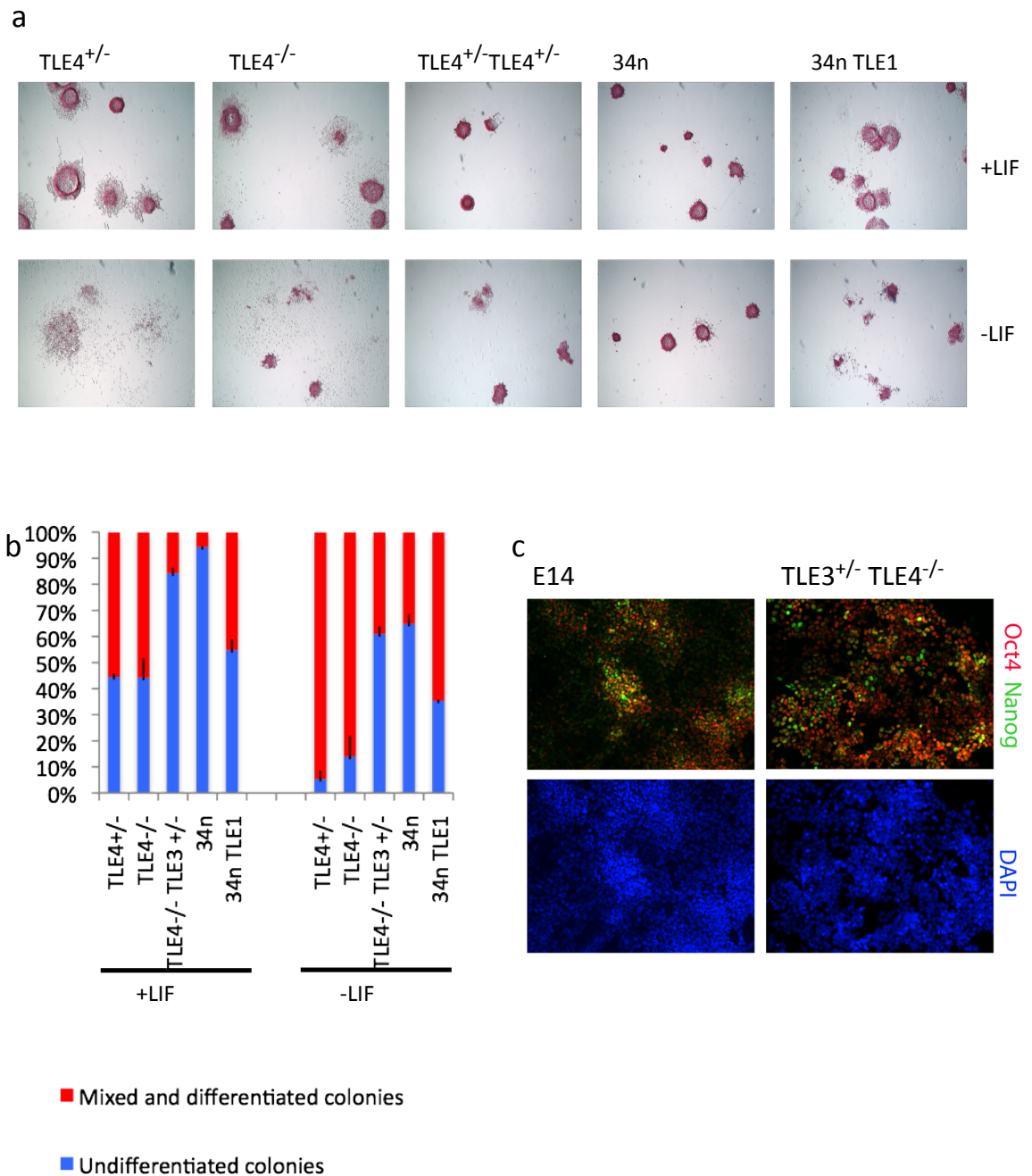


Fig 4.2 Self renewal ability of cells with reduced TLE activity at colonial density

TLE mutant cells were plated in normal media in the presence or absence of LIF at a density of 50/cm² and were left to grow into colonies for 5d. Plates were then fixed and stained for alkaline phosphatase activity and examined under a microscope. **(a)** Representative pictures of colonies in each condition. **(b)** Colonies were counted and classed according to the apparent level of self renewal or differentiation as judged by AP staining and morphology. The figure represents the average percentage of each class per plate over 4 biological replicates. **(c)** Comparison of Oct4 (red) and Nanog (green) expression between the E14tg2a line and generated TLE4^{-/-} TLE3^{+/-} line in the absence of LIF.

microscopy (Fig 4.2c). TLE4^{-/-} TLE3^{+/-} cells have noticeably higher levels of both markers even without LIF promoted self-renewal.

4.3 TLE1 expression results in modest reductions in some pluripotency markers.

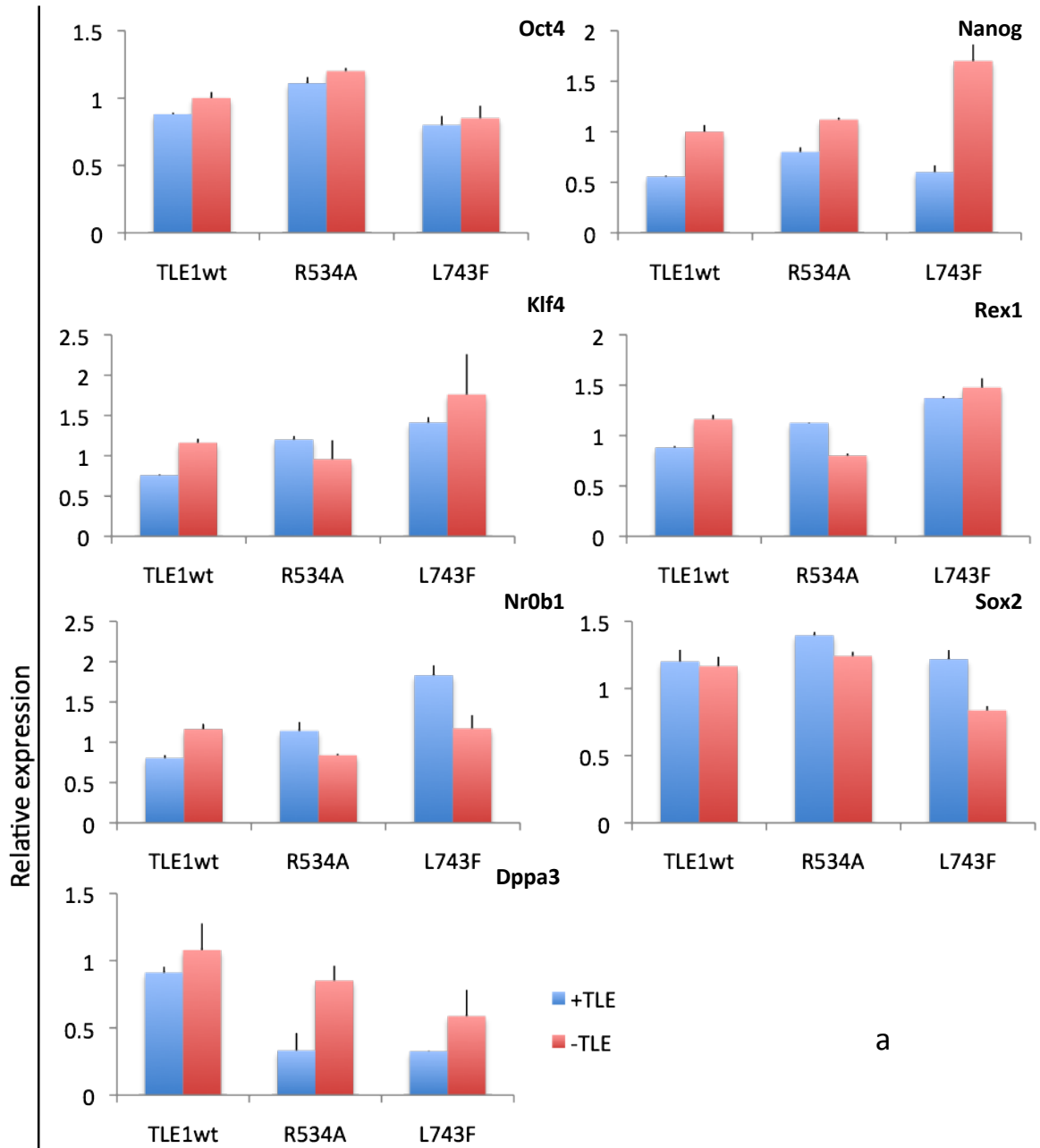
Because of the self-renewal defect in TLE1 overexpressing ES cells, molecular markers of self-renewal and pluripotency were investigated in these lines. cDNA was prepared from these cells and recombined subclones without overexpressed TLE1 and analysed by quantitative rtPCR (Fig 4.3a). *Oct4*, *Nanog*, *Sox2* and *Dppa3* were all modestly reduced in TLE1 overexpressing lines. While these effects are modest to negligible at the RT-PCR level, they are consistently repeated in immunohistochemistry and appeared more dramatic at the protein level (see below). In the absence of LIF ES cells readily make primitive endoderm and mesoderm. Interestingly, alongside the decrease in some pluripotency markers, I also observed an increase in the primitive endoderm markers *Gata4* and *Gata6* for some lines.

The reduction in the expression of key ES transcription factors was also apparent at the protein level. Immunohistochemistry for cultures grown with and without TLE1 in the presence or absence of the cytokine LIF are shown in Figure 4.3b-d. Wild type TLE1 and both point mutations reduced the expression of *Oct4*, *Sox2*, and *Nanog*, and TLE over expressing lines appeared to down regulate these markers to a greater extent in LIF withdrawal than did rescued clones.

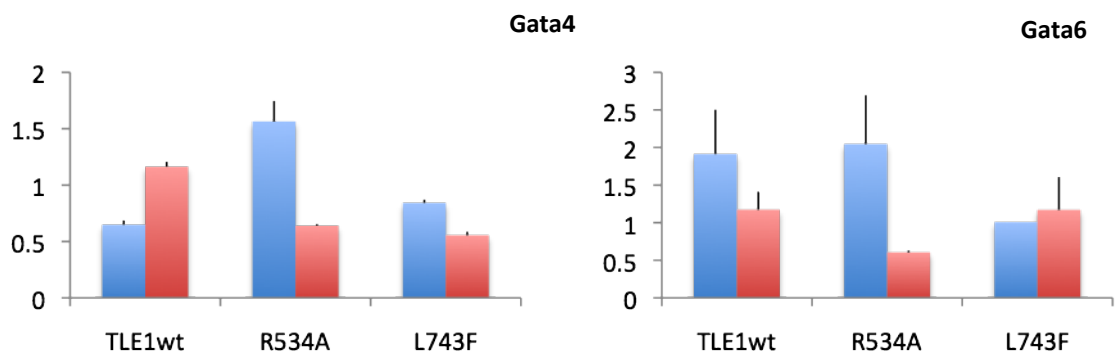
4.4 TLE3 and TLE4 compound mutants express high levels of pluripotency genes

To complement the overexpression experiments and further investigate the increased ability of TLE mutant ES cells to self renew, a similar analysis of molecular markers was carried out. The different TLE mutants were tested in the following growth conditions: GMEM and 10%FCS with LIF, after LIF withdrawal for 3 and 6 days. cDNA was prepared from each sample and subjected to quantitative PCR analysis for a range of different ES and differentiated cell markers (Fig 4.4a). This figure shows an

Pluripotency markers



Primitive Endoderm markers



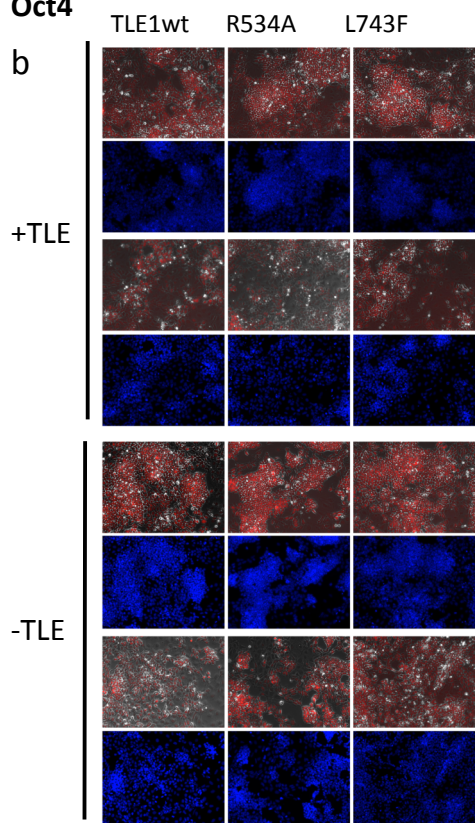
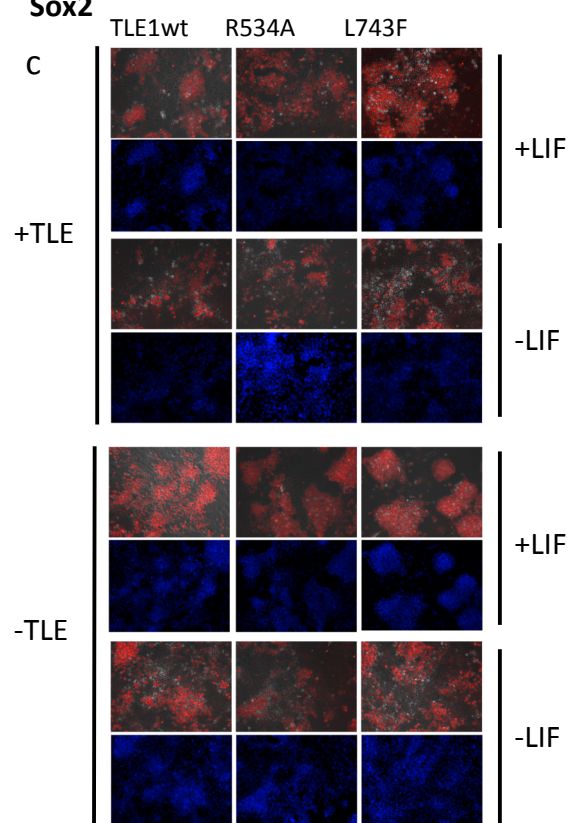
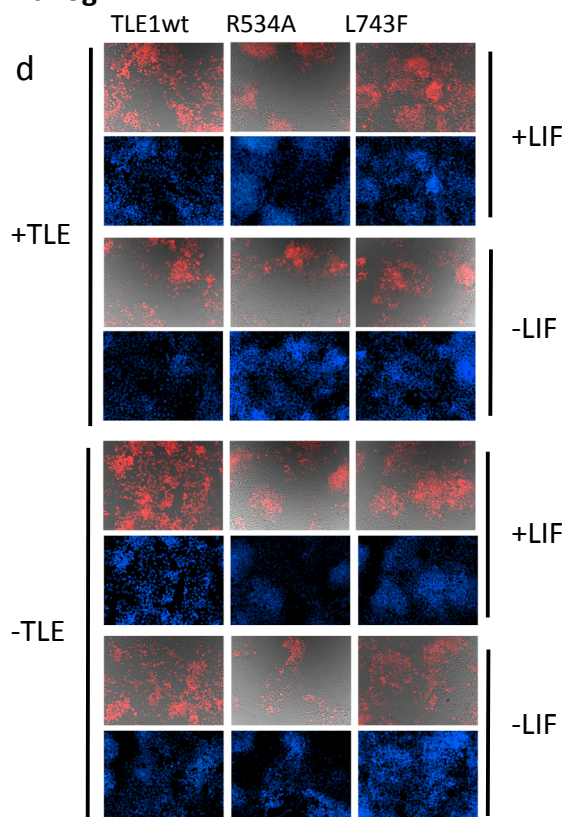
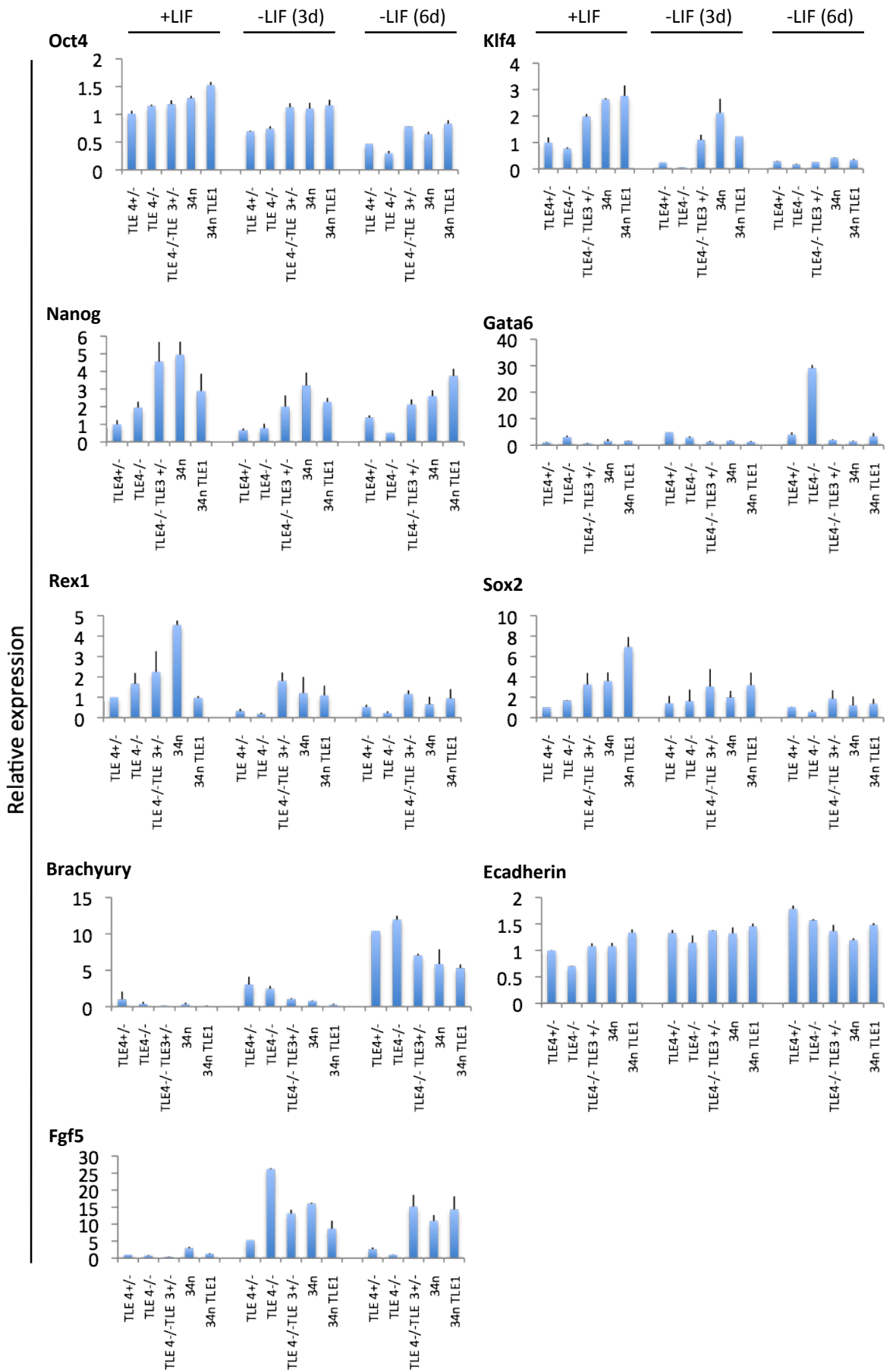
Oct4**Sox2****Nanog**

Fig 4.3 Pluripotency and primitive endoderm marker expression in TLE1 overexpressors

cDNA prepared from TLE1 overexpressors and recombined subclones was analysed by real time qPCR **(a)**. The pluripotency markers Oct4, Nanog, Klf4, Rex1, Nr0b1, Sox2 and Dppa3 and the primitive endoderm markers Gata4 and Gata6 were looked at. Expression levels are normalized to TBP for each sample and shown relative to TLE1wt cells with TLE overexpression removed. Protein expression was also analysed for the pluripotency markers Oct4 **(b)**, Sox2 **(c)** and Nanog **(d)**. Cells were grown for 3d in the presence or absence of LIF before being fixed and stained with the appropriate primary antibodies and fluorophore conjugated secondaries. Representative fields were photographed by fluorescence microscopy.

a



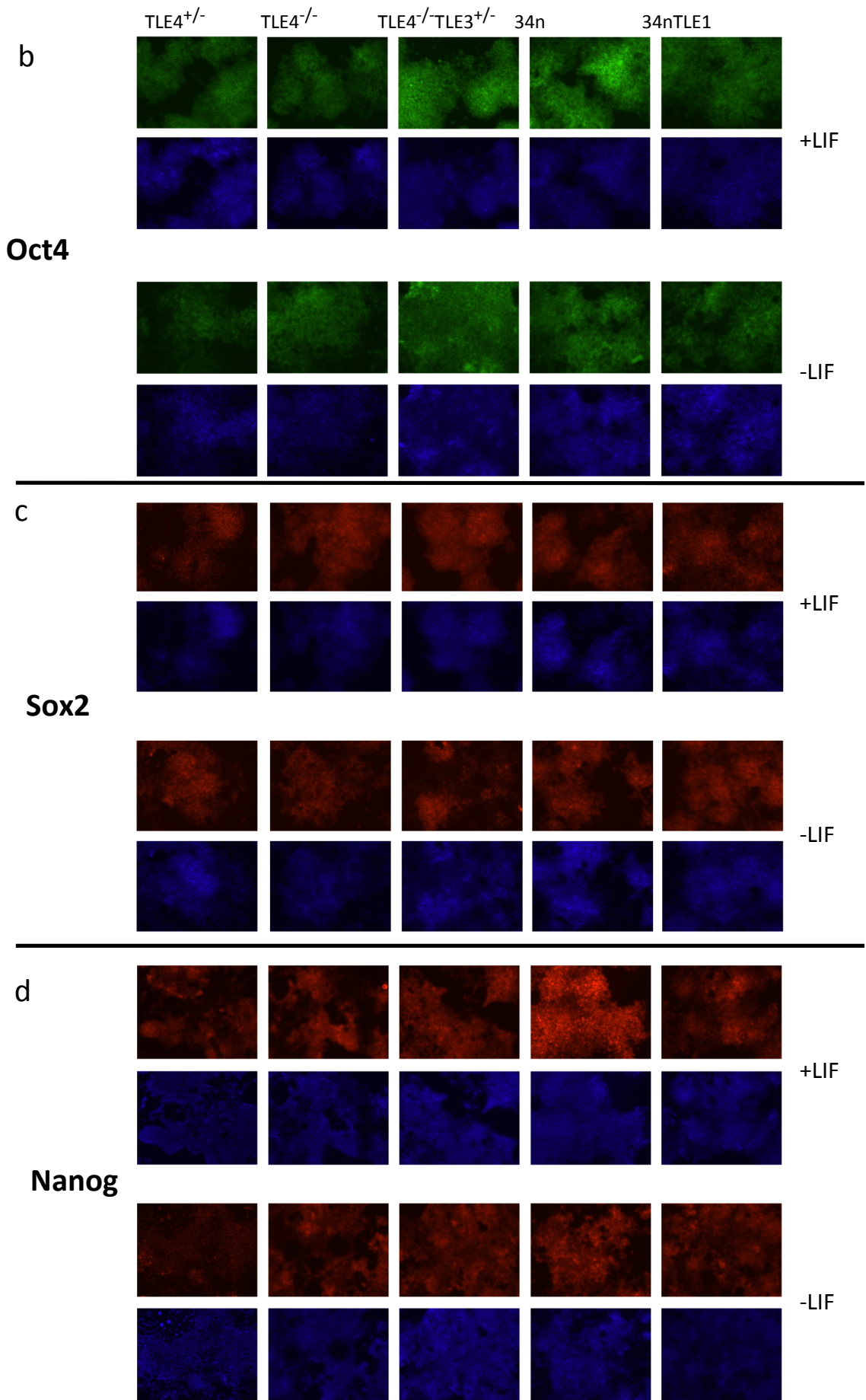


Fig 4.4 Pluripotency and differentiation marker expression in TLE mutant cells

(a) TLE mutant cells were grown in the presence of LIF and the absence of LIF for 3 days and 6 days. RNA was prepared from these and used to synthesize cDNA for analysis by real time qPCR. The ES markers Oct4, Sox2, Klf4, Nanog, Rex1, Ecadherin and Fgf5 and the differentiation marker Brachyury were looked at. Expression levels are normalized to TBP and shown relative to those for TLE4^{+/-} cells in LIF. Cells were also grown for analysis by immunofluorescence. After being grown with or without LIF for 3d, cells were fixed and stained with primary antibodies for Oct4 **(b)**, Sox2 **(c)**, and Nanog **(d)**. They were developed with fluorophore conjugated secondary antibodies and viewed by fluorescence microscopy showing representative fields. Arrows show areas of highest expression.

increase in many pluripotency and self-renewal associated markers, as TLE alleles are lost. *Oct4*, *Nanog*, *Klf4*, *Sox2* and *Rex1* all showed this general trend in LIF media. Addition of a TLE1 expression vector partially rescued the increased *Nanog* and *Sox2* in 34n cells, though a rescue was not observed for all markers. When LIF was withdrawn from the entire set of cell lines, the overall levels of pluripotency gene expression were reduced across the board, although the reduction in gene expression is less extreme in TLE3/TLE4 compound mutants. Even after 6 days of LIF withdrawal the TLE4^{-/-} TLE3^{+/-} and 34n cells expressed significant levels of key ES cell markers.

Interestingly, levels of *Fgf5* remained high in the TLE3/4 compound mutants. *Fgf5* is normally expressed early in differentiation, and is usually associated with epiblast and EpiSCs. *Fgf5* appeared to increase with normal kinetics in the TLE3/4 compound mutations, but remained highly expressed out to 6 days of LIF withdrawal. While the *Ecadherin* can also be seen as an epiblast marker, reduced TLE levels did not effect its expression. The mesendoderm marker *Brachyury* was also reduced in mutant cells as TLE levels decline, suggesting a block to spontaneous differentiation to this lineage, even after LIF withdrawal. No consistent effect was seen on the PrEn marker *Gata6*, although interestingly, high levels were seen in one particular line TLE4^{-/-} after LIF withdrawal.

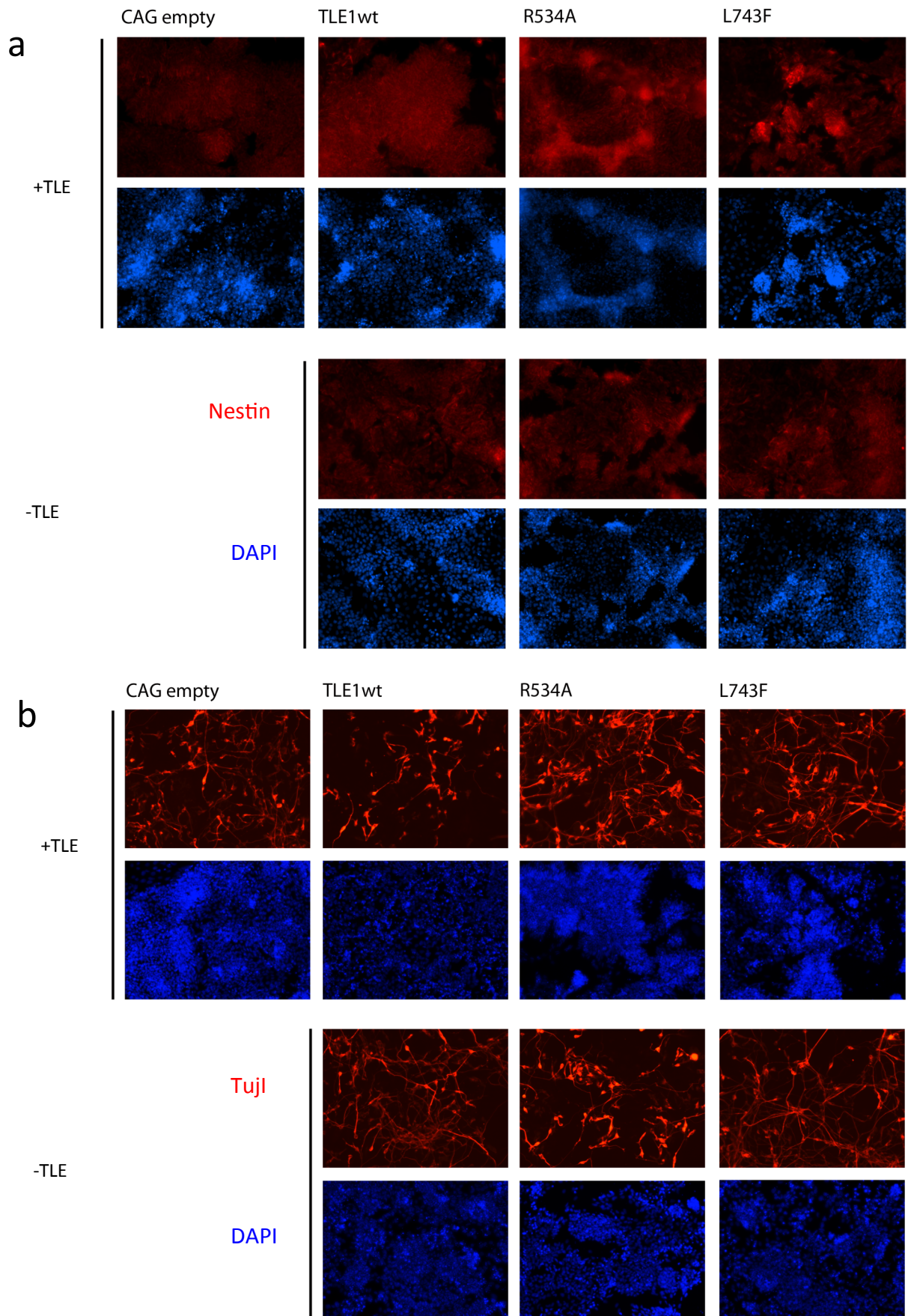
Expression of ES markers was also assayed at the protein level by immunohistochemistry. Cells were grown as before, for 3 days with or without LIF and were stained with antibodies to OCT4, SOX2 and NANOG. The effect on OCT4 (Fig 4.4b) and SOX2 (Fig 4.4c) was less pronounced, although consistently upregulated. With respect to OCT4 staining specifically, TLE4^{-/-} TLE3^{+/-} mutants and particularly 34n cells showed patches of extremely high OCT4 expression (arrow in Fig 4.4b). This expression appeared rescued by ectopic TLE1. NANOG expression was more dramatically upregulated in response to reduced TLE levels and its expression was clearly maintained in the absence of LIF (Fig 4.4d).

4.5 TLE overexpressing cells are prone to differentiation in multiple lineages.

While TLE1 overexpressing ES cells appeared prone to spontaneous primitive endoderm differentiation, I wanted to test their capacity to differentiate toward additional lineages; neural and mesendodermal. To this end I exploited defined differentiation protocols to generate both lineages.

Initially I tested the capacity of these cell lines to form neural progenitors at a fixed time points. The effective generation of high levels of neural progenitors can readily be achieved by the culture of ES cells in minimal media (N2B27) in the absence of any cytokines (Ying et al. 2003). A schematic of this differentiation protocol is shown in Fig 4.5.1d. After three days under these conditions, these cultures consisted largely of NESTIN positive early neural precursors (Fig 4.5.1a). If the cultures were left in N2B27 for a further 4 days, they began to resemble terminally differentiated neurons, expressing neuronal marker β -III TUBULIN (TUJ1) (4.5.1b). Overexpression lines were compared to recombined subclones and cells with vector alone. Cells expressing TLE1 and especially the point mutations R534A and L743F exhibited greater numbers of strongly nestin positive cells at day 3. By day 7 the two point mutations and in particular R543A showed significant inductions of TUJ1. This observation was born out by significant increases in the number and density of elongated neurons in culture. Interestingly, while TLE1 wild type overexpressing lines generated significant levels of NESTIN positive precursors, they did not exhibit enhanced numbers or staining for TUJ1. In fact, cells with TLE1wt have reduced levels of TUJ1. Reduction of terminally differentiated neurons by wild type TLE1 is expected, as it is a known repressor of neuronal differentiation. However the increase in neurons when TLE1 mutations are used is more interesting. It would imply that repression of neural differentiation by TLE1 is in conjunction with WRPW motif containing cofactors such as HES1, as L743F is specific for this binding deficiency. This has previously been shown by the expression of these mutations in primary cultures of cortical neurons (Buscarlet et al. 2008).

To determine whether the over expression of these mutant TLEs was effecting the extent or rate of neural differentiation and to assess a range of additional markers I



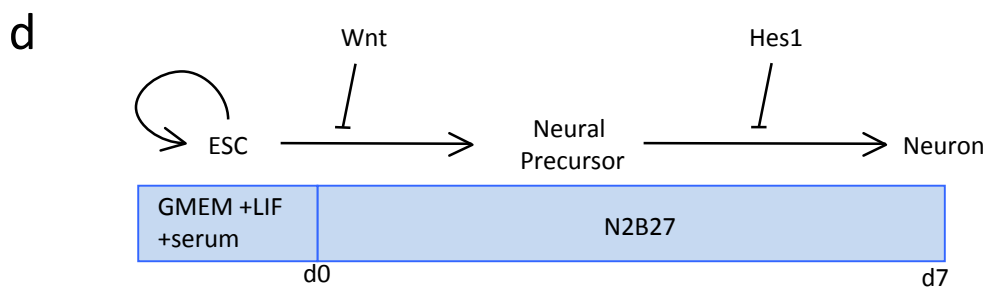
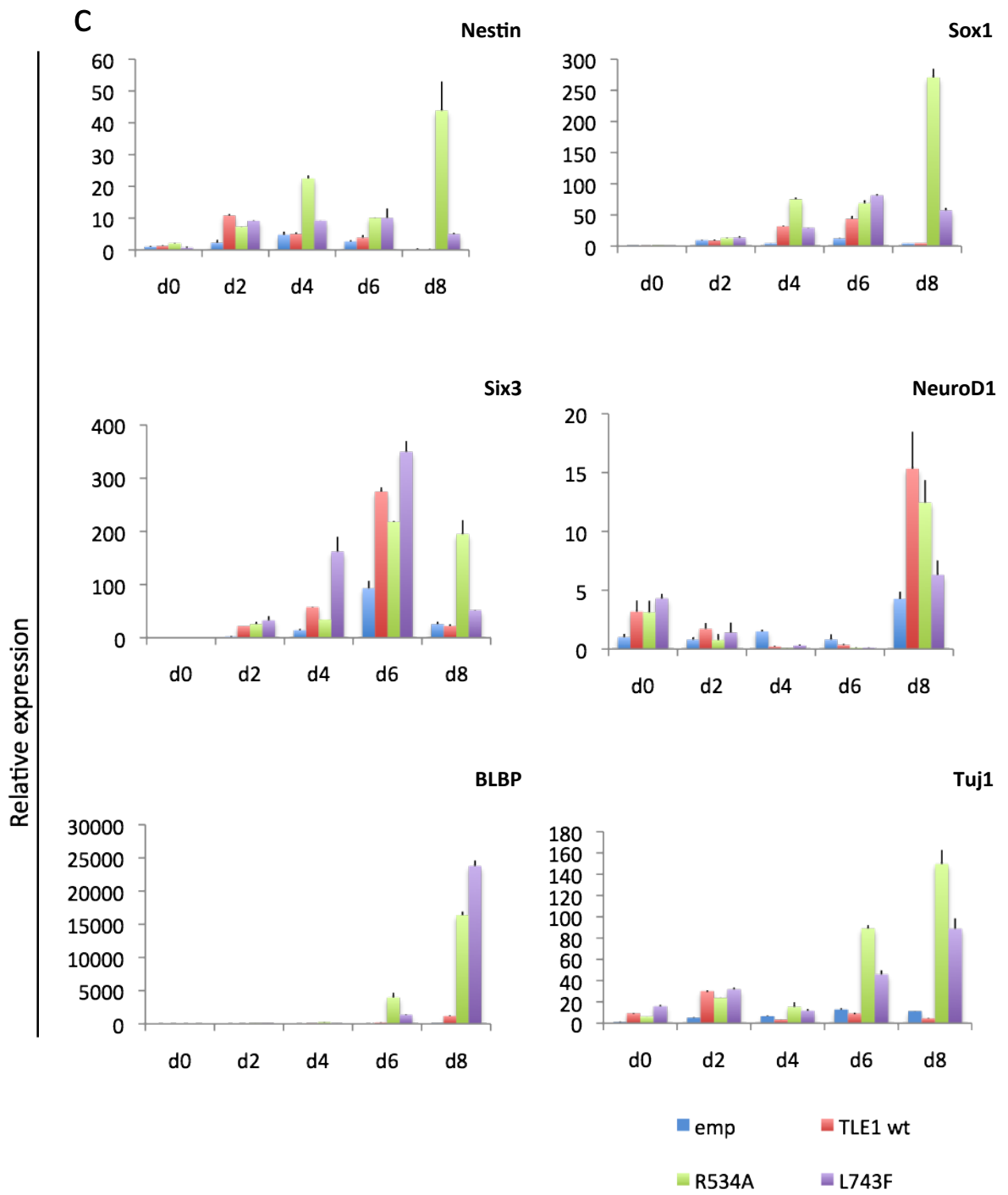


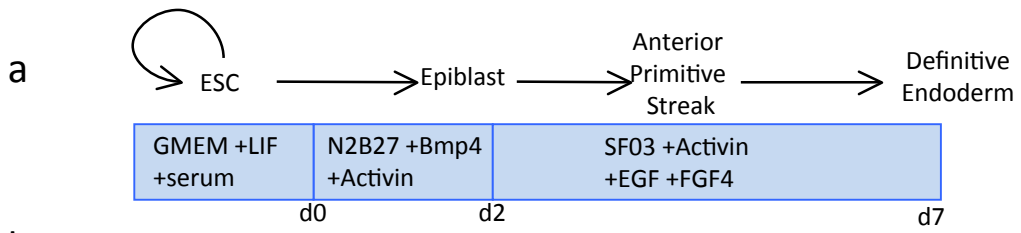
Fig 4.5.1 Neural differentiation of TLE overexpressing ES cells

TLE overexpressing cells and those with the vector alone were subjected to the monolayer neural differentiation protocol. Differentiation efficiency was first analysed by immunofluorescence. Cells were fixed and stained with the appropriate primary antibody and a fluorophore conjugated secondary at day 3 for nestin **(a)** and day 7 for Tuj1 **(b)**. Cells were also differentiated in the same way for neural marker analysis by real time qPCR **(c)**. Cells were harvested before (d0) and at days 2, 4, 6 and 8 of the protocol. RNA extraction and cDNA amplification was performed on the samples. cDNA was used for real-time qPCR analysis of the neural lineage marker genes Sox1, Nestin, NeuroD1, Six3, BLBP and Tuj1. This was performed in technical triplicate. Transcript levels are normalized to TBP and shown relative to the levels in empty vector cells at d0. **(d)** Schematic of the neural differentiation protocol showing equivalent developmental stages and pathways acting on this process.

assessed a time course for neural differentiation by quantitative RT-PCR. Cells were differentiated as before and cDNA was produced from cultures at 0, 2, 4, 6 and 8 days of differentiation (Fig 4.5.1c). Both neural precursor markers *Nestin* and *Sox1* were expressed at higher levels in TLE1 overexpressors, however, as with the NESTIN staining this was particularly pronounced in the lines harbouring TLE1 point mutations. Interestingly, expression of these early markers was retained in CAG TLE1 R534A cells even at the latest time point. *Six3* and *NeuroD1* are both expressed in neural precursors. Expression of these is higher in both wild type and point mutant overexpression lines. However, this result contrasted with the expression of late neural markers such as *Tuj1* and *BLBP*, which are only upregulated in the cell lines expressing TLE mutations that fail to bind WRPW. This observation is similar to that observed the immunohistochemistry and is interesting. As the wild type protein can both repress Notch and Wnt signalling this is not surprising. However, the increase in neurons in response to two TLE1 mutations is interesting as it implies that this effect relies on interaction with TCF like proteins and therefore would be related to Wnt signalling.

Previous work in our laboratory has shown that repression of wnt signalling mediated by TLE4 is involved in the control of anterior definitive endoderm (ADE) formation in both mice and *Xenopus* (Zamparini et al. 2006). The transcriptional repression of TLE4 by Hex promotes ADE formation in embryos by derepressing wnt signalling and suppressing mesoderm induction. It was therefore interesting to ask if forced expression of a TLE protein would modulate mesoderm or endoderm induction. Advantage was taken of a protocol newly developed in this laboratory, which uses defined conditions to differentiate ES cells first to primitive streak derivatives, then to endoderm and anterior endoderm (Fig 4.5.2a) (Morrison et al. 2008).

TLE1 overexpressing cells and the control line were subjected to this protocol and samples were taken at 0, 2, 5 and 7 days and used to generate RNA/cDNA for quantitative RT-PCR (Fig 4.5.2b). Consistent with my previous observations, the TLE1 overexpressing cell lines appeared more effective at generating early derivatives of differentiation. The early mesoderm/primitive streak markers *Brachyury* and *Wnt3a* were higher in all TLE1 overexpressors at day 5. Interestingly, overexpression of TLE1wt and TLE1 R534A exhibited modestly higher levels of the axial mesendoderm



b

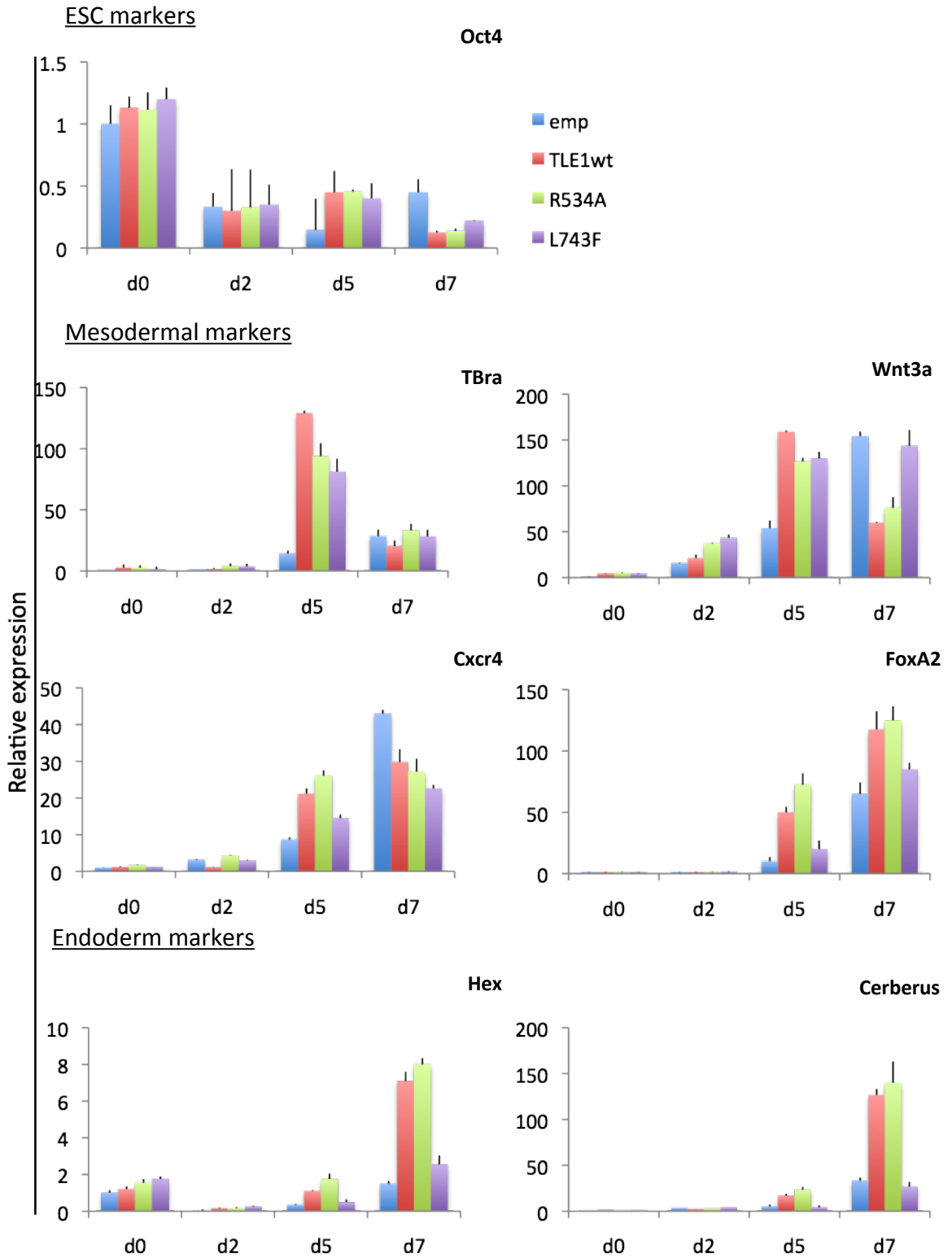


Fig 4.5.2 Mesendoderm differentiation of TLE overexpressing ES cells

(a) Schematic of the ADE differentiation protocol showing equivalent developmental stages. **(b)** Cell lines overexpressing TLE and cells with the vector alone were differentiated towards endoderm. They were harvested before (d0) and at days 2, 5 and 7 of the protocol. Samples were used for RNA extraction followed by cDNA synthesis. Expression of lineage marker genes was analysed by real-time qPCR for each cell line and time point. Each data point represent the average of two biological replicates with PCR performed in technical triplicate. Levels are normalized to TBP and shown relative to empty vector cells at d0.

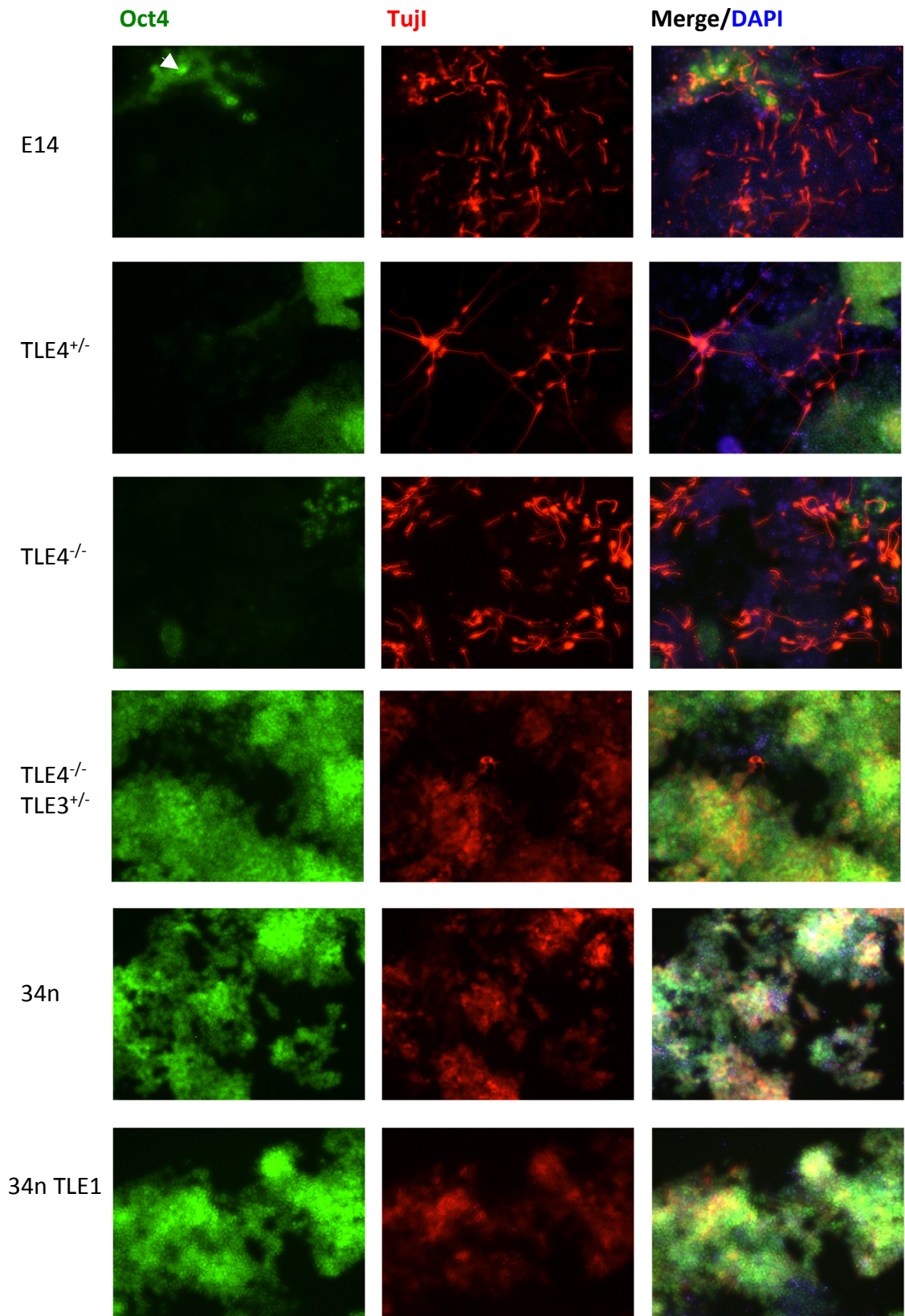
marker *FoxA2* and significantly higher levels of the two ADE genes, *Hex* and *Cerberus*. While the increase in ADE markers appears to be the opposite observation than originally predicted it is consistent with a number of observations about anterior endoderm. First, late specification of anterior endoderm is dependent on Wnt antagonism and second, HEX activity is dependent on TLE1 as a co-repressor. Therefore in the TLE1 overexpressors, HEX would be predicted to be more broadly active. The increase in endodermal markers is not seen with the L743F mutation. The TLE1 L743F line also displays higher *Wnt3a* transcript levels compared to the wild type TLE1 or R534A. This suggests that a eh-1 containing protein may mediate a specific TLE1 dependent suppression of endodermal identity and this may also help to reconcile the observations here with those of Zamparini et al. A summary of gene expression changes is provided in Fig S.1.1 (neural differentiation) and Fig S.1.2 (mesendodermal differentiation).

4.6 Differentiation of TLE mutants.

TLE mutant ES cells have been shown to have enhanced self-renewal ability due to reduced spontaneous differentiation. However it was not known whether they could overcome this initial block and undergo differentiation if they were given the correct inductive signals. To investigate this, I used defined protocols for both neural and mesendodermal differentiation to determine how ubiquitous the block to differentiation was.

As TLE1 overexpressors were better able to differentiate towards the neural lineage, I hypothesized that the loss of function lines might exhibit the opposite phenotype. Cells were plated out in the monolayer neural differentiation protocol as previously described and allowed to differentiate for up to 7 days. They were then stained with antibodies for TUJ1 to mark neurons and OCT4 to mark undifferentiated ES cells. Even at late time points in this protocol, some cells in this protocol failed to downregulate OCT4 as has previously been shown (Lowell et al. 2006). However, these normally represent a minority of these cultures. Thus while TLE4 single mutants and E14 cells formed areas containing elongated TUJ1 positive neurons as expected (Fig 4.6.1a), there were also

a



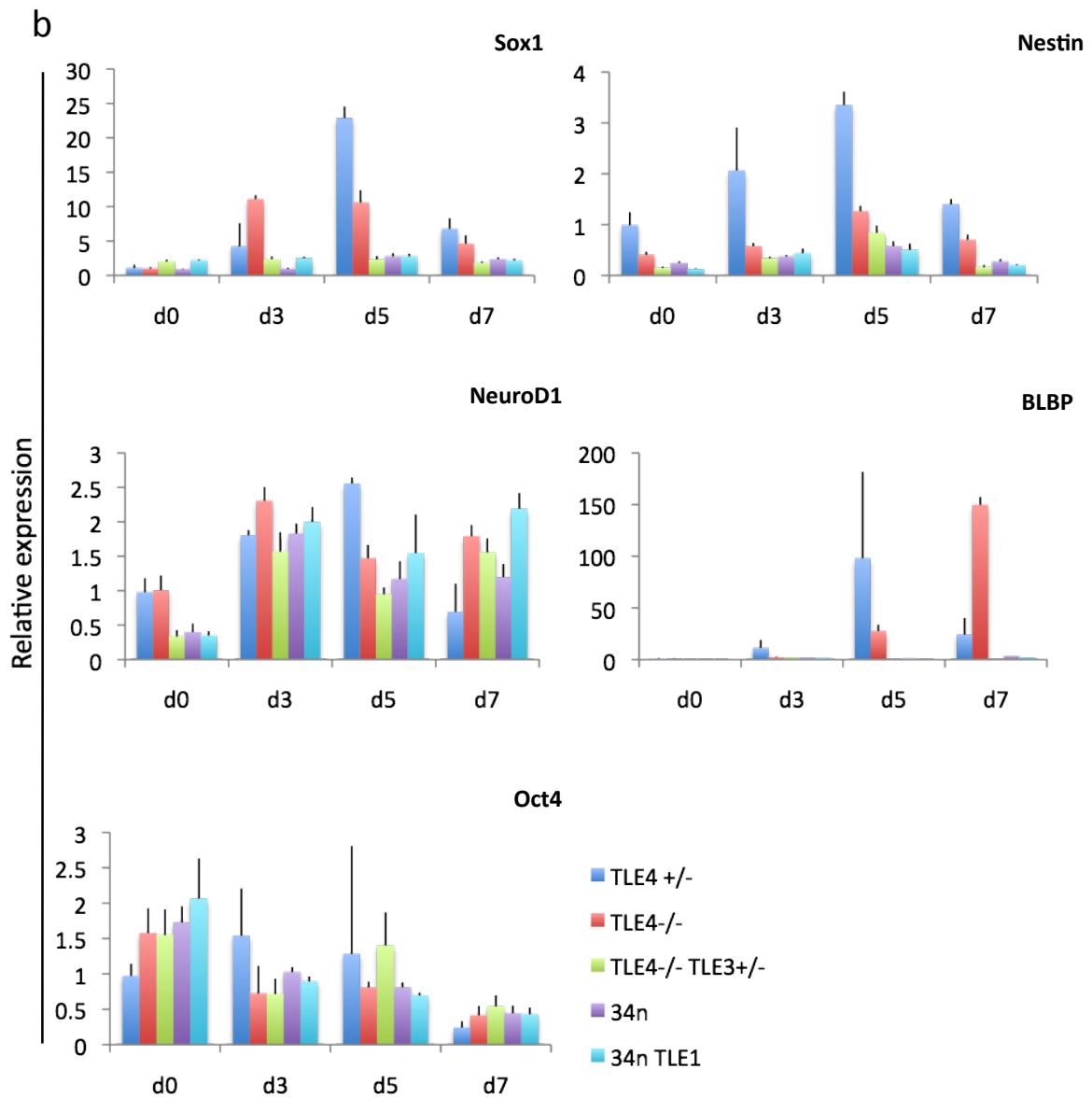


Fig 4.6.I Neural Differentiation of TLE mutant ES cells

TLE mutant ES cells were grown and subjected to the monolayer neural differentiation protocol. **(a)** Marker expression was analysed by immunofluorescence. Cells were differentiated in the same way and fixed and stained at day 7 for Oct4 (green) and Tuj1 (red) with the appropriate primary antibodies and fluorophore conjugated secondaries. They were visualized by fluorescence microscopy with DAPI used as a counterstain. Cells were harvested before (d0) and at days 3, 5 and 7 of the protocol. **(a)** RNA extraction and cDNA amplification was performed on the samples. cDNA was used for real-time qPCR analysis of the neural lineage marker genes Sox1, Nestin, NeuroD1, BLBP and the self renewal marker Oct4. Data shown represents the average of two biological replicates with PCR performed on each in technical triplicate. Levels are normalized to TBP and shown relative to TLE4^{+/-} cells at d0.

some OCT4 positive cells (arrowhead in Fig 4.6.1a). However, this staining does not colocalize with the cell bodies of TUJ1 positive neurons and thus represents a minority of undifferentiated cells. Cultures from the TLE3/4 compound lines on the other hand, did not generate neurons. Faint, diffuse staining with the TUJ1 antibody was observed but these cells did not have the obvious elongated morphology of neurons. This staining may represent another cytoskeletal or mitochondrial form of tubulin. In addition, the majority of these cells failed to down regulate OCT4, despite prolonged culture in N2B27 without cytokines. Forced expression of TLE1 failed to rescue this phenotype, although this lack of rescue may be due to an insufficient level of TLE or the unlikely possibility that there are functional differences within the family of TLEs. Further work will be required to resolve these possibilities.

To investigate kinetics of differentiation at the transcriptional level, a time course of neural differentiation was subjected to a range of RT-PCR markers. Cells were differentiated as before and sampled at days 0, 3, 5 and 7 of the protocol. cDNA was synthesized and analysed by quantitative rtPCR (Fig 4.6.1b). The neuroectoderm marker *Sox1* was upregulated from day 3 in TLE4 single mutant cells, but TLE3/TLE4 double mutant cells failed to upregulate *Sox1* at any time point. However, this block to differentiation does not appear complete, as *Oct4* message did appear reduced by day 7. This suggests a level of post translation regulation as the effect on *Oct4* at the protein level appeared much more dramatic. *Nestin* followed a similar pattern and increased most in TLE4^{+/-}. *NeuroD1* expression was also upregulated in all the cell lines tested. Interestingly, *NeuroD1* is not exclusive to neural precursors though, and could represent a different lineage. The mature neuronal/glial marker *BLBP* was high in TLE4 single mutants by the end of the protocol but was almost completely absent in TLE3/TLE4 double mutants.

As with the TLE overexpressors, I tested the capacity of the TLE allelic series to form mesoderm and endoderm under defined conditions. TLE mutants and the rescued lines were plated out for the monolayer ADE protocol summarized in Fig 3.13a. They were left to differentiate and samples taken for cDNA synthesis at d0, d2, d5 and d7 of the protocol. Transcript levels for mesoderm and endoderm markers were analysed by quantitative rtPCR for each sample (Fig 4.6.2). In contrast to the neural differentiation

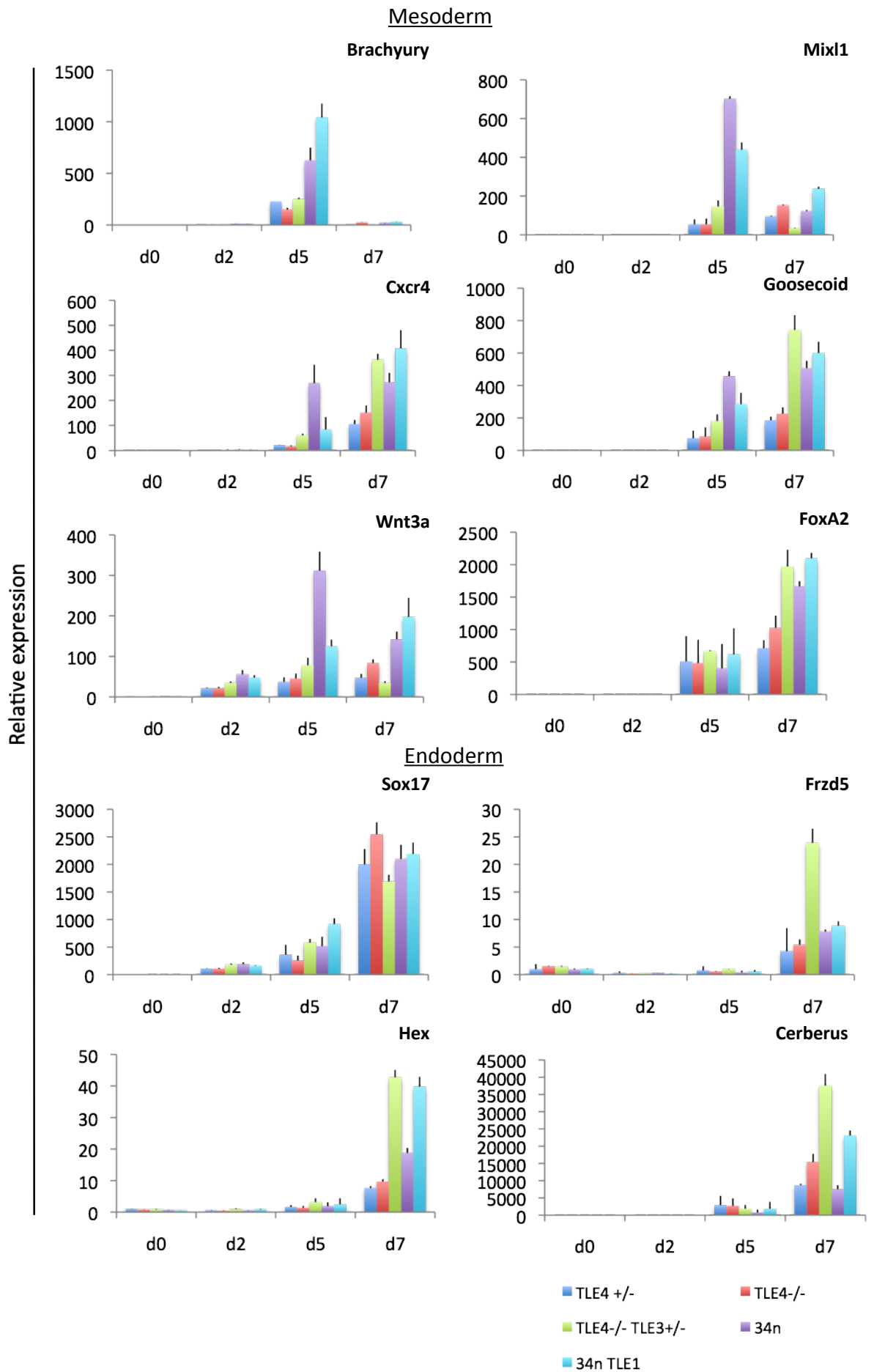


Fig 4.6.2 Mesendoderm differentiation of TLE mutant ES cells

TLE3/4 mutant and 34n TLE1 rescued ES cells were differentiated towards anterior definitive endoderm. They were harvested before (d0) and at days 2, 5 and 7 of the protocol. Samples were used for RNA extraction followed by cDNA synthesis. Expression of lineage marker genes was analysed by real-time qPCR for each cell line and time point. Data shown represents the average of two biological replicates with PCR performed on each in technical triplicate

protocol, differentiation by this protocol appeared to be enhanced in TLE mutant cells based on marker upregulation. The mesoderm markers *Gooseoid*, *Mixl1*, *Cxcr4*, *Brachyury*, *FoxA2* and *Wnt3a* were all expressed at higher levels in response to reduced TLE activity. Interestingly, specific anterior mesendoderm makers, *Gooseoid*, *Frzd5*, *Hex* and *Cerberus* were all expressed at high levels in the TLE4^{-/-} TLE3^{+/-} than 34n cells. Also, the double nulls were particularly ineffective at making these lineages, while the 34n rescued cells are. This suggest that while a reduction in TLE is required for optimal mesendoderm induction, a critical level of TLE maybe necessary for the activity of homeobox transcription factors such as HEX and GOOSECOID, which use TLEs as corepressors, to properly pattern the emerging endoderm and suppress mesoderm induction. In general however, TLE mutants seemed to be more efficient at forming mesoderm during the protocol. Primitive streak markers *Brachyury*, *Mixl1* and *Wnt3a* were dramatically upregulated in mutants. The gene expression changes observed in the TLE mutant cell differentiation experiments are also summarised in Figs S.1.1 and S.1.2.

4.7 ES marker expression of TLE mutant cells in the 2i culture system

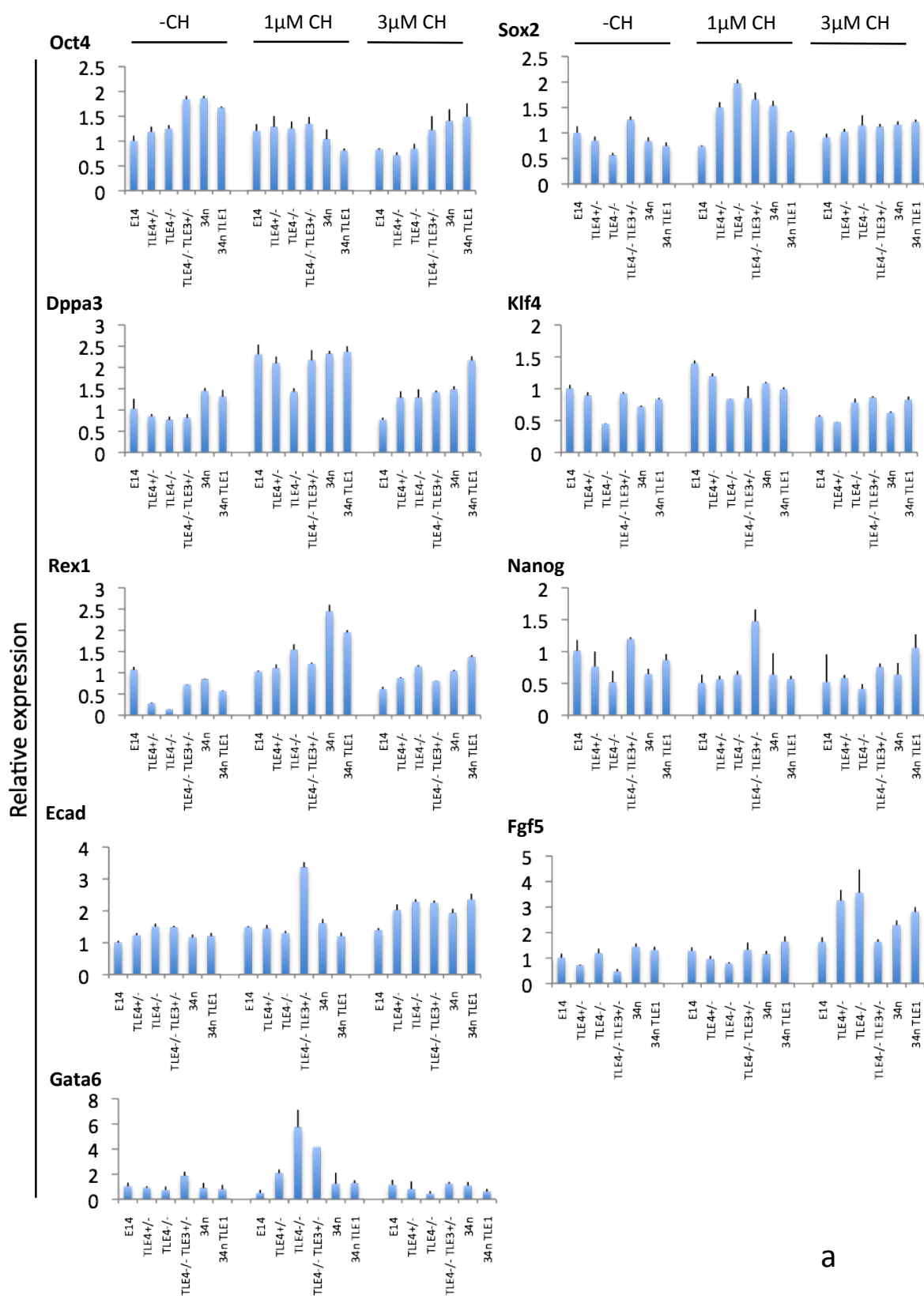
TLE proteins have previously been implicated in the regulation of ES self renewal, albeit indirectly via TCF3. TCF3 has been shown to bind the Nanog promoter in ES cells and repress its transcription (Pereira et al. 2006). Mutation of the TLE binding domain of the TCF3 protein negated this repression, suggesting a TLE protein was acting as a corepressor. TCF3 binding has also been shown by CHIP-on-chip to other pluripotency associated genes such as *Oct4* and the bound TCF3 colocalizes with TLE2 (Tam et al. 2008). Interestingly, TLE5, which has been purported to act as a dominant negative TLE in some circumstances, is also expressed in ES cells. Its expression is regulated by STAT3 and declines upon LIF withdrawal induced reduction of STAT3 (Sekkaï et al. 2005). These studies suggest a model where repression of ES associated genes by Tcf3 in conjunction with TLE corepressors, is necessary for ES cells to differentiate efficiently. TCF3 can act as a transcriptional activator or repressor and this depends on whether it is complexed with β CATENIN or corepressors such as CtBP or

TLEs. The balance between these two types of complex is controlled by Wnt signalling. We formulated a hypothesis that the increase in TLE mutant cells self-renewal abilities is due to an amplification of the Wnt pathway by reduction of Tcf mediated repression.

ES cells can be grown in defined conditions without serum using the 2i culture system. Cells are cultured in N2B27 media with two small molecule inhibitors to control signalling pathways and keep ES cells in a self-renewing state (Ying et al. 2008). PD032501 blocks commitment to differentiation by suppressing phospho-ERK. CHIR99021 is a GSK3 inhibitor and its addition appears to enhance cell growth and viability. Moreover, other GSK3 β inhibitors have been used to maintain ES cells in an undifferentiated state. However, the dependence of the defined 2i system on GSK3 inhibition allowed me to test whether the enhanced capacity of TLE3/4 compound mutants enables the to self renew in the absence of CHIR99021.

TLE mutant cells were plated in 2i media containing the recommended normal PD0325901 concentration (1 μ M) and CHIRON99021 at the normal concentration (3 μ M), 1 μ M or without CHIRON99021. They were grown and passaged in this for 5 days to allow gene expression changes. cDNA was then prepared from them for analysis by quantitative PCR (Fig 4.7a) and samples were also antibody stained for OCT4 expression (Fig 4.7b). In low or absent CHIRON, some ES markers such as *Oct4*, *Sox2* and *Nanog* were higher in the 34n line than lines with more TLE, but there was no clear trend across the allelic series. No consistent effect was seen on *Gata6*, however one interesting observation was high levels of this marker in the TLE4^{-/-} cells in 1 μ M CHIRON. However, when the lines were grown in normal CHIRON (3 μ M), differences between normally exhibited between these cell lines were less apparent, suggesting that TLE repression might feed indirectly into activate MAP kinase signalling that is effectively inhibited by the 2i condition. OCT4 protein expression was also largely unaffected across the allelic series in normal or moderately reduced CHIRON (Fig 4.7b). Again, levels did appear higher in 34n cells than other lines in the absence of CHIRON. However, cell survival in this condition also appeared greater as shown by increased DAPI fluorescence, thus OCT4 expression may be increased as a consequence of this. The data presented in this experiment is inconclusive. However it

does not appear to support the hypothesis that TLEs are working through the wnt pathway alone to regulate self-renewal.



a

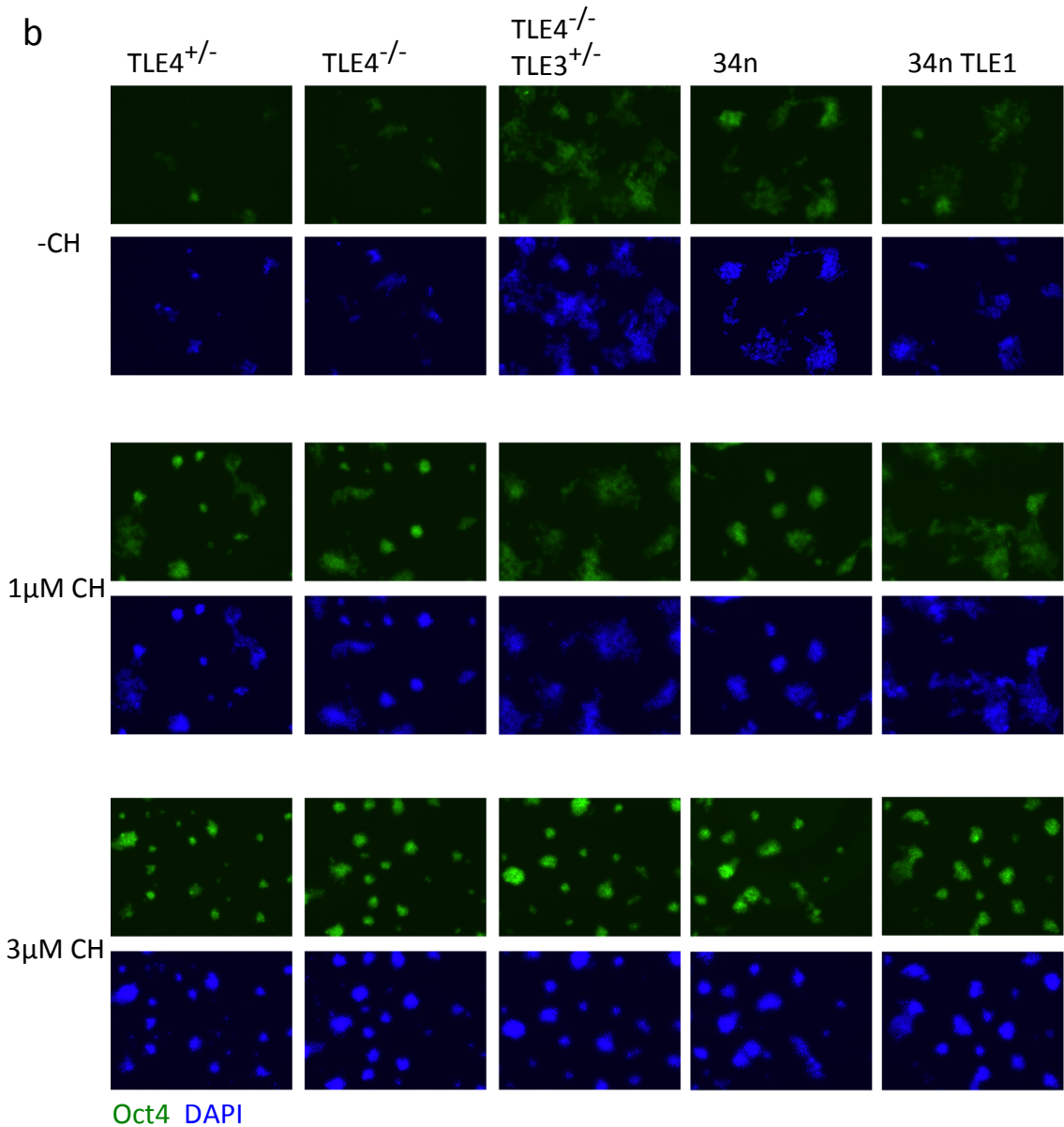


Fig 4.7 ES marker expression of TLE mutant cells in 2i with altered CHIRON concentration

TLE mutant ES cells were grown and passaged in 2i media with different CHIRON concentrations for 5 days. The concentrations of CHIRON99021 in different 2i medias were 3μM, 1μM and 0μM. PD0325901 and LIF in the media were kept constant. **(a)** Cells were then harvested and used for RNA extraction and cDNA synthesis. Real time qPCR analysis was performed for the markers Oct4, Sox2, Klf4, Rex1, Nanog, Dppa3, Ecadherin and Fgf5. Expression levels are normalized to TBP values for each sample and shown relative to those for E14 -CHIRON. Analysis was performed in technical triplicate for each data point. **(b)** Oct4 levels were also analysed in the same experiment using immunofluorescence. Cells were fixed and stained after 5 days using Oct4 primary antibody and a fluorescent secondary. They were visualized by fluorescence microscopy with using DAPI as a counterstain and representative fields photographed.

4.8 Discussion

In this chapter I have identified several interconnected roles for TLE proteins in the regulation of early lineage specification and ES cell self-renewal. Growing TLE overexpressing and TLE mutant cells at clonal density revealed differences in the cells self-renewal abilities. While ES cells with less TLE activity were able to self renew with high efficiency, ES cells overexpressing TLE were more prone than wild type cells to differentiation. Furthermore, the effect of loss of both TLE3 and TLE4 is strong enough to allow LIF independent self-renewal. These opposing phenotypes suggest TLE in ES cells facilitates the passage from a self-renewing to a more differentiated state. Overexpression of both wild type and point mutants of TLE1 increase differentiation, demonstrating that the effect is not dependant on eh1 or WRPW classes of TLE cofactors and could involve TCF proteins for example. This would agree with previous studies showing a role for TLEs in TCF mediated repression of *Nanog* and *Oct4* (Pereira et al. 2006; Tam et al. 2008). However the phenotype of TLE overexpression is milder than that of TLE loss. This is in agreement with TLEs function as a corepressor with no independent DNA binding. Although increased TLE may amplify the effects of any TLE dependant proteins, it cannot independently affect specific processes without a DNA binding partner. In contrast loss of TLE would be a limiting factor in itself, reducing the ability of differentiation promoting TLE dependant repressors to act, thereby exerting a greater effect. This is also reflected in a molecular analysis of self-renewal and differentiation related markers.

TLE overexpressing ES cells had a moderate decrease in certain self-renewal markers such as *Oct4*, *Sox2* and *Nanog* as assayed by both quantitative rtPCR and antibody staining. However in TLE mutant ES cells, an opposite and more pronounced effect was observed. Transcript levels of self-renewal markers such as *Oct4*, *Nanog*, *Klf4*, and *Sox2* all showed a general trend of increased expression as TLE levels reduced. TLE3/TLE4 compound mutants had the highest levels of these factors. Even after extended periods of LIF withdrawal, these cells maintained high levels of these factors, especially *Oct4*. In contrast, the mesendoderm marker *Brachyury* was reduced, demonstrating reduced spontaneous differentiation. No consistent effect was observed on the primitive endoderm markers *Gata4* or *Gata6* that could be correlated to total

TLE levels although *Gata6* was significantly higher in TLE4^{-/-} cells. This is a similar result to the high *Gata6* levels seen in the same cells in 2i with reduced CHIRON. The significance of this is unclear but may reflect differences between individual TLEs.

Transition of ES cells to specific differentiated cell types is controlled by both downregulation of the self-renewal promoting network and by control of early lineage promoting factors to steer differentiation. A role for TLEs in the latter was also identified. TLEs have previously been implicated in the control of differentiation in embryonic development and interact with developmental regulators such as Fox and homeobox proteins, Hes1 and Goosecoid (Yao et al. 2000; Izzi et al. 2007; Yaklichkin et al. 2007). Here I show that TLE1 overexpression promotes early differentiation towards the neural lineage from ES cells. This is in agreement with the increased ability of these cells to differentiate as discussed above and the repression of Wnt signalling which has been shown to promote neural differentiation (Aubert et al. 2002). Notch signalling can promote neural progenitor specification (Lowell et al. 2006) therefore TLE antagonism of Notch ICD/RBPJ mediated transcription may suppress neural differentiation. Lack of Notch antagonism by the point mutants would give these Wnt-suppressing proneural activities but no Notch-suppressing antineural activity, explaining their strong neural differentiation promoting effect. Previous studies describe TLEs as repressors of terminal neural differentiation and this agrees with the observation that TLE1wt ES cells produce less TUJ1 positive neurons in a differentiation protocol. However, the increased number of these neurons in cells overexpressing TLE1 point mutants with a specific deficiency in WRPW interactions suggests this neural suppression is dependant on WRPW containing proteins for example Hes1. These experiments supports similar observations from TLE1 overexpression in primary cultures of neural progenitors (Buscarlet et al. 2008) and extends the role of TLEs to an earlier stage of differentiation. In contrast, TLE3/TLE4 compound mutant ES cells were less able to differentiate to the early neural lineage as shown by reduced *Sox1* and persistent *Oct4* expression. They appear completely unable to produce terminally differentiated neural cell types. A model is suggested whereby TLE proteins promote early specification towards the neural lineage by repression of pluripotency genes and

Wnt repression, then provide a secondary function at later stages to regulate neural differentiation through the Notch pathway.

As well as the neural lineage, a role in mesendoderm lineage specification was also highlighted. In a mesendoderm differentiation protocol, cells overexpressing TLE1 and point mutations had a greatly increased propensity to differentiate towards this lineage as shown by increased primitive streak markers such as *Wnt3a* and *Brachyury*. This is in agreement with the previous observations of TLE1 overexpressing cells more readily differentiating and a more marked downregulation of *Oct4* at the end of the protocol. Although they might be expected to have the reciprocal phenotype, TLE3/TLE4 mutants also express more PS markers as TLE levels decrease. This apparently contradictory observation can be explained by the reduction in Wnt antagonism by loss of TLE. Wnt signalling promotes early mesendodermal differentiation therefore if the initial obstacle to differentiation by reduced pluripotency network repression can be overcome, TLE3/TLE4 mutants can differentiate towards this lineage with greater efficiency. At later stages of this protocol, cells are directed towards anterior endoderm and cells with reduced levels of TLE express higher anterior endoderm markers such as *Hex*, *Cerberus* and *Fzd5*. This is in agreement with the previous study by Zamparini et al that showed reduced TLE4 causes derepression of Wnt signalling, leading to upregulation of anterior endodermal Wnt target genes such as *Cerberus*. TLE1 and TLE1 R534A overexpressing cells also have increased anterior endoderm markers *Hex* and *Cerberus*. This is in apparent conflict with the previous observations. However, TLEs also act as cofactors with endodermal homeobox transcription factors such as HEX and GOOSECOID. These observations suggest dual positive and negative roles for TLEs in anterior endoderm differentiation at different stages, depending on the context of expressed cofactors. In agreement with this, reduction in TLE levels in the TLE3/TLE4 mutants up to a point allows better mesendodermal differentiation, but complete loss of both genes inhibits it.

The possible roles identified for TLE proteins in self-renewal and lineage specification are summarized in schematic form in Fig 4.8.

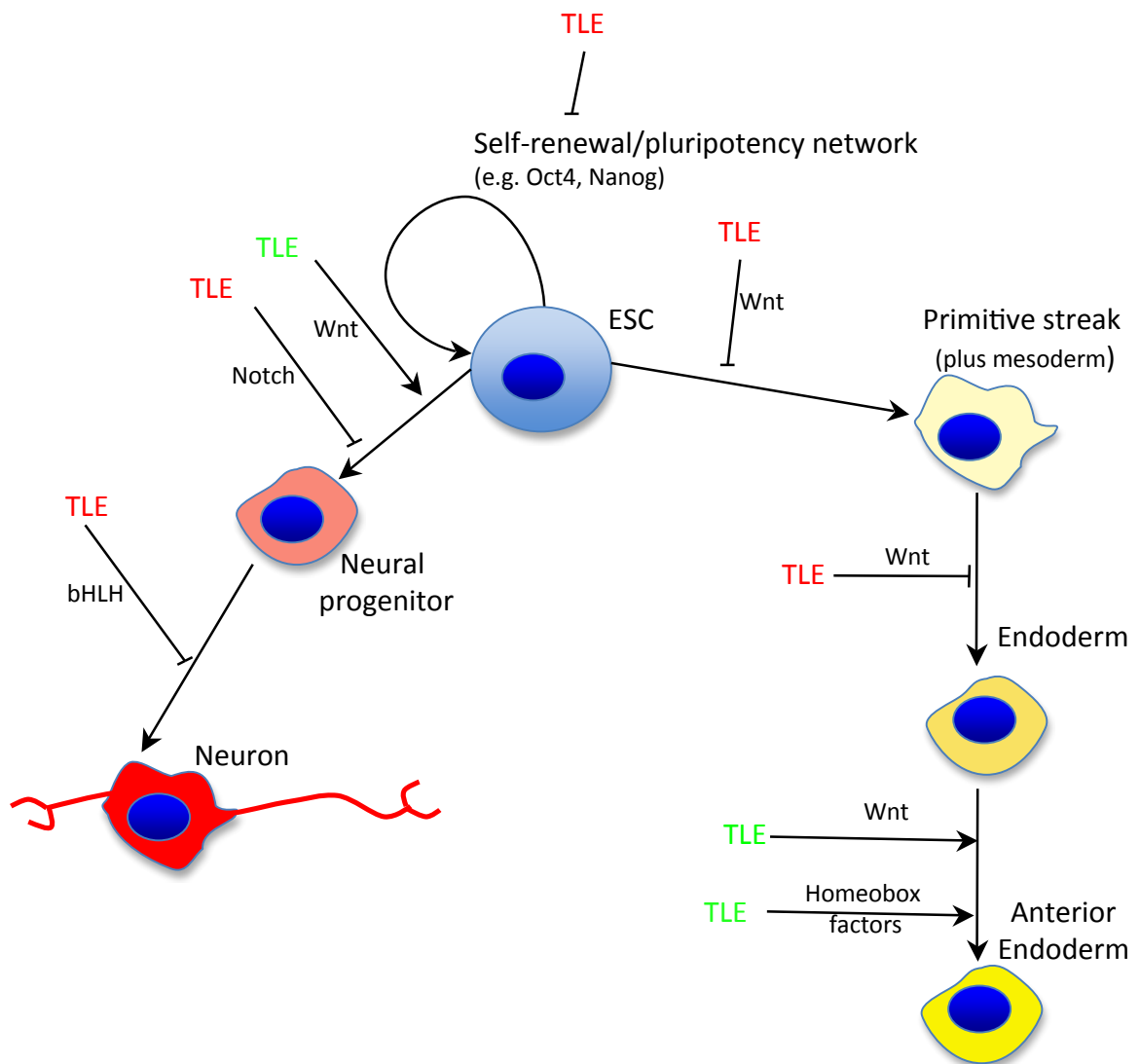


Fig 4.8 Speculative model for roles of TLEs in ES cell self renewal and lineage specification

Model for some of the possible roles of TLE in ES cell self renewal, neural and mesendodermal differentiation. Positive (green) and negative (red) roles for TLE mediated repression are shown for each process. TLE reduces self renewal by inhibiting self renewal genes. TLE increases neural differentiation through inhibiting self renewal and antagonising Wnt signaling, but can also decrease it through Notch and bHLH mediated repression. TLE inhibits mesendoderm/primitive streak and later anterior endoderm through wnt antagonism, but can also promote this differentiation initially through decreased self renewal ability, later interactions with homeobox transcription factors such as Hex and Goosecoid and later Wnt signaling antagonism.

Chapter 6

Final Discussion

Final Discussion

In this thesis, I have provided some novel insights into the roles of TLE family corepressors in early lineage specification and regulation of ES cell differentiation. This was facilitated by the generation of a range of tools that allowed both gain and loss of TLE, and perturbation of specific TLE activities.

TLE proteins have been observed in both ES cells and early mouse embryos. Although they appear to be expressed throughout the embryonic portion of the conceptus, their expression pattern at gastrulation and beyond is highly dynamic. Moreover, even at the blastocyst stage, TLE4 seemed to exhibit slight heterogeneity in the ICM compared to the more uniform expression in the epiblast. In addition, a heterogeneous expression pattern was observed for TLE4 in ES undifferentiated ES cell cultures. These observations suggest a level of control over TLE expression, although the role of these proteins in early development and differentiation has not previously been studied in depth. Later developmental roles for TLEs have been described and experiments in this work expand these roles to earlier stages. TLE proteins were first identified as a neural suppressor in *Drosophila* (*Groucho*) and this role was later extended to mammals. However, previous studies concentrated on later stages of neural specification. Experiments here show that TLE1 has a positive effect on the initial specification of neural progenitors, probably through Wnt antagonism, and an opposing negative effect through an eh1 containing cofactor, probably via the Notch pathway.

Experiments in this thesis explore the role of TLE1, TLE3 and TLE4 in early lineage specification events. Consistent with their distinct and dynamic expression patterns, different TLE mutants appear to have diverse effects on differentiation, for example differences in neural and endoderm markers between TLE4 and TLE4/TLE4 compound mutants and increased Gata6 observed in TLE4^{-/-} cells in some experiments. While these effects could simply reflect the gene dose, the possibility remains that there are differences between the activities of individual TLEs. While TLE1 is purported to have identical biochemical properties to other TLEs, it only partially rescues TLE3/TLE4 mutants. This may be a result of failing to rescue the heterogeneous gene activity with a constitutively active TLE1 vector or cultural adaptation to forced TLE1 expression, but could also imply subtle differences between the proteins that have not previously been

identified. Clearly more extensive rescue experiments using inducible expression are required to distinguish between these possibilities.

Previous work in our lab (Zamparini et al. 2006) identified TLE family members as repressed targets of the homeobox transcription factor *Hex*, in anterior endoderm specification. Although this work was carried out in *Xenopus*, the gene interaction networks involved appeared conserved in the mouse, and suggested a possible role for Wnt signal amplification by repression of TLEs in regulation of mammalian anterior endoderm specification too. Experiments in this work lend further evidence to this idea. Mutant cells with reduced TLE activity were better able to differentiate into anterior endoderm as marked by genes such as *Hex* and *Fzd5*. In addition, primitive streak markers were increased at earlier stages of differentiation, in agreement with the need for the Wnt pathway in establishing the primitive streak and subsequently mesoderm and endoderm, and this would also drive ES cells towards endoderm. Roles for Wnt signalling in establishing dorsoanterior identity are well known in the frog. In mouse, Wnt is classically thought of as a posteriorizing influence due to its role in establishing the primitive streak, however disruption of the wnt pathway prevents the correct positional expression of anterior markers like *Hex* before the establishment of the PS (Huelsken et al. 2000). Additionally, *Hex* and *Cerberus* are not expressed anteriorly when β *catenin* is deleted specifically in the AVE (Lickert et al. 2002). These findings imply a role for Wnt signalling in anterior endodermal specification in mammals too and even suggest a Nieuwkoop like role for AVE.

In addition to Wnt antagonism, TLEs are also implicated in later patterning of anterior endoderm in a positive role. Cells with reduced TLE made ADE very efficiently, however complete lack of TLE3 and TLE4 prevented this. ES cells expressing high levels of TLE1 also expressed high levels of ADE markers. TLEs have been shown to act as corepressors with anterior endodermal markers *Gooseoid* and *Hex* (Jiménez et al. 1999; Swingler et al. 2004). *Gooseoid* represses the mesendoderm marker *Mixl1* and this has been linked to TLE activity (Izzi et al. 2007). A model is suggested where TLE becomes necessary as a corepressor for anterior endoderm inducing homeobox factors to correctly pattern this tissue. In my experiments, increased TLE would only act in this process in a subset of ES cells that have already become endoderm, but would here amplify the effects of endoderm inducing proteins that require TLEs. In an

analogous manner, a pituitary dysplasia phenotype caused by an imbalance between the factors PROP1 and HESX1 can be amplified by ectopic expression of TLE1 acting as a HESX1 corepressor (Dasen et al. 2001). Interestingly, TLE1 R534A increased endoderm markers in the same way as TLE1^{wt} while the less severe point mutation (L743F) did not. Therefore, losing the WRPW interactions decreased endoderm specification, and then subsequently losing eh1 interactions too increased it again. This suggests a WRPW protein may be promoting mesendodermal differentiation while an eh1 containing protein inhibits it. Further investigation of this through an increased panel of markers and inducible TLE1 expression would help resolve this.

TLEs were also observed to affect the balance between self-renewal and differentiation in ES cells. Reduced TLE increased self-renewal and inhibited differentiation while increased TLE had the opposite effects. This did not appear due to inhibition of specific lineages as no consistent effects were seen on early neurectoderm, mesendoderm or primitive endoderm differentiation markers in normal ES culture. However, loss of TLE strongly upregulated self-renewal/pluripotency associated genes, most strongly *Oct4* and *Nanog*, while the reciprocal phenotype was seen with TLE1 overexpression, suggesting this is the mechanism by which TLE affects self renewal.

The transition from naïve, uncommitted cells in an early embryo or a culture of undifferentiated ES cells towards specialised somatic lineages can be seen as being regulated by opposing interlinked processes. The pluripotency/self-renewal gene network must be maintained to allow the growth and maintenance of pluripotent precursors but then downregulated at the appropriate time to allow commitment of cells. The fine balance between these opposing programs allows rapid switching from self-renewal to differentiation of uncommitted cells in a developing embryo. In ES culture, random, stochastic fluctuations in gene networks may cause individual cells to transition towards a more differentiated lineage such as epiblast or primitive endoderm, but with no intrinsic or extrinsic cues to stabilize this transition, and the continued activity of the pluripotency network, these precursors cannot commit stably. The most uncommitted ICM-like cells in the non-excited state have been termed the “ground state” and would have to transition through an epiblast-like state to differentiate. The low NANOG set in a population of cells heterogeneously expressing this marker, could be seen as transitioning away from the ground state (Ying et al. 2008). An alternative

explanation recently supported by work in our lab, is that all ES cells with an active pluripotency network are equally uncommitted and can transition freely between precursors and ICM like state. In this model, there would exist metastable, self-renewing populations of early precursors to both primitive endoderm and primitive ectoderm (Canham et al. 2010). As TLE4 is expressed heterogeneously in ES cells and represses NANOG, an interesting possibility is raised where TLE4 is marking one or more lineage specific groups of precursor cells. It seems unlikely this is a PrEn precursor as no consistent effect was seen on markers like *Gata4* or *Gata6*. However, the positive effects of TLE on neural specification suggest it could be a primitive ectoderm like population. It would be interesting to further investigate this idea through marker expression and by analysing the how the TLE3 and TLE4 reporters correlate with NANOG in ES cells. In addition, TLE3 mORANGE would enable purification of high TLE3 expressing live cells by flow cytometry, which could be tested for their capacity to differentiate towards specific lineages such as neural.

Other experiments suggested by the outcomes of this work include further analysis of the molecular basis of *Nanog* or *Oct4* repression by TLEs. This could be investigated by ChIP analysis of promoter acetylation in these genes in mutants compared to wild type, as TLE would be expected to deacetylate promoters via HDAC recruitment if the effect is direct. To directly probe the role of wnt modulation by TLEs, it would be useful to have a point mutant that lacked HDAC interaction. A *Drosophila Groucho* mutant with a short Q domain deletion, MB5, was recently shown to have absent TCF binding without affecting tetramerization ability (Mieszczanek et al. 2008) and could be replicated in mammalian TLE1. The 34n cells provide a useful background for testing TLE activities. Combining this cell line with Tet regulatable overexpression of specific TLEs or point mutants with altered activities would have several advantages. It would avoid any cultural adaptations to high TLE levels caused by long-term overexpression, which may be the cause of the incomplete rescue seen by TLE1 overexpression in the 34n cells seen here. It would also mean highly controllable TLE activity and allow the analysis of defined aspects of TLE activity at specific timepoints during differentiation, in order to answer the questions raised by experiments in this thesis.

		TLE1 wt	R534A	L743F
d0	up	NeuroD1	NeuroD1	NeuroD1
	down			
d2	up	Six3	Six3	Six3
	down		Nestin	
d4	up	Nestin, Sox1, Six3	Sox1, Six3	Sox1, Six3
	down			
d6	up	Sox1	Nestin, Sox1, BLBP, Tuj1	Nestin, Sox1, BLBP, Tuj1
	down			
d8	up		Nestin, Sox1, BLBP, Tuj1	Nestin, Sox1, BLBP, Tuj1
	down			

		TLE4 ^{-/-}	TLE4 ^{-/-} TLE3 ^{+/-}	34n	34n TLE1
d0	up	Oct4	Oct4	Oct4	Oct4
	down	Nestin	Nestin, NeuroD1	Nestin, NeuroD1	Nestin, NeuroD1
d3	up	Sox1			
	down	Nestin, BLBP, Oct4	Nestin, BLBP, Oct4	Sox1, Nestin, BLBP, Oct4	Nestin, BLBP, Oct4
d5	up			Sox1, Nestin, NeuroD1, BLBP	Sox1, Nestin, NeuroD1, BLBP
	down	Sox1, Nestin, NeuroD1, BLBP	Sox1, Nestin, NeuroD1, BLBP		
d7	up	NeuroD1, BLBP	NeuroD1	NeuroD1	NeuroD1
	down	Sox1, Nestin1	Sox1, Nestin1, BLBP	Nestin, Sox1, BLBP	Nestin, Sox1, BLBP

Fig S.1.1 Summary table of gene expression changes in neural differentiation for TLE1 overexpressing and TLE mutant cells

Genes are listed in the table depending on whether they are up or down in relation to levels in the control cell line in each cell type an timepoint (CAG empty for overexpression lines, TLE4^{+/-} for mutant lines)

		TLE1 wt	R534A	L743F
d0	up			
	down			
d2	up	Wnt3a	Wnt3a	Wnt3a
	down			
d5	up	Oct4, Brachyury, Wnt3a, Cxcr4, FoxA2, Hex, Cerberus	Oct4, Brachyury, Wnt3a, Cxcr4, FoxA2, Hex, Cerberus	Oct4, Brachyury, Wnt3a
	down			
d7	up	FoxA2, Hex, Cerberus	FoxA2, Hex, Cerberus	
	down	Oct4, Cxcr4, Wnt3a	Oct4, Cxcr4, Wnt3a	Oct4, Cxcr4

		TLE4 ^{-/-}	TLE4 ^{-/-} TLE3 ^{+/-}	34n	34n TLE1
d0	up				
	down				
d2	up				
	down				
d5	up		Mixl1, Cxcr4, Goosecoid, Wnt3a	Brachyury, Mixl1, Cxcr4, Goosecoid, Wnt3a	Brachyury, Mixl1, Cxcr4, Goosecoid, Wnt3a, Sox17
	down				
d7	up		Cxcr4, Goosecoid, FoxA2, Frzd5, Hex, Cerberus	Cxcr4, Goosecoid, FoxA2, Wnt3a	Cxcr4, Goosecoid, FoxA2, Wnt3a, Hex, Cerberus
	down				

Fig S.1.2 Summary table of gene expression changes in endodermal differentiation for TLE1 overexpressing and TLE mutant cells

Genes are listed in the table depending on whether they are up or down in relation to levels in the control cell line in each cell type an timepoint (CAG empty for overexpression lines, TLE4^{+/-} for mutant lines)

Common Abbreviations

A	Amperes
AVE	Anterior Visceral Endoderm
ADE	Anterior Definitive Endoderm
AP	Alkaline Phosphatase
bp	base pair
BSA	Bovine Serum Albumin
°C	Degrees Centigrade
CO ₂	Carbon Dioxide
DMSO	Dimethyl Sulphoxide
DNA	Deoxyribonucleic Acid
dNTP	Deoxynucleotide Triphosphate
DTT	Dithiothreitol
DVE	Distal Visceral Endoderm
EDTA	Ethylenediamine Tetra-acetate
EGO	Early Gastrula Organizer
ESC	Embryonic Stem Cell
EtOH	Ethanol
FCS	Fetal Calf Serum
g	grams
GFP	Green Fluorescent Protein
GMEM	Glasgow's Modified Eagle's Medium
H ₂ O	Water
hr	hour
ICM	Inner Cell Mass
KAc	Potassium Acetate
kb	kilobase
kD	Kilodaltons

l	litre
LB	Luria Broth
m	minute
μ	micro
M	Molar
MgCl ₂	Magnesium Chloride
N	nano
nm	nanometres
NaCl	Sodium Chloride
NaOH	Sodium hydroxide
PBS	Phosphate Buffered Saline
PBST	Phosphate Buffered Saline with Tween20
PCR	Polymerase Chain reaction
PLAP	Placental Alkaline Phosphatase
PFA	Paraformaldehyde
PrE	Primitive Endoderm
PS	Primitive Streak
RNA	Ribonucleic Acid
rpm	revolutions per minute
RT	Room Temperature
SDS	Sodium Dodecyl Sulfate
TE	Tris-EDTA
TE-SDS	Tris-EDTA with SDS
TAE	Tris Acetate EDTA
UV	Ultra Violet
V	Volts
w/v	Weight Volume

Appendix - Publication

Inhibition of Cortical Neuron Differentiation by Groucho/TLE1 Requires Interaction with WRPW, but Not Eh1, Repressor Peptides*

Received for publication, January 28, 2008, and in revised form, June 13, 2008. Published, JBC Papers in Press, July 8, 2008, DOI 10.1074/jbc.M800722200

Manuel Buscarlet[‡], Alessandro Perin[‡], Adam Laing[§], Joshua Mark Brickman^{§1}, and Stefano Stifani^{‡2}

From the [‡]Centre for Neuronal Survival, Montreal Neurological Institute, McGill University, Montreal, Quebec H3A 2B4, Canada and the [§]Institute for Stem Cell Research, MRC Centre for Regenerative Medicine, King's Buildings, West Mains Road, Edinburgh EH9 3JQ, United Kingdom

In both invertebrates and vertebrates, transcriptional co-repressors of the Groucho/transducin-like Enhancer of split (Gro/TLE) family regulate a number of developmental mechanisms, including neuronal differentiation. The pleiotropic activity of Gro/TLE depends on context-specific interactions with a variety of DNA-binding proteins. Most of those factors engage Gro/TLE through two different types of short peptide motifs, the WRP(W/Y) tetrapeptide and the Engrailed homology 1 (Eh1) sequence (FXLXXIL). The aim of this study was to elucidate the contribution of WRP(W/Y) and Eh1 motifs to mammalian Gro/TLE anti-neurogenic activity. Here we describe point mutations within the C-terminal WD40 repeat domain of Gro/TLE1 that do not perturb protein folding but disrupt the ability of Gro/TLE1 to inhibit the differentiation of cerebral cortex neural progenitor cells into neurons. One of those mutations, L743F, selectively blocks binding to Hes1, an anti-neurogenic basic helix-loop-helix protein that harbors a WRPW motif. In contrast, the L743F mutation does not disrupt binding to Engrailed1 and FoxG1, which both contain Eh1 motifs, nor to Tcf3, which binds to the Gro/TLE N terminus. These results demonstrate that the recruitment of transcription factors harboring WRP(W/Y) tetrapeptides is essential to the anti-neurogenic function of Gro/TLE1.

Transcriptional co-repressors of the Groucho/transducin-like Enhancer of split (Gro/TLE)³ family play critical roles during multiple developmental processes, including neuronal differentiation in the developing mammalian forebrain (1). Gro/

TLEs act as co-repressors for a variety of DNA-binding transcription factors. Some of those proteins are dedicated transcriptional repressors while others mediate repression or transactivation depending on specific contexts (1–4). Through interactions with a large number of transcriptional regulators, Gro/TLEs are involved in the gene regulatory functions of a variety of signaling pathways, including Notch, Wnt/Wingless, transforming growth factor- β superfamily, and epidermal growth factor receptor signal transduction mechanisms (1–6). Moreover, growing evidence suggests important roles for Gro/TLEs in integrating these different signaling cascades during several developmental processes (1, 5).

The regulation of neuronal differentiation was one of the first functions of Gro/TLE proteins to be characterized. During *Drosophila* neural development, Gro participates in the Notch-mediated lateral inhibition mechanism that restricts the number of committed neuroblasts within proneural clusters containing initially equipotential presumptive neural progenitor cells (7, 8). Neuroblasts undergoing commitment activate the Notch receptor in adjacent cells, resulting in the transcriptional induction of genes encoding basic helix loop helix (bHLH) proteins of the Hairy/Enhancer of split (Hes) family. These DNA-binding proteins recruit Gro to form complexes that repress the expression, as well as biochemical activity, of proteins that promote neuronal differentiation, like the bHLH factors encoded by *achaete-scute* complex and *atonal* genes (9–11). Loss-of-function mutations of *Drosophila gro* result in the differentiation of supernumerary neurons, similar to the phenotype caused by disruption of *Notch* or *Enhancer of split* genes (7, 8).

Mammalian Gro/TLE proteins also perform anti-neurogenic functions. Gro/TLE1 and Gro/TLE3 are expressed in undifferentiated neural progenitor cells of the ventricular zone of the telencephalic vesicles (12–14). Forced expression of *Gro/TLE1* in the forebrain of transgenic mice causes an inhibition/delay of neuronal development *in vivo* (15). Similarly, exogenous expression of *Gro/TLE1* in primary cultures of undifferentiated neural progenitor cells from the dorsal telencephalon causes decreased neuronal differentiation and an accumulation of proliferating progenitor cells (14).

The molecular mechanisms underlying Gro/TLE-mediated inhibition of neuronal differentiation in the mammalian forebrain remain to be defined. Gro/TLEs form complexes, and repress transcription, with a number of DNA-binding proteins expressed during forebrain neuronal differentiation. These

* This work was supported in part by a Residency Fellowship from the University of Padova (Neurosurgical Unit, Treviso Hospital, Treviso, Italy) (to A. P.), an MRC Studentship (to A. L.), by grants from the Wellcome Trust and Scottish Funding Council (to J. M. B.), and the Canadian Institutes of Health Research (MOP-13957) (to S. S.). The costs of publication of this article were defrayed in part by the payment of page charges. This article must therefore be hereby marked "advertisement" in accordance with 18 U.S.C. Section 1734 solely to indicate this fact.

¹ A recipient of an MRC Senior Non-Clinical Fellowship.

² A Chercheur National of the Fonds de la Recherche en Sante du Quebec. To whom correspondence should be addressed: Montreal Neurological Institute, 3801 Rue University, Montreal, Quebec H3A2B4, Canada. Fax: 514-398-1319; E-mail: stefano.stifani@mcgill.ca.

³ The abbreviations used are: Gro/TLE, Groucho/transducin-like Enhancer of split; bHLH, basic helix loop helix; Eh1, Engrailed homology 1; En1, Engrailed1; GFP, green fluorescent protein; Hes, Hairy/Enhancer of split; WD, WD40 repeat; GST, glutathione S-transferase; HA, hemagglutinin; WT, wild type.

Regulation of Gro/TLE1 Anti-neurogenic Activity

include, but are not limited to, bHLH proteins of the Hes family, like Hes1 (10, 14, 16, 17), forkhead box proteins, such as FoxG1 (18–20), and homeodomain proteins of the Six (21, 22), Pax (23), and Otx (24) families. Most transcription factors that bind to Gro/TLE interact with the C-terminal WD40 repeat (WD) domain of the latter and can be grouped into two main classes based on the fact that they utilize two different types of short peptide sequences to recruit Gro/TLE co-repressors. Those “repressor peptides” belong to either the WRP(W/Y) (termed WRPW hereafter) or Engrailed homology 1 (Eh1; FXLXXIL) motif families (1). Although different in sequence, both WRPW and Eh1 peptides bind to an overlapping, but not completely identical, site on the surface of the Gro/TLE WD domain (25).

Here we describe studies aimed at determining the contribution of different groups of transcription factors to the ability of Gro/TLE1 to inhibit the differentiation of cerebral cortex (cortical) neural progenitor cells into neurons. Our results show that Gro/TLE1 recruitment via repressor peptides of the WRPW family is essential for Gro/TLE1-mediated inhibition of neuronal differentiation. In contrast, the ability to interact with proteins that either contain repressor peptides of the Eh1 type or bind to the Gro/TLE N terminus is not sufficient to mediate Gro/TLE1 anti-neurogenic function. These results characterize the mechanisms underlying Gro/TLE1 activity during cortical neurogenesis.

EXPERIMENTAL PROCEDURES

Site-directed Mutagenesis and DNA Plasmids—DNAs encoding mutated forms of Gro/TLE1 harboring the mutations V486S, C488R, R534A, E550K, and L743F were generated by site-directed mutagenesis using the QuikChange II site-directed mutagenesis kit (Stratagene, La Jolla, CA), using pCMV2-FLAG-Gro/TLE1 (14) as substrate. Oligonucleotide primers used for mutagenesis were as follows (mutations are underlined): V486S-F: 5'-CAACCACGGGG-AGTCGGTGTGCGCTGTGA, C488R-F: 5'-CGGGGAGG-TGGTGAGAGCTGTGACCATCAGC, R534A-F: 5'-CTG-AACAGAGACAATTATATCGCTTCCTGTAAATTGCT-ACCCG, E550K-F: 5'-CTCATAGTGGGAGGGAAAGCCAG-TACTTTGTCC, and L743F-F: 5'-GAGTCCTCGTCAGTGT-TTAGCTGTGACATCTC. *pcDNA3-GAL4dbd-Gro/TLE1* plasmids were generated by amplifying by PCR the entire coding sequence of each mutant using the appropriate pCMV2-FLAG-Gro/TLE1 plasmids as template, followed by subcloning into the EcoRV site of *pcDNA3-GAL4dbd* plasmid, which encodes the DNA-binding domain of GAL4 (GAL4dbd). Vectors *pEBG-Hes1*, *pEBG-Hes1(ΔWRPW)*, *pEGFP*, *pCMV2-FLAG-Gro/TLE1*, *pCMV2-HA-FoxG1*, *pMyc-Tcf3*, *pCMV2-HA-En1*, *p5xGAL4UAS-SV40p-luciferase*, and *pRSV-β-galactosidase* were described (14, 16, 18, 20).

Transcription Assays—For studies using a GAL4-responsive promoter, HEK293 cells were transfected using the SuperFect reagent (Qiagen) as described (14, 20). The total amount of transfected DNA was adjusted in each case at 3 μg per well using *pcDNA3*. Transcription assays were performed using 1.5 μg/well of reporter construct *p5xGAL4UAS-SV40p-luciferase* in the presence or absence of plasmids *pcDNA3-GAL4dbd* or *pcDNA3-GAL4dbd-Gro/TLE1* (WT, V486S, C488R, R534A,

E550K, or L743F) (1.0 μg/well). In each case, 0.5 μg/well of β-galactosidase expression plasmid, *pRSV-β-gal*, was used to normalize for transfection efficiency. Twenty-four hours after transfection, cells were subjected to determination of luciferase activity as described (14, 16, 19, 26). Results were expressed as mean values ± S.D. Expression of GAL4dbd-Gro/TLE1 fusion proteins was detected using an anti-Gro/TLE1 antibody (1:1,000) (14).

Interaction Assays in Transfected Cells and Western Blotting Analysis—HEK293 cells were cultured and transfected using SuperFect. In each experiment, cells were co-transfected with 1.0 μg of *pCMV2-FLAG-Gro/TLE1* (WT, V486S, C488R, R534A, E550K, or L743F) and 1.0 μg of either *pEBG-HES1* (or *pEBG-HES1(ΔWRPW)* as control), *pCMV2-HA-FoxG1*, *pMyc-Tcf3*, or *pCMV2-HA-En1*. Cell lysates were prepared and GST co-precipitations or co-immunoprecipitations using either anti-HA (Covance, Berkeley, CA) or anti-Gro/TLE1 (14) antibodies were performed as described (14, 20, 27). This was followed by Western blotting analysis using anti-FLAG (1:10,000; Sigma), anti-GST (1:500; Santa Cruz Biotechnology, Santa Cruz, CA), anti-HA (1:5,000), or anti-Myc (1:200; BD Pharmingen, San Diego, CA) antibodies.

Cortical Neural Progenitor Cell Cultures—Primary cultures of neural progenitor cells were established from dorsal telencephalic cortices dissected from embryonic day (E) 12–14 mouse embryos as described (27–31). Cells were seeded into four-well chamber slides (Nalgene Nunc, Rochester, NY) coated with 0.1% poly-D-lysine and 0.2% laminin (BD Biosciences, Bedford Park, MD), cultured in Neurobasal medium supplemented with 1% N₂, 2% B27, 0.5 mM glutamine, 1% penicillin-streptomycin (Invitrogen), and 40 ng/ml of FGF2 (Collaborative Research, Bedford, MA). After 48 h *in vitro*, cells were transfected with plasmids encoding either enhanced green fluorescent protein (GFP) alone (0.2 μg/well), or both GFP (0.2 μg/well) and Gro/TLE1 (*pCMV2-FLAG-Gro/TLE1* (WT, V486S, C488R, R534A, E550K, or L743F)) (0.8 μg/well). When needed, the total amount of DNA was adjusted to 1.0 μg using *pcDNA3*. DNA was mixed with 50 μl of OptiMEM medium (Invitrogen), followed by incubation for 5 min. An equal volume of OptiMEM medium were mixed separately with Lipofectamine 2000 reagent (Invitrogen; 2 μl/μg of DNA) and then combined with the DNA mixture and incubated for 20 min at room temperature. The DNA-Lipofectamine 2000 mixture was then added dropwise to each well. Three days later, cells were fixed and subjected to immunocytochemistry using antibodies against the proliferating cell marker Ki67 (1:200; BD Pharmingen), the neural progenitor cell marker nestin (1:400; Chemicon, Temecula, CA), the neuronal cell marker βIII-tubulin (1:300; Promega), the neuronal cell marker neuron specific nuclear protein (NeuN) (1:100; Chemicon), the astrocyte cell marker glial fibrillary acidic protein (GFAP; 1:300; Sigma), or activated caspase-3 (1:200; BD Pharmingen). Cells were counterstained with Hoechst 33258 (Sigma) before examination by fluorescence microscopy (14, 27, 31). Grayscale images were digitally assigned to the appropriate red or green channel using Northern Eclipse software (Empix, Ontario, Canada). Three to six random fields of each condition (per experiment) were used for quantitation of the percent of GFP-positive cells co-expressing

specific markers (28–31). Results were expressed as the mean values \pm S.D. At least six separate experiments were conducted in each case, and statistical analysis was performed using the Student's *t*-test.

RESULTS

Characterization of Point Mutations in the WD Domain of Gro/TLE1 That Do Not Disrupt Protein Folding—Previous mutation and structural studies of WD domain containing proteins like β -transducin repeat-containing protein 1 (32), the β -subunit of G protein-coupled receptors (33, 34), and the yeast Gro/TLE analogue Tup1 (35) have revealed that residues implicated in protein-protein interactions are preferentially located at similar positions on the external surface surrounding the central channel of the β -propeller. Multiple blades and residues are implicated in those interactions. More specifically, surface residues located at the start of the first β -sheet or just after the second one are often implicated in protein-protein interactions (32).

In agreement with those findings, analysis of the crystal structure of the Gro/TLE1 WD domain demonstrated that one side of the central pore of the β -propeller harbors overlapping binding sites for both WRPW and Eh1 peptides (25). This common transcription factor-binding pocket contains key surface residues located within separate blades of the β -propeller. Some of those residues are essential for interaction with both WRPW and Eh1 peptides, while others are required for binding to the former but not the latter (25).

The crystal structure of the WD domain of Gro/TLE1 (25, 36) was utilized in conjunction with naturally occurring mutations at evolutionarily conserved residues in Gro/TLE-related proteins such as *Drosophila* Gro (25), *Caenorhabditis elegans* UNC-37 (37, 38), and yeast Tup1 (35, 39) to select five residues within the WD domain of Gro/TLE1 as *in vitro* mutagenesis targets (Fig. 1, A–C). More specifically, we generated the following mutations: V486S (similar to the Gro mutations V435A and V435L), C488R (analogous to mutations C348R in Tup1 and C437M in Gro), R534A (analogous to mutation R483H in Gro), E550K (analogous to mutations E463N in Tup1, E394K in UNC-37, and E499A in Gro), and L743F (analogous to mutation L692F in Gro) (Fig. 1D).

Based on crystallographic data (25, 36), these mutations were not expected to disrupt the overall structure of the WD domain. In agreement with this prediction, we observed that all mutated proteins migrated on denaturing polyacrylamide gels like wild-type Gro/TLE1 (Fig. 1E), were able to translocate to the nucleus (Fig. 1F), and retained the ability to repress transcription from a basally active promoter when expressed as fusion proteins with the DNA-binding domain of the yeast protein GAL4 (Fig. 2). Together, these results demonstrate that the point mutations in the WD domain of Gro/TLE1 selected for this study do not significantly perturb the structure and biochemical activity of Gro/TLE1.

Different Effects of WD Domain Mutations on the Ability of Gro/TLE1 to Interact with WRPW or Eh1 Repressor Peptides—To assess the possible effects of the WD domain mutations on the anti-neurogenic activity of Gro/TLE1, we first determined whether they would block Gro/TLE1 interaction with different

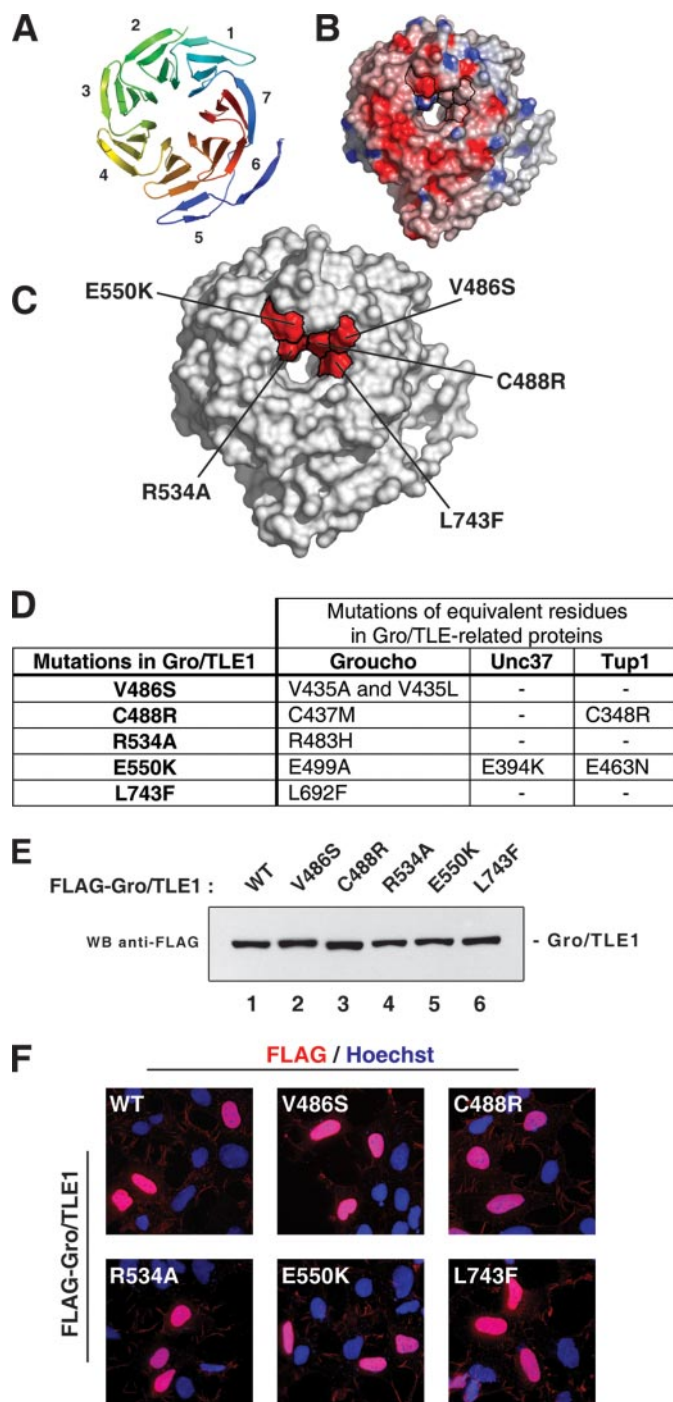


FIGURE 1. Characterization of Gro/TLE1 WD domain mutations. A, schematic representation of the Gro/TLE1 C-terminal β -propeller composed of seven blades each consisting of a four-stranded β -sheet (36). B, surface mapping and electrostatic potential representation of the β -propeller (color coding: red for negative charges and blue for positive charges) showing charged residues surrounding the predicted central hydrophilic channel where WRPW(P/Y) and Eh1 repressor peptides bind. C, mapping of the five point mutations (V486S, C488R, R534A, E550K, and L743F) introduced in the Gro/TLE1 WD domain, shown in red. D, list of mutations analyzed in this study and equivalent mutations in *Drosophila* Gro, *C. elegans* UNC-37, and yeast Tup1. E, Western blotting (WB) analysis using an anti-FLAG antibody of WT or mutated forms of FLAG epitope-tagged Gro/TLE1 proteins expressed in HEK293 cells. F, nuclear localization of wild-type or mutated Gro/TLE1 proteins determined by immunofluorescence analysis of transfected HEK293 cells using an anti-FLAG antibody.

Regulation of Gro/TLE1 Anti-neurogenic Activity

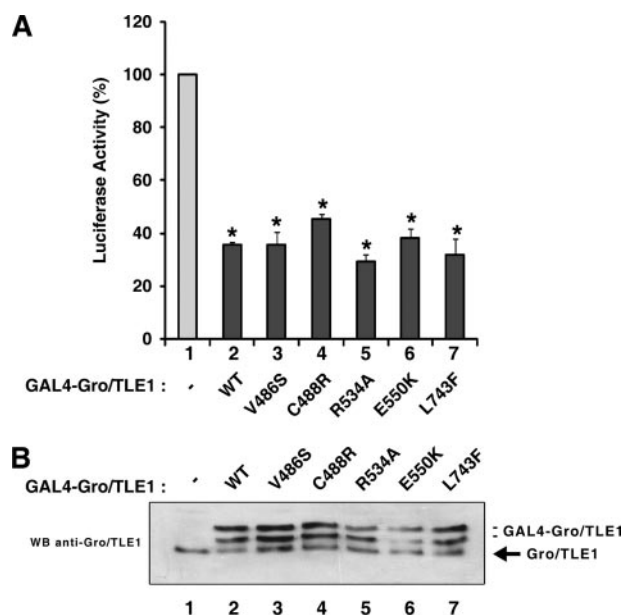


FIGURE 2. Analysis of transcription repression activity of wild-type and mutated Gro/TLE1 proteins. *A*, HEK293 cells were transfected with a *p5xGAL4UAS-SV40p-luciferase* reporter construct (1.5 μ g/transfection) in the absence (bar 1) or presence of WT (bar 2) or mutated (bars 3–7) forms of GAL4dbd-Gro/TLE1 (1 μ g/transfection). Basal luciferase activity in the absence of effector plasmids was considered 100%, and values in the presence of effector plasmids were expressed as the mean \pm S.D. of at least three separate experiments performed in duplicate; *, $p < 0.001$. *B*, Western blotting (WB) analysis of Gro/TLE1 proteins used in the transcription assays using anti-Gro/TLE1 antibody. GAL4dbd-Gro/TLE1 consistently migrated as a doublet; the migration of this doublet was slower than endogenous Gro/TLE1 (see arrow). The level of expression of exogenous GAL4dbd-Gro/TLE1 proteins was similar to that of endogenous Gro/TLE1.

transcription partners. Several Gro/TLE-binding factors that contain either WRPW or Eh1 motifs are expressed during cortical neuron development in cells where Gro/TLE1 is also expressed (18, 21–24). We therefore selected specific Gro/TLE1 transcription partners that would represent examples of different categories of proteins. The bHLH factor Hes1 was selected as a prototypical WRPW motif-bearing protein. Moreover, Hes1 is a critical regulator of cortical neurogenesis (40–42). Engrailed1 (En1) was chosen as a typical example of a protein that uses an Eh1 motif to recruit Gro/TLE proteins (43). We also examined Tcf3, as an example of a transcription partner that interacts with the N terminus, and not the WD domain, of Gro/TLE (44).

Co-transfections followed by pull-down (Fig. 3A) or co-immunoprecipitations (Fig. 3, B and C) assays showed that separate WD mutations had different effects on Gro/TLE1 ability to interact with those proteins. All mutations completely blocked or severely reduced the interaction with Hes1 (Fig. 3A), suggesting that each of those residues is important for optimal WRPW peptide recognition. In contrast, the interaction of Gro/TLE1 with En1 was disrupted only by mutations C488R, R534A, and E550K, but not by the V486S and L743F mutations (Fig. 3B). These findings show that WRPW- and Eh1 motif recognition by the WD domain of Gro/TLE1 is mediated by both overlapping and separate residues. In particular, the contribution of Leu-743 is essential for WRPW peptide binding but not for Eh1 motif recognition. In contrast to the results with Hes1 and En1, all Gro/TLE1 WD mutations retained the ability to

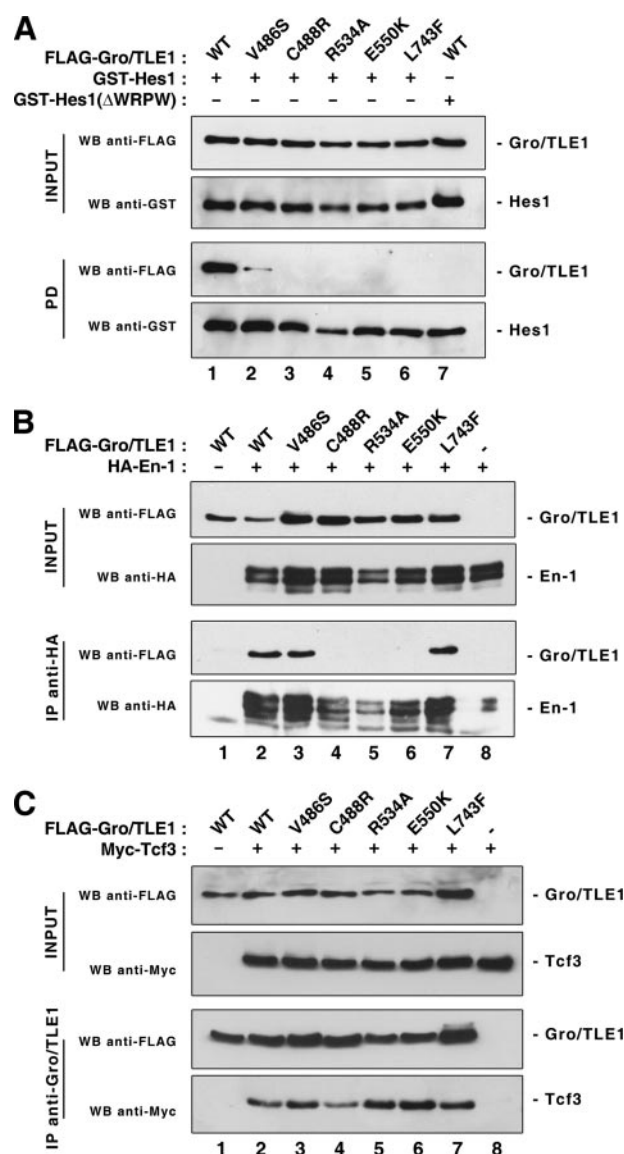


FIGURE 3. Effect of different Gro/TLE1 WD domain mutations on interaction with Hes1, En1, or Tcf3. *A*, HEK293 cells were co-transfected with plasmids encoding FLAG epitope-tagged WT or mutated Gro/TLE1 and either a fusion protein of GST and full-length Hes1 (lanes 1–6) or truncated Hes1 lacking the WRPW motif required for Gro/TLE binding (Δ WRPW) (lane 7). Each cell lysate (INPUT) was incubated with glutathione-Sepharose beads and the precipitated material (PD, pull-down), together with 1:10 of each input lysate, was subjected to Western blotting (WB) analysis with anti-FLAG or anti-GST antibodies. *B* and *C*, HEK293 cells were co-transfected with plasmids encoding FLAG epitope-tagged wild-type or mutated Gro/TLE1 proteins, as indicated, and either HA epitope-tagged En1 (B) or Myc epitope-tagged *Xenopus*-Tcf3 (C). Each cell lysate (INPUT) was subjected to immunoprecipitation (IP) with either anti-HA (B) or anti-Gro/TLE1 (C) antibodies. Immunoprecipitates, together with 1:10 of each input lysate, were analyzed by Western blotting with the indicated antibodies.

bind to Tcf3 (Fig. 3C). In agreement with this finding, each mutated protein repressed trans-activation mediated by β -catenin/Tcf complexes in transfected cells (data not shown). These results are consistent with the notion that Tcf/Lef proteins interact with the N-terminal domain of Gro/TLE (44).

We next examined the ability of mutated Gro/TLE1 proteins to bind to the forkhead transcription factor FoxG1, which is a critical regulator of telencephalic neurogenesis (45). Previous *in vitro* studies have suggested that Gro/TLE1 binds to FoxG1

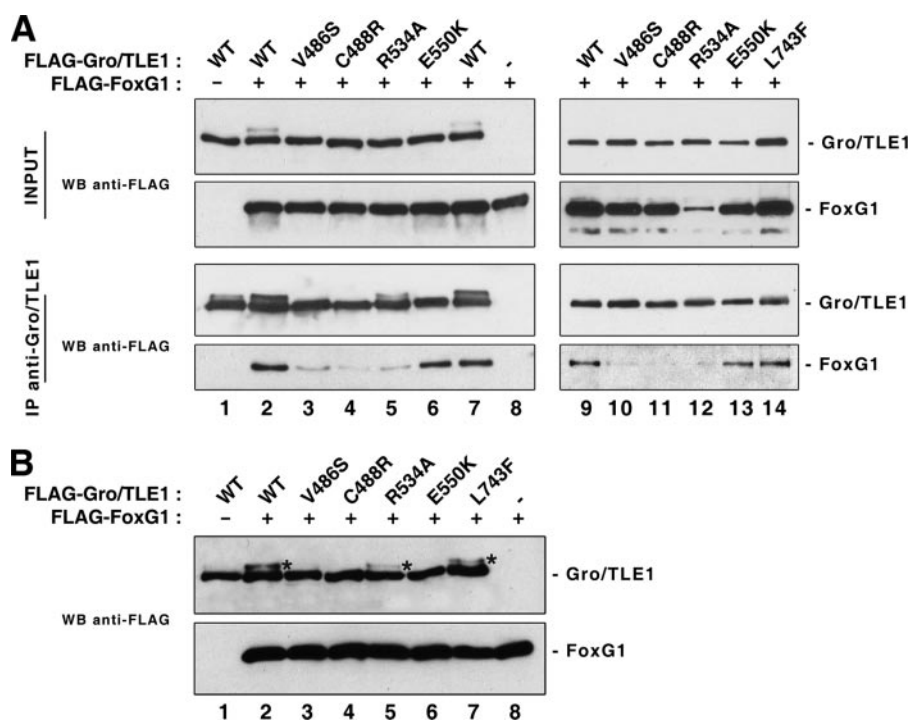


FIGURE 4. Effect of different Gro/TLE1 WD domain mutations on interaction with FoxG1. *A*, HEK293 cells were co-transfected with plasmids encoding FLAG epitope-tagged WT or mutated Gro/TLE1 proteins, as indicated, and FLAG-tagged FoxG1. Each cell lysate (*INPUT*) was subjected to immunoprecipitation (*IP*) with an anti-Gro/TLE1 antibody. Immunoprecipitates, together with 1:10 of each input lysate, were subjected to SDS-polyacrylamide gel electrophoresis on either 6% (*lanes 1–8*) or 10% (*lanes 9–14*) gels, followed by Western blotting (*WB*) with an anti-FLAG antibody. *B*, HEK293 cells were co-transfected with the indicated combinations of proteins, followed by fractionation of cell lysates on a 6% SDS-polyacrylamide gel and Western blotting with an anti-FLAG antibody. Asterisks are placed next to the slower form of Gro/TLE1 observed in the presence of FoxG1.

using both its C-terminal WD domain and N-terminal Q domain (18). This possibility is consistent with the presence of both a putative Eh1 motif (FSINSLV) at the N terminus of FoxG1 and a separate Gro/TLE1 binding sequence at a more C-terminal location (18, 19), suggesting that FoxG1 uses multiple sequences to engage Gro/TLE1. Co-immunoprecipitation studies showed that mutations E550K and L743F did not significantly affect the Gro/TLE1 ability to bind to FoxG1 (Fig. 4*A*). The other mutations reduced but did not completely block this interaction. These observations suggest that the mode of Gro/TLE1 recruitment by FoxG1 is complex and involves separate domains. Nevertheless, the observation that FoxG1 still interacts with the L743F mutant suggests further that Leu-743 is critical for binding to WRPW peptides but not other Gro/TLE1 binding sequences.

Analysis of Gro/TLE1 proteins on low percentage polyacrylamide gels allowed the resolution of separate Gro/TLE1 species with different electrophoretic mobility (Fig. 4*A*, *lanes 1–7*, and Fig. 4*B*). Reduced electrophoretic mobility of Gro/TLE1 has been shown previously to result from increased phosphorylation, a process that is promoted by interaction with several transcription partners, including FoxG1, and is referred to as “cofactor-activated phosphorylation” (14, 16). We found that mutations that reduced binding to FoxG1, such as V486S, C488R, and R534A, also reduced the increased phosphorylation of Gro/TLE1 observed in the presence of FoxG1 (Fig. 4*B*, see *lanes 2–5*). Importantly, mutation E550K, which does not

prevent binding to FoxG1, completely blocked the cofactor-activated phosphorylation of Gro/TLE1 (Fig. 4*B*, *lane 6*). These findings suggest an essential role for Glu-550 in the regulation of Gro/TLE1 phosphorylation, possibly by mediating protein-protein interactions with critical factors.

Taken together, these results suggest that different WD domain mutations provide a useful means of uncoupling transcription repression partner recognition, permitting the examination of the specific contributions of separate protein classes to the biological functions of Gro/TLE1.

Requirement for WRPW Motif Recruitment for Gro/TLE1 Anti-neurogenic Activity—Forced expression of Gro/TLE1 inhibits/delays cortical neuron differentiation in the telencephalon of developing transgenic mouse embryos and cultures of cortical neural progenitor cells (14, 15). To clarify the contribution of transcription factors containing WRPW or Eh1 motifs to its anti-neurogenic function, we exogenously expressed wild-type or

mutated Gro/TLE1 proteins in primary cultures of neural progenitor cells obtained from dissected dorsal telencephalon from E12–E14 mouse embryos (Fig. 5, *A* and *B*). This defined primary culture system (“cortical progenitor cells”) has been used on multiple occasions to investigate the functions of extrinsic and intrinsic regulators of cortical neuron differentiation (27–31, 46–49). Enhanced GFP was co-expressed with Gro/TLE1 to visualize the transfected cells, which were analyzed for the expression of markers of proliferating cells, undifferentiated neural progenitors, postmitotic neurons, or astrocytes after 5 days *in vitro* (Fig. 5*B* and data not shown). As previously described (14), exogenous expression of wild-type Gro/TLE1 resulted in an increase in the number of cells co-expressing GFP and the mitotic cell marker Ki67, compared with control (Fig. 5*C*). Wild-type Gro/TLE1 caused a similar increase in the number of nestin-positive neural progenitor cells (Fig. 5*D*). These effects were accompanied by a significant reduction in the number of GFP-positive cells exhibiting a neuronal morphology and expressing the neuronal cell markers, NeuN and β III-tubulin (Fig. 5, *F* and *G*). GFAP-positive astrocytes accounted for a small fraction of the cells in culture and Gro/TLE1 expression had no detectable effect on their number (Fig. 5*E*). The number of transfected cells showing signs of programmed cell death, like the expression of activated caspase-3, was small under all conditions tested (Fig. 5*H*). These results show a role for Gro/TLE1 in delaying/inhibiting the differentiation of cortical progenitor cells into neurons.

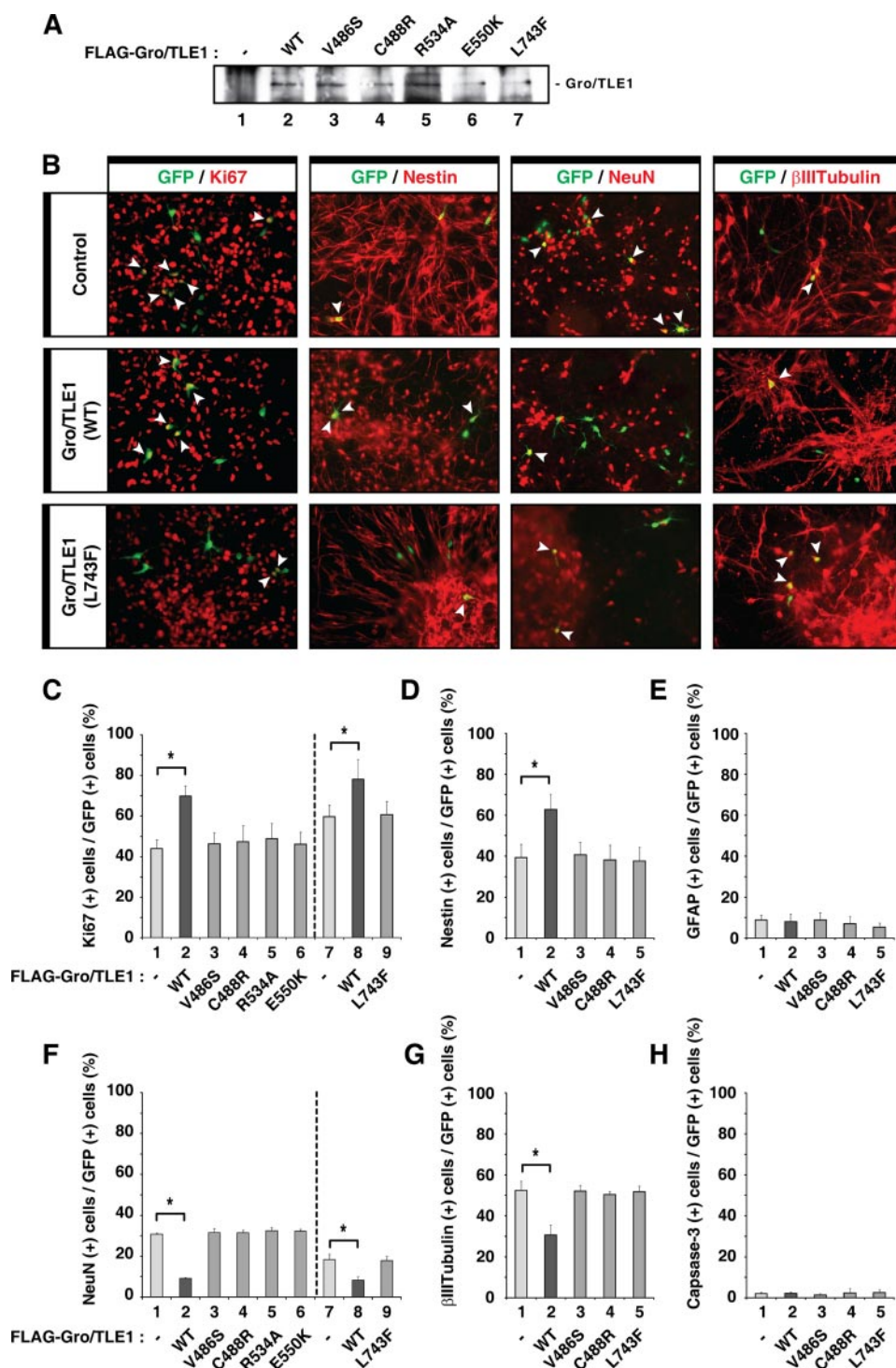


FIGURE 5. Effect of Gro/TLE1 proteins on cortical neuron differentiation. A, primary cultures of E13.0 mouse embryonic cortical progenitor cells were transfected with plasmids encoding FLAG-tagged forms of Gro/TLE1 (lanes 2–7), followed by immunoprecipitation (IP) and Western blotting (WB) analysis of the transfected proteins with anti-FLAG antibody; untransfected cells were analyzed in lane 1. B, cortical progenitor cells were transfected with either GFP alone (Control, top row) or a combination of GFP and wild-type Gro/TLE1 (middle row), Gro/TLE1^{L743F} (bottom row), or other mutated forms of Gro/TLE1 (not shown). Approximately 48 h later, cells were fixed and subjected to double-labeling analysis of the expression of GFP (green) and either the progenitor cell markers Ki67 and nestin, the neuronal markers NeuN and βIII-tubulin (red), the astrocyte marker GFAP or activated caspase-3 (not shown). Arrowheads point to examples of double-labeled cells. C–H, quantitation of the percentage of GFP-positive cells that also expressed the indicated markers. Results are shown as the mean ± S.D. (>500 cells were counted in each case; n ≥ 6; *p < 0.001 using the Student's *t* test). F and G, βIII-tubulin immunoreactivity marks both younger and older neuron populations, whereas NeuN immunoreactivity labels preferentially more mature neurons. As a result, larger numbers of neurons are detected using the anti-βIII-tubulin antibody compared with the anti-NeuN antibody.

The anti-neurogenic effect of Gro/TLE1 was abolished by mutations that selectively disrupt interaction with WRPW, but not Eh1, repressor peptides, such as V486S and L743F (Fig. 5, C and D, F and G). The E550K mutation, which prevents interaction with Hes1 and En1 but does not block binding to FoxG1, also abrogated the anti-neurogenic affect of Gro/TLE1 (Fig. 5, C and F). The same was true for mutations, like C488R and R534A, which disrupt the interaction of Gro/TLE1 with Hes1, En1, and Foxg1, but not Tcf3 (Fig. 5, C and D, F and G). None of the mutated Gro/TLE1 proteins caused significant changes in the number of cells expressing GFAP or activated caspase-3 (Fig. 5, E and H). Taken together, these results indicate that the anti-neurogenic activity of Gro/TLE1 depends on the recruitment of WRPW motif family proteins. They suggest further that Hes family members are the primary anti-neurogenic partners of Gro/TLE1 during cortical neuron development.

DISCUSSION

In this report, we sought to determine whether the ability of Gro/TLE1 to inhibit/delay the transition of cortical progenitor cells into neurons depends on interactions with proteins containing the WRPW or/and Eh1 repressor peptides, or neither of those. By analyzing a panel of WD domain mutations that selectively impair the interaction of Gro/TLE1 with different transcriptional cofactors, we have shown that WRPW motif recognition is essential for Gro/TLE1 anti-neurogenic activity.

Essential Role of Specific WD Domain Residues in Repressor Peptide Recognition—Using information derived from previous structural and genetic studies, we generated a panel of point mutations within the C-terminal WD domain of Gro/TLE1 that do not disrupt the overall structure of this β-propeller, as indicated by the ability of the mutated proteins to translocate to the nucleus and repress

both basal and activated transcription in transfected cells. These mutations can be grouped into two categories based on their effect on repressor peptide recognition. One group (category-1 mutations) disrupts interactions with both WRPW and Eh1 peptides whereas the second (category-2) blocks binding to the former but not the latter.

Mutations C488R, R534A, and E550K behaved as category-1 mutations in our study. Those three residues sit near the mouth of the central pore of the β -propeller (25, 36) and participate in key interactions with the C-terminal tryptophan, N-terminal tryptophan, and arginine of the WRPW peptide, respectively (25). In the case of the Eh1 motif (FXLXXIL), those residues make key contacts with leucine 7, phenylalanine 1, and isoleucine 3, respectively (25). The essential roles of those amino acids are further highlighted by their evolutionary conservation among Gro/TLE orthologs and analogs and the severe effects of naturally occurring mutations at those sites. More specifically, amino acid positions corresponding to Glu-550 in Gro/TLE1 are conserved in *Drosophila* Gro (Glu-499), *C. elegans* UNC-37 (Glu-394), and yeast Tup1 (Glu-463). Mutations targeting this position were found for Tup1 (E463N) (39) and UNC-37 (E394K) (38). In both cases, these mutations significantly perturb the biological functions of these proteins. Similarly, the position equivalent to Arg-534 of Gro/TLE1 is mutated (R483H) in a *Drosophila gro* allele that causes widespread perturbation of the embryonic functions of this gene (25). Taken together, these observations are consistent with the notion that category-1 residues are critical for Gro/TLE protein ability to engage a large number of transcription partners.

We have found that V486S and L743F behave as category-2 mutations. Those residues are part of a hydrophobic recess located at the mouth of the central pore, and are involved in interactions with the side chain of the C-terminal tryptophan of the WRPW peptide (25). This hydrophobic depression appears to be flexible enough to accommodate the equally flexible side chains of isoleucine-3, isoleucine-6, and leucine-7 of the Eh1 motif even in the presence of Val-486 or Leu-743 mutations (this study and Ref. 25). Analysis in *Drosophila* shows that mutation of Leu-629 (equivalent to Leu-743 of Gro/TLE1) causes embryonic phenotypes that are somewhat weaker than those resulting from mutations of WD domain residues required for interactions with both WRPW and Eh1 peptides (25), consistent with only a partial perturbation of protein-protein interactions.

The effects of the WD domain mutations on cofactor binding do not seem to be due to a generalized misfolding of Gro/TLE1, because all the mutated proteins were competent to interact with, and repress trans-activation mediated by, Tcf proteins. These observations suggest further that those mutations should not cause a generalized loss of the many functions of Gro/TLE1, as they are not predicted to affect all of its protein-protein interactions. It should be noted, however, that we cannot rule out the possibility that at least some of those mutations might disrupt interactions with global cofactors that bind to the WD domain and are required by most, if not all, transcription partners, including those that bind to the N terminus of Gro/TLE1.

Uncoupling of Repressor Peptide Recognition Reveals an Essential Role for WRPW Motif Recognition in Gro/TLE1 Anti-

neurogenic Activity—The present studies show that category-1 mutations, which block Gro/TLE1 ability to interact with both WRPW and Eh1 peptides, also disrupt its inhibitory effect on cortical neuron differentiation. Category-2 mutations, which do not prevent binding to proteins that harbor an Eh1 motif (like En1 or FoxG1) or proteins that bind exclusively to the Gro/TLE1 N-terminal Q domain (like Tcf3), also disrupt Gro/TLE1 anti-neurogenic function. These results indicate that the ability to become recruited by transcription factors that either belong to the Eh1 peptide group or engage Gro/TLE via the N-terminal region of the latter is not sufficient to mediate Gro/TLE1 anti-neurogenic activity. Thus, even though members of these protein groups are expressed in forebrain progenitor cells, they do not appear to be involved in Gro/TLE1-mediated inhibition of cortical neurogenesis. Instead, our findings show that Gro/TLE1 depends on interactions with proteins containing WRPW motifs to inhibit the cortical progenitor-to-neuron transition.

This interpretation agrees with several previous findings. Hes1 (a prototypical WRPW motif protein) and Gro/TLE are co-expressed in cortical neural progenitor cells, form complexes, and repress transcription together (14, 16, 18, 20). Moreover, both Hes1 and Gro/TLE1 were shown to associate in cultured neural stem cells with the promoter of pro-neuronal genes, like *Mash1* (17). Misexpression of *Gro/TLE1* in the developing forebrain causes reduced neuronal differentiation *in vivo*, as does its exogenous expression in cultured cortical neural progenitor cells (Refs. 14, 15 and this study). These effects are similar to the inhibition of neuronal differentiation and maintenance of neural stem/progenitor cells caused by misexpression of *Hes1*, *Hes3*, or *Hes5* in the embryonic brain (41, 50, 51). Conversely, *Hes1*;*Hes5* double knock-out mice show a premature differentiation of neural stem/progenitor cells into neurons (52). Together with our present findings, these results strongly suggest that Gro/TLE1 works together with Hes proteins to regulate the transition of cortical neural progenitor cells into neurons.

The physiological significance of the ability of Gro/TLE1 to form complexes with other factors expressed during cortical neurogenesis remains to be defined. It is possible that through such interactions Gro/TLE1 might participate in mechanisms important for other cellular processes, like the regulation of the rate of cell proliferation of neural progenitors, or the specification of selected neuronal fates. In that regard, previous studies have shown that different Gro/TLE family members continue to be expressed in different populations of post-mitotic cortical neurons, suggesting non-overlapping roles in the establishment and/or maintenance of neuronal identity (47, 53).

Gro/TLE family members regulate a large number of developmental processes. The availability of mutations that selectively perturb interactions with specific families of Gro/TLE transcription partners is expected to facilitate the elucidation of the molecular mechanisms underlying the pleiotropic activities of this family of transcriptional co-repressors.

Acknowledgments—We thank Yeman Tang and Kerline Joachim for excellent technical assistance.

REFERENCES

1. Buscarlet, M., and Stifani, S. (2007) *Trends Cell Biol.* **17**, 353–361
2. Chen, G., and Courey, A. J. (2000) *Gene* **249**, 1–16
3. Courey, A. J., and Jia, S. (2001) *Genes Dev.* **15**, 2786–2796
4. Gasperowicz, M., and Otto, F. (2005) *J. Cell Biochem.* **95**, 670–687
5. Hasson, P., and Paroush, Z. (2006) *Br. J. Cancer* **94**, 771–775
6. Zamparini, A. L., Watts, T., Gardner, C. E., Tomlinson, S. R., Johnston, G. I., and Brickman, J. M. (2006) *Development* **133**, 3709–3722
7. Heitzler, P., Bourouis, M., Ruel, L., Carteret, C., and Simpson, P. (1996) *Development* **122**, 161–171
8. Bray, S. J. (2006) *Nat. Rev. Mol. Cell Biol.* **7**, 678–689
9. Paroush, Z., Finley, R. L., Kidd, T., Wainwright, S. M., Ingham, P. W., Brent, R., and Ish-Horowicz, D. (1994) *Cell* **79**, 805–815
10. Fisher, A. L., Ohsako, S., and Caudy, M. (1996) *Mol. Cell Biol.* **16**, 2670–2677
11. Giagtzoglou, N., Alifragis, P., Koumbanakis, K. A., and Delidakis, C. (2003) *Development* **130**, 259–270
12. Dehni, G., Liu, Y., Husain, J., and Stifani, S. (1995) *Mech. Dev.* **53**, 369–381
13. Leon, C., and Lobe, C. G. (1997) *Dev. Dyn.* **208**, 11–24
14. Nuthall, H. N., Joachim, K., and Stifani, S. (2004) *Mol. Cell Biol.* **24**, 8395–8407
15. Yao, J., Liu, Y., Lo, R., Tretjakoff, I., Peterson, A., and Stifani, S. (2000) *Mech. Dev.* **93**, 105–115
16. Nuthall, H. N., Husain, J., McLaren, K. W., and Stifani, S. (2002) *Mol. Cell Biol.* **22**, 389–399
17. Ju, B. G., Solum, D., Song, E. J., Lee, K. J., Rose, D. W., Glass, C. K., and Rosenfeld, M. G. (2004) *Cell* **119**, 815–829
18. Yao, J., Lai, E., and Stifani, S. (2001) *Mol. Cell Biol.* **21**, 1962–1972
19. Sonderegger, C. K., and Vogt, P. K. (2003) *Oncogene* **22**, 1749–1757
20. Marcal, N., Patel, H., Dong, Z., Belanger-Jasmin, S., Hoffman, B., Helgason, C. D., Dang, J., and Stifani, S. (2005) *Mol. Cell Biol.* **25**, 10916–10929
21. Kobayashi, M., Nishikawa, K., Suzuki, T., and Yamamoto, M. (2001) *Dev. Biol.* **232**, 315–326
22. Appolloni, I., Calzolari, F., Corte, G., Perris, R., and Malatesta, P. (2008) *Cereb. Cortex* **18**, 553–562
23. Benes, F. M., Lim, B., Matzilevich, D., Walsh, J. P., Subburaiu, S., and Minns, M. (2007) *Proc. Natl. Acad. Sci. U. S. A.* **104**, 10164–10169
24. Panto, M. R., Zappala, A., Tuorto, F., and Cicirata, F. (2004) *Eur. J. Neurosci.* **19**, 2893–2902
25. Jennings, B. H., Pickles, L. M., Wainwright, S. M., Roe, S. M., Pearl, L. H., and Ish-Horowicz, D. (2006) *Mol. Cell* **22**, 645–655
26. Grbavec, D., Lo, R., Liu, Y., and Stifani, S. (1998) *Eur. J. Biochem.* **258**, 339–349
27. Belanger-Jasmin, S., Llamas, E., Tang, Y., Joachim, K., Osiceanu, A. M., Jhas, S., and Stifani, S. (2007) *J. Neurochem.* **103**, 2022–2034
28. Ghosh, A., and Greenberg, M. E. (1995) *Neuron* **15**, 89–103
29. Toma, J. G., El-Bizri, H., Barnabe-Heider, F., Aloyz, R., and Miller, F. D. (2000) *J. Neurosci.* **20**, 7648–7656
30. Sun, Y., Nadal-Vicens, M., Mison, S., Lin, M. Z., Zubiaga, A., Hua, X., Fan, G., and Greenberg, M. E. (2001) *Cell* **104**, 365–376
31. Jhas, S., Ciura, S., Belanger-Jasmin, S., Dong, Z., Llamas, E., Theriault, F. M., Joachim, K., Tang, Y., Liu, L., Liu, J., and Stifani, S. (2006) *J. Neurosci.* **26**, 11061–11071
32. Wu, G., Xu, G., Schulman, B. A., Jeffrey, P. D., Harper, J. W., and Pavletich, N. P. (2003) *Mol. Cell* **11**, 1445–1456
33. Wall, M. A., Coleman, D. E., Lee, E., Iniguez-Lluhi, J. A., Posner, B. A., Gilman, A. G., and Sprang, S. R. (1995) *Cell* **83**, 1047–1058
34. Sondek, J., Bohm, A., Lambright, D. G., Hamm, H. E., and Sigler, P. B. (1996) *Nature* **379**, 369–374
35. Sprague, E. R., Redd, M. J., Johnson, A. D., and Wolberger, C. (2000) *EMBO J.* **19**, 3016–3027
36. Pickles, L. M., Roe, S. M., Hemingway, E. J., Stifani, S., and Pearl, L. H. (2002) *Structure* **10**, 751–761
37. Miller, D. M., 3rd, Niemeier, C. J., and Chitkara, P. (1993) *Genetics* **135**, 741–753
38. Pflugrad, A., Meir, J. Y., Barnes, T. M., and Miller, D. M., 3rd (1997) *Development* **124**, 1699–1709
39. Komachi, K., and Johnson, A. D. (1997) *Mol. Cell Biol.* **17**, 6023–6028
40. Sasai, Y., Kageyama, R., Tagawa, Y., Shigemoto, R., and Nakanishi, S. (1992) *Genes Dev.* **6**, 2620–2634
41. Ishibashi, M., Moriyoshi, K., Sasai, Y., Shiota, K., Nakanishi, S., and Kageyama, R. (1994) *EMBO J.* **13**, 1799–1805
42. Ishibashi, M., Ang, S. L., Shiota, K., Nakanishi, S., Kageyama, R., and Guillemot, F. (1995) *Genes Dev.* **9**, 3136–3148
43. Jimenez, G., Paroush, Z., and Ish-Horowicz, D. (1997) *Genes Dev.* **11**, 3072–3082
44. Brantjes, H., Roose, J., van De Wetering, M., and Clevers, H. (2001) *Nucleic Acids Res.* **29**, 1410–1419
45. Xuan, S., Baptista, C. A., Balas, G., Tao, W., Soares, V. C., and Lai, E. (1995) *Neuron* **14**, 1141–1152
46. Menard, C., Hein, P., Paquin, A., Savelson, A., Yang, X. M., Lederfein, D., Barnabe-Heider, F., Mir, A. A., Sterneck, E., Peterson, A. C., Johnson, P. F., Vinson, C., and Miller, F. D. (2002) *Neuron* **36**, 597–610
47. Shen, Q., Wang, Y., Dimos, J. T., Fasano, C. A., Phoenix, T. N., Lemischka, I. R., Ivanova, N. B., Stifani, S., Morrissey, E. E., and Temple, S. (2006) *Nat. Neurosci.* **9**, 743–751
48. Jepsen, K., Solum, D., Zhou, T., McEvelly, R. J., Kim, H. J., Glass, C. K., Hermanson, O., and Rosenfeld, M. G. (2007) *Nature* **450**, 415–419
49. Friocourt, G., Kanatani, S., Tabata, H., Yozu, M., Takahashi, T., Antypa, M., Ragueneau, O., Chelly, J., Ferec, C., Nakajima, K., and Parnavelas, J. G. (2008) *J. Neurosci.* **28**, 5794–5805
50. Hirata, H., Ohtsuka, T., Bessho, Y., and Kageyama, R. (2000) *J. Biol. Chem.* **275**, 19083–19089
51. Ohtsuka, T., Sakamoto, M., Guillemot, F., and Kageyama, R. (2001) *J. Biol. Chem.* **276**, 30467–30474
52. Ohtsuka, T., Ishibashi, M., Gradwohl, S., Nakanishi, S., Guillemot, F., and Kageyama, R. (1999) *EMBO J.* **18**, 2196–2207
53. Yao, J., Liu, Y., Husain, J., Lo, R., Palaparti, A., Henderson, J., and Stifani, S. (1998) *Dev. Growth Differ.* **40**, 133–146

References

Acampora, D., V. Avantaggiato F. Tuorto and A. Simeone (1997). "Genetic control of brain morphogenesis through Otx gene dosage requirement." Development 124: 3639-3650.

Adjaye, J., J. Huntriss, R. Herwig, A. BenKahla, T. Brink, C. Wierling, C. Hultschig, D. Groth, M. Yaspo, H. Picton, R. Godsen and H Lehrac (2005). "Primary differentiation in the human blastocyst: comparative molecular portraits of inner cell mass and trophectoderm cells." Stem Cells 23(10): 1514-1525.

Aghaallaei, N., B. Bajoghli, I. Walter and T. Czerny (2005). "Duplicated members of the Groucho/Tle gene family in fish." Developmental Dynamics 234: 143-150.

Ambrosetti, D., H. Scholer, L. Dailey and C. Basilico (2000). "Modulation of the activity of multiple transcriptional activation domains by the DNA binding domains mediates the synergistic action of Sox2 and Oct-3 on the FGF5 enhancer." Journal of Biological Chemistry 275: 23387-23397.

Ang, S., A. Wierda, D. Wong, K. Stevens, S. Cascio, S., J. Rossant and K. Zaret. (1993). "The formation and maintenance of the definitive endoderm lineage in the mouse: involvement of HNF3/forkhead proteins." Development 119: 1301-1315.

Antczak, M. and J. Van Blerkom (1997). "Oocyte influences on early development: the regulatory proteins leptin and STAT3 are polarized in mouse and human oocytes and differentially distributed within the cells of the preimplantation stage embryo." Mol Hum Reprod 3(12): 1067-1086.

Arnold, S. and E. Robertson (2009). "Making a commitment: cell lineage allocation and axis patterning in the early mouse embryo." Nat Rev Mol Cell Biol 10(2): 91-103.

Ashfield, R., A. Patel, S. Bossone, H. Brown, R. Campbell, K. Marcu and N. Proudfoot (1994). "MAZ-dependent termination between closely spaced human complement genes." The EMBO Journal 13(23): 5656.

Aubert, J., H. Dunstan, I. Chambers and A. Smith (2002). "Functional gene screening in embryonic stem cells implicates Wnt antagonism in neural differentiation." Nat Biotech 20(12): 1240-1245.

Bajoghli, B. (2007). "Evolution of the Groucho/Tle gene family: gene organization and duplication events." Development Genes and Evolution.

- Beddington, R.** (1994). "Induction of a second neural axis by the mouse node." Development 120: 613-620.
- Beddington, R. and E. Robertson** (1999). "Axis Development and Early Asymmetry in Mammals." Cell 96: 195-209.
- Belo, J., D. Bachiller, E. Agius, C. Kemp, A. Borges, S. Marques, S. Piccolo and E. De Robertis** (2000). "Cerberus-like is a secreted BMP and nodal antagonist not essential for mouse development." Genesis 26(4): 265-270.
- Belo, J., T. Bouwmeester, L. Leyns and N. Kertesz** (1997). "Cerberus-like is a secreted factor with neuralizing activity expressed in the anterior primitive endoderm of the mouse gastrula." Mechanisms of Development 68: 45-97.
- Ben-Haim, N., C. Lu, M. Guzman-Ayala, L. Pescatore, D. Constam, F. Naef, E. Robertson and D. Constam** (2006). "The nodal precursor acting via activin receptors induces mesoderm by maintaining a source of its convertases and BMP4." Dev Cell.
- Brannon, M., M. Gomperts, L. Sumoy, R. Moon and D. Kimelman** (1997). "A β -catenin/XTcf-3 complex binds to the siamois promoter to regulate dorsal axis specification in *Xenopus*." Genes & Development 11: 2359-2370.
- Brantjes, H., J. Roose, M. van De Wetering and H. Clevers** (2001). "All Tcf HMG box transcription factors interact with Groucho-related co-repressors." Nucleic Acids Res 29(7): 1410-1419.
- Brennan, J., C. Lu, D. Norris and T. Rodriguez** (2001). "Nodal signalling in the epiblast patterns the early mouse embryo." Nature 411: 965-968.
- Brickman, J., C. Jones, M. Clements, J. C. Smith and R. S. Beddington** (2000). "Hex is a transcriptional repressor that contributes to anterior identity and suppresses Spemann organizer function." Development 127(11): 2303-2315.
- Buehr, M., S. Meek, K. Blair, J. Yang, J. Ure, J. Silva, R. Mclay, J. Hall, Q. Ying and A. Smith** (2008). "Capture of Authentic Embryonic Stem Cells from Rat Blastocysts." Cell 135(7): 1287-1298.
- Burdon, T., C. Stracey, I. Chambers, J. Nichols and A. Smith** (1999). "Suppression of SHP-2 and ERK signalling promotes self-renewal of mouse embryonic stem cells." Developmental Biology 210(1): 30-43.
- Burks, P., H. Isaacs and M. Pownall** (2008). "FGF signaling modulates transcriptional repression by *Xenopus* groucho-related-4." Biol Cell 101: 301-308.

Buscarlet, M., A. Perin, A. Laing, J. M. Brickman and S. Stifani (2008). "Inhibition of Cortical Neuron Differentiation by Groucho/TLE1 Requires Interaction with WRPW, but Not Eh1, Repressor Peptides." Journal of Biological Chemistry 283(36): 24881-24888.

Buscarlet, M. and S. Stifani (2007). "The 'Marx' of Groucho on development and disease." Trends in Cell Biology 17(7): 353-361.

Canham, M., A. Sharov, M. H. Ko and J. Brickman (2010). "Functional heterogeneity of embryonic stem cells revealed through translational amplification of an early endodermal transcript." PLoS Biol 8(5): e1000379.

Carnac, G., L. Kodjabachian, J. B. Gurdon and P. Lemaire (1996). "The homeobox gene Siamois is a target of the Wnt dorsalisation pathway and triggers organiser activity in the absence of mesoderm." Development 122(10): 3055-3065.

Chambers, I., D. Colby, M. Robertson, J. Nichols, S. Lee, S. Tweedie and A. Smith (2003). "Functional expression cloning of Nanog, a pluripotency sustaining factor in embryonic stem cells." Cell 113(5): 643-655.

Chambers, I., J. Silva, D. Colby, J. Nichols, B. Nijmeijer, M. Robertson, J. Vrana, K. Jones, L. Grotewold and A. Smith (2007). "Nanog safeguards pluripotency and mediates germline development." Nature 450(7173): 1230-1234.

Chambers, I. and S. Tomlinson (2009). "The transcriptional foundation of pluripotency." Development 136(14): 2311.

Chazaud, C. and J. Rossant (2006). "Disruption of early proximodistal patterning and AVE formation in Apc mutants." Development 133: 3379-3387.

Chen, G., J. Fernandez, Mische, S. and A. Courey (1999). "A functional interaction between the histone deacetylase Rpd3 and the corepressor groucho in Drosophila development." Genes & Development 13: 2218-2230.

Chen, G., P. Nguyen and A. Courey (1998). "A Role for Groucho Tetramerization in Transcriptional Repression." Molecular and Cellular Biology 18: 7259-7268.

Cinnamon, E., A. Helman, R. Ben-Haroush Schyr, A. Orian, G. Jimenez and Z. Paroush (2008). "Multiple RTK pathways downregulate Groucho-mediated repression in Drosophila embryogenesis." Development 135(5): 829-837.

Dang, J., T. Inukai, H. Kurosawa, K. Goi, T. Inaba, N. T. Lenny, J. R. Downing, S. Stifani and A. T. Look (2001). "The E2A-HLF oncoprotein activates Groucho-related genes and suppresses Runx1." Mol Cell Biol 21(17): 5935-5945.

Daniels, D. L. and W. I. Weis (2005). " β -catenin directly displaces Groucho/TLE repressors from Tcf/Lef in Wnt-mediated transcription activation." Nat Struct Mol Biol 12(4): 364-371.

Dasen, J. S., J. P. Barbera, T. S. Herman, S. O. Connell, L. Olson, B. Ju, J. Tollkuhn, S. H. Baek, D. W. Rose and M. G. Rosenfeld (2001). "Temporal regulation of a paired-like homeodomain repressor/TLE corepressor complex and a related activator is required for pituitary organogenesis." Genes Dev 15(23): 3193-3207.

Daudet, N. and J. Lewis (2005). "Two contrasting roles for Notch activity in chick inner ear development: specification of prosensory patches and lateral inhibition of hair-cell differentiation." Development 132(3): 541-551.

Ding, J., L. Yang, Y. Yan, A. Chen, N. Desai, Wynshaw-Boris, A. and M. Shen (1998). "Cripto is required for correct orientation of the anterior-posterior axis in the mouse embryo." Nature 395: 702-707.

Eberhard, D., G. Jiménez, B. Heavey and M. Busslinger (2000). "Transcriptional repression by Pax5 (BSAP) through interaction with corepressors of the Groucho family." The EMBO Journal 19(10): 2292-2303.

Evans, M. and M. Kaufman (1981). "Establishment in culture of pluripotential cells from mouse embryos." Nature 292(5819): 154-156.

Fekany, K., Y. Yamanaka, T. Leung, H. Sirotkin, J. Topczewski, M. A. Gates, M. Hibi, A. Renucci, D. Stemple, A. Radbill, A. Schier, W. Driever, T. Hirano, W. Talbot and L. Solnica-Krezel (1999). "The zebrafish bozozok locus encodes Dharma, a homeodomain protein essential for induction of gastrula organizer and dorsoanterior embryonic structures." Development 126(7): 1427-1438.

Fisher, A. L. and M. Caudy (1998). "Groucho proteins: transcriptional corepressors for specific subsets of DNA-binding transcription factors in vertebrates and invertebrates." Genes Dev 12(13): 1931-1940.

Flores-Saaib, R. and A. Courey (2000). "Analysis of Groucho-histone interactions suggests mechanistic similarities between Groucho-and Tup1-mediated repression." Nucleic Acids Res 28(21): 4189-4169.

Friedel, R., A. Plump, X. Lu, K. Spilker, Jolicoeur, C. and M Tessier-Lavigne (2005). "Gene targeting using a promoterless gene trap vector ("targeted trapping") is an efficient method to mutate a large fraction of genes." Proceedings of the National Academy of Sciences 102(27): 13188-13193.

Friedman, J. R. and K. H. Kaestner (2006). "The Foxa family of transcription factors in development and metabolism." Cell Mol Life Sci 63(19-20): 2317-2328.

Gasperowicz, M. and F. Otto (2005). "Mammalian Groucho homologs: Redundancy or specificity?" J. Cell. Biochem. 95(4): 670-687.

Gerhart, J., M. Danilchik, T. Doniach, Roberts, S., Rowning, B. and R. Stewart (1989). "Cortical rotation of the *Xenopus* egg: consequences for the anteroposterior pattern of embryonic dorsal development." Development(Supplement): 37-51.

Glinka, A., H. Delius, C. Blumenstock and C. Niehrs (1996). "Combinatorial signalling by Xwnt-11 and Xnr3 in the organizer epithelium." Mechanisms of Development 60(2): 221-231.

Glinka, A., W. Wu, H. Delius, Monaghan P., Blumenstock, C. and C. Niehrs (1998). "Dickkopf-1 is a member of a new family of secreted proteins and functions in head induction." Nature.

Gossler, A., A. Joyner, J. Rossant and W. Skarnes (1989). "Mouse embryonic stem cells and reporter constructs to detect developmentally regulated genes." Science 244(4903): 463-464.

Grbavec, D. and S. Stifani (1996). "Molecular interaction between TLE1 and the carboxyl-terminal domain of HES-1 containing the WRPW motif." Biochem Biophys Res Commun 223(3): 701-705.

Green, S. and A. Johnson (2005). "Genome-wide Analysis of the Functions of a Conserved Surface on the Corepressor Tup1." Molecular Biology of the Cell 16: 2605-2613.

Hao, J., T. Li, X. Qi, D. Zhao and G. Zhao (2006). "WNT/[beta]-catenin pathway up-regulates Stat3 and converges on LIF to prevent differentiation of mouse embryonic stem cells." Developmental Biology 290(1): 81-91.

Harland, R. and J. Gerhart (1997). "Formation and function of Spemann's organizer." Annu Rev Cell Dev Biol 13: 611-667.

Hasson, P., N. Egoz, C. Winkler, G. Volohonsky, Jia, S., Dinur, T., Volk T., Courey, A. and Z. Paroush (2004). "EGFR signaling attenuates Groucho-dependent repression to antagonize Notch transcriptional output." Nature Genetics 37: 101-105.

Heasman, J. (2006). "Maternal determinants of embryonic cell fate." Semin Cell Dev Biol 17(1): 93-98.

Heasman, J., D. Ginsberg, B. Geiger, K. Goldstone, T. Pratt, C. Yoshida-Noro and C. Wylie (1994). "A functional test for maternally inherited cadherin in *Xenopus*

shows its importance in cell adhesion at the blastula stage." *Development* 120(1): 49-57.

Ho, C. Y., C. Houart, S. W. Wilson and D. Y. Stainier (1999). "A role for the extraembryonic yolk syncytial layer in patterning the zebrafish embryo suggested by properties of the hex gene." *Curr Biol* 9(19): 1131-1134.

Hoffman, B., B. Zavaglia, M. Beach and C. Helgason (2008). "Expression of Groucho/TLE proteins during pancreas development." *BMC Developmental Biology* 8(1): 81.

Hsieh, J.-C., L. Lee, L. Zhang, S. Wefer, K. Brown, C. DeRossi, M. E. Wines, T. Rosenquist and B. C. Holdener (2003). "Mesd encodes an LRP5/6 chaperone essential for specification of mouse embryonic polarity." *Cell* 112(3): 355-367.

Huangfu, D., K. Osafune, R. Maehr, Guo, W., Eijkelenboon, A., Chen, S., Muhlestein, W. and D. Melton (2008). "Induction of pluripotent stem cells from primary human fibroblasts with only Oct4 and Sox2." *Nature Biotechnology* 26: 1267-1275.

Huelsken, J., R. Vogel, V. Brinkmann, B. Erdmann, C. Birchmeier and W. Birchmeier (2000). "Requirement for beta-catenin in anterior-posterior axis formation in mice." *J Cell Biol* 148(3): 567-578.

Izzi, L., C. Silvestri, I. von Both, E. Labbé, L. Zakin, J. L. Wrana and L. Attisano (2007). "Foxh1 recruits Gsc to negatively regulate Mixl1 expression during early mouse development." *The EMBO Journal* 26(13): 3132-3143.

Jennings, B. H. and D. Ish-Horowicz (2008). "The Groucho/TLE/Grg family of transcriptional co-repressors." *Genome Biol* 9(1): 205.

Jennings, B., L. Pickles, S. Wainwright, S. Roe, L. Pearl and D. Ish-Horowicz (2006). "Molecular recognition of transcriptional repressor motifs by the WD domain of the Groucho/TLE corepressor." *Mol Cell* 22(5): 645-655.

Jiménez, G., C. Verrijzer and D. Ish-Horowicz (1999). "A conserved motif in goosecoid mediates groucho-dependent repression in *Drosophila* embryos." *Molecular and Cellular Biology* 19(3): 2080-2087.

Kaji, K., K. Norrby, A. Paca, M. Mileikovsky, P. Mohseni and K. Woltjen (2009). "Virus-free induction of pluripotency and subsequent excision of reprogramming factors." *Nature* 458(7239): 771-775.

Kawamura, A., S. Koshida, H. Hijikata, A. Ohbayashi, H. Kondoh and S. Takada (2005). "Groucho-associated transcriptional repressor ripply1 is required for

proper transition from the presomitic mesoderm to somites." Dev Cell 9(6): 735-744.

Kawamura, A., S. Koshida and S. Takada (2008). "Activator-to-repressor conversion of T-box transcription factors by the Ripply family of Groucho/TLE-associated mediators." Molecular and Cellular Biology 28(10): 3236.

Kessler, D. (1997). "Siamois is required for formation of Spemann's organizer." Proc Natl Acad Sci USA 94(24): 13017.

Kimura-Yoshida, C., H. Nakano, D. Okamura and K. Nakao (2005). "Canonical Wnt signaling and its antagonist regulate anterior-posterior axis polarization by guiding cell migration in mouse visceral endoderm." Dev Cell 9: 639-650.

Klein, P. S. and D. A. Melton (1996). "A molecular mechanism for the effect of lithium on development." Proc Natl Acad Sci USA 93(16): 8455-8459.

Knust, E., K. Tietze and J. Campos-Ortega (1987). "Molecular analysis of the neurogenic locus Enhancer of split of *Drosophila melanogaster*." The EMBO Journal 6(13): 4113.

Kondow, A., K. Hitachi, K. Okabayashi, N. Hayashi and M. Asashima (2007). "Bowline mediates association of the transcriptional corepressor XGrg-4 with Tbx6 during somitogenesis in *Xenopus*." Biochem Biophys Res Commun 359(4): 959-964.

Koop, K., L. MacDonald and C. Lobe (1996). "Transcripts of Grg4, a murine groucho-related gene, are detected in adjacent tissues to other murine neurogenic gene homologues during embryonic development." Mech Dev 59: 73-87.

Kunath, T., M. Saba-El-Leil, M. Almousailleakh, J. Wray, S. Meloche and A. Smith (2007). "FGF stimulation of the Erk1/2 signalling cascade triggers transition of pluripotent embryonic stem cells from self-renewal to lineage commitment." Development 134(16): 2895-2902.

Lai, E. (2004). "Notch signaling: control of cell communication and cell fate." Development 131: 965-973.

Leon, C. and C. Lobe (1997). "Grg 3, a murine Groucho-related gene, is expressed in the developing nervous system and in Mesenchyme-Induced Epithelial Structures." Developmental Dynamics 208: 11-24.

Lepourcelet, M and Shivdasani R.(2002). "Characterization of a Novel Mammalian Groucho Isoform and Its Role in Transcriptional Regulation." Journal of Biological Chemistry 277(49): 47732-47740.

Leyns, L., T. Bouwmeester, S. Kim, S. Piccolo and E. De Robertis (1997). "Frzb-1 is a secreted antagonist of Wnt signaling expressed in the Spemann organizer." Cell 88: 747-756.

Li, J., C. Sutter, D. Parker, T. Blauwkamp, M. Fang and K. Cadigan (2007). "CBP/p300 are bimodal regulators of Wnt signaling." The EMBO Journal 26(9): 2284.

Li, L., B. Baibakov and J. Dean (2008). "A subcortical maternal complex essential for preimplantation mouse embryogenesis." Dev Cell 15(3): 416-425.

Lickert, H., S. Kutsch, Kanzler, B., Tamai, Y., Taketo, M. and R. Kemmler (2002). "Formation of multiple hearts in mice following deletion of [beta]-catenin in the embryonic endoderm." Dev Cell 3(2): 171-181.

Lindsley, D. L. and E. H. Grell (1968). "Genetic Variations of *Drosophila Melanogaster*." Carnegie Institution of Washington, Washington DC.

Liu, P., M. Wakamiya, M. Shea, U. Albrecht, Behringer, R., and A. Bradley (1999). "Requirement for Wnt3 in vertebrate axis formation." Nature genetics 22: 361-365.

Liu, Y. and P. A. Labosky (2008). "Regulation of Embryonic Stem Cell Self-Renewal and Pluripotency by Foxd3." Stem Cells 26(10): 2475-2484.

Logan, C., J. Miller, M. Ferkowicz and D. McClay (1999). "Nuclear beta-catenin is required to specify vegetal cell fates in the sea urchin embryo." Development 126(2): 345-357.

Lowell, S., A. Benchoua, B. Heavey and A. G. Smith (2006). "Notch promotes neural lineage entry by pluripotent embryonic stem cells." PLoS Biol 4(5): e121.

Lu, C., E. Robertson and J. Brennan (2004). "The mouse frizzled 8 receptor is expressed in anterior organizer tissues." Gene Expression Patterns 4: 569-572.

Mallo, M., F. del Amo and T. Gridley (1993). "Cloning and developmental expression of Grg, a mouse gene related to the groucho transcript of the *Drosophila* Enhancer of split complex." Mechanisms of Development 42(1-2): 67-76.

Mallo, M., M. Gendron-Maguire, M. L. Harbison and T. Gridley (1995). "Protein characterization and targeted disruption of Grg, a mouse gene related to the groucho transcript of the *Drosophila* Enhancer of split complex." Dev Dyn 204(3): 338-347.

Marçal, N., H. Patel, Z. Dong, S. Belanger-Jasmin, B. Hoffman, C. D. Helgason, J. Dang and S. Stifani (2005). "Antagonistic effects of Grg6 and Groucho/TLE on the

transcription repression activity of brain factor 1/FoxG1 and cortical neuron differentiation." Molecular and Cellular Biology 25(24): 10916-10929.

Martinez Barbera, J. P., M. Clements, P. Thomas, T. Rodriguez, D. Meloy, D. Kioussis and R. S. Beddington (2000). "The homeobox gene Hex is required in definitive endodermal tissues for normal forebrain, liver and thyroid formation." Development 127(11): 2433-2445.

Masui, S., Y. Nakatake, Y. Toyooka and D. Shimosato (2007). "Pluripotency governed by Sox2 via regulation of Oct3/4 expression in mouse embryonic stem cells." Nature Cell Biology 9(6): 635-635.

Mayr, T., U. Deutsch, M. Kühl, H. Drexler, F. Lottspeich, R. Deutzmann, D. Wedlich and W. Risau (1997). "Fritz: a secreted frizzled-related protein that inhibits Wnt activity." Mechanisms of Development 63(1): 109-125.

McKendry, R., S. Hsu, Harland R., and R Grosschedl (1997). "LEF-1/TCF proteins mediate wnt-inducible transcription from the Xenopus nodal-related 3 promoter." Developmental Biology 192: 420-431.

Mieszczanek, J., M. de La Roche and M. Bienz (2008). "A role of Pygopus as an anti-repressor in facilitating Wnt-dependent transcription." Proceedings of the National Academy of Sciences 105(49): 19324.

Mikawa, T., A. M. Poh, K. A. Kelly, Y. Ishii and D. E. Reese (2004). "Induction and patterning of the primitive streak, an organizing center of gastrulation in the amniote." Dev Dyn 229(3): 422-432.

Milili, M., L. Gauthier, J. Veran, M. Mattei and C. Schiff (2002). "A new Groucho TLE 4 protein may regulate the repressive activity of Pax 5 in human B lymphocytes." Immunology 106(4): 447-455.

Mitsui, K., Y. Tokuzawa, H. Itoh, K. Segawa, M. Murakami, K. Takahashi, M. Maruyama, M. Maeda and S. Yamanaka (2003). "The homeoprotein Nanog is required for maintenance of pluripotency in mouse epiblast and ES cells." Cell 113(5): 631-642.

Miyabayashi, T., J. Teo, M. Yamamoto, M. McMillan, C. Nguyen and M. Kahn (2007). "Wnt/ β -catenin/CBP signaling maintains long-term murine embryonic stem cell pluripotency." Proceedings of the National Academy of Sciences 104(13): 5668.

Miyasaka, H., B. Choudhury, E. Hou and S. Li (1993). "Molecular cloning and expression of mouse and human cDNA encoding AES and ESG proteins with strong similarity to Drosophila enhancer of split groucho protein." Eur J Biochem 216(1): 343-352.

Morimoto, M., N. Sasaki, M. Oginuma, M. Kiso, K. Igarashi, K.-i. Aizaki, J. Kanno and Y. Saga (2007). "The negative regulation of Mesp2 by mouse Ripply2 is required to establish the rostro-caudal patterning within a somite." Development 134(8): 1561.

Morrish, D., Y. Kudo, I. Caniggia, J. Cross, D. Evain-Brion, M. Gasperowicz, M. Kokozidou, C. Leisser, K. Takahashi and J. Yoshimatsu (2007). "Growth factors and trophoblast differentiation--workshop report." Placenta 28: S121.

Morrison, G., I. Oikonomopoulou, R. Migueles, S. Soneji, A. Livigni, T. Enver and J. Brickman (2008). "Anterior Definitive Endoderm from ESCs Reveals a Role for FGF Signaling." Cell Stem Cell 3(4): 402-415.

Morrison, G. M. and J. M. Brickman (2006). "Conserved roles for Oct4 homologues in maintaining multipotency during early vertebrate development." Development 133(10): 2011-2022.

Mukhopadhyay, M., S. Shtrom and C. Rodriguez-Esteban (2001). "Dickkopf1 is required for embryonic head induction and limb morphogenesis in the mouse." Dev Cell 1: 423-424.

Murray, J., D. Campbell, N. Morrice, G. Auld, N. Shpiro, R. Marquez, M. Peggie, J. Bain, G. Bloomberg, F. Grahammer, F. Lang, P. Wulff, D. Kuhl and P. Cohen (2004). "Exploitation of KESTREL to identify NDRG family members as physiological substrates for SGK1 and GSK3." Biochem J 384(Pt 3): 477-488.

Nakagawa, M., M. Koyanagi, Tanabe, K. and S. Yamanaka (2007). "Generation of induced pluripotent stem cells without Myc from mouse and human fibroblasts." Nature Biotechnology 26(1): 101-106.

Nichols, J., I. Chambers, T. Taga and A. Smith (2001). "Physiological rationale for responsiveness of mouse embryonic stem cells to gp130 cytokines." Development 128(12): 2333-2339.

Nichols, J., B. Zevnik, K. Anastassiadis, H. Niwa, Klewe-Nebenius, D. and A. Smith (1998). "Formation of pluripotent stem cells in the mammalian embryo depends on the POU transcription factor Oct4." Cell 95: 379-391.

Niwa, H., T. Burdon, I. Chambers and A. Smith (1998). "Self-renewal of pluripotent embryonic stem cells is mediated via activation of STAT3." Genes Dev 12(13): 2048.

Niwa, H., J. Miyazaki and A. Smith (2000). "Quantitative expression of Oct-3/4 defines differentiation, dedifferentiation or self-renewal of ES cells." Nature genetics 24: 372-376.

Nord, A., K. Vranizan, W. Tingley, A. C. Zambon, K. Hanspers, L. G. Fong, Y. Hu, P. Bacchetti, T. Ferrin, P. Babbitt, S. Doniger, W. Skarnes, S. Young and B. Conklin (2007). "Modeling insertional mutagenesis using gene length and expression in murine embryonic stem cells." PLoS ONE 2(7): e617.

Nuthall, H., K. Joachim and S. Stifani (2004). "Phosphorylation of Serine 239 of Groucho/TLE1 by Protein Kinase CK2 Is Important for Inhibition of Neuronal Differentiation." Molecular and Cellular Biology 24(19): 8395.

Okita, K., T. Ichisaka and S. Yamanaka (2007). "Generation of germline-competent induced pluripotent stem cells." Nature 448(7151): 313-317.

Paroush, Z. and R. Finley (1994). "Groucho is required for Drosophila neurogenesis, segmentation, and sex determination and interacts directly with hairy-related bHLH proteins." Cell 79(5): 805-815.

Pera, M. and P. Tam (2010). "Extrinsic regulation of pluripotent stem cells." Nature 465(7299): 713-720.

Perea-Gomez, A., K. A. Lawson, M. Rhinn, L. Zakin, P. Brûlet, S. Mazan and S. L. Ang (2001). "Otx2 is required for visceral endoderm movement and for the restriction of posterior signals in the epiblast of the mouse embryo." Development 128(5): 753-765.

Perea-Gomez, A., F. Vella, W. Shawlot, M. Oulad-Abdelghani, C. Chazaud, C. Meno, V. Pfister, L. Chen, E. Robertson, H. Hamada, R. Behringer and S.-L. Ang (2002). "Nodal Antagonists in the Anterior Visceral Endoderm Prevent the Formation of Multiple Primitive Streaks." Developmental Cell 3: 745-756.

Pereira, L., F. Yi and B. J. Merrill (2006). "Repression of Nanog gene transcription by Tcf3 limits embryonic stem cell self-renewal." Mol Cell Biol 26(20): 7479-7491.

Pflugrad, A., J. Meir, T. Barnes and D. Miller (1997). "The Groucho-like transcription factor UNC-37 functions with the neural specificity gene unc-4 to govern motor neuron identity in *C. elegans*." Development 124(9): 1699-1709.

Piccolo, S., E. Agius, L. Leyns, S. Bhattacharyya, H. Grunz, T. Bouwmeester and E. D. Robertis (1999). "The head inducer Cerberus is a multifunctional antagonist of Nodal, BMP and Wnt signals." Nature 397: 707-710.

Piotrowska, K. and M. Zernicka-Goetz (2001). "Role for sperm in spatial patterning of the early mouse embryo." Nature 409(6819): 517-521.

Powell, S., N. Zilz, Y. Beazer-Barclay, T. Bryan, S. Hamilton, S. Thibodeau, B. Vogelstein and K. Kinzler (1992). "APC mutations occur early during colorectal tumorigenesis." Nature 359(235-237): 235-237.

Range, R., J. Venuti and D. McClay (2005). "LvGroucho and nuclear β -catenin functionally compete for Tcf binding to influence activation of the endomesoderm gene regulatory network in the sea urchin embryo." Developmental Biology 279(1): 252-267.

Rathjen, J., J. Lake, M. Bettess, J. Washington, G. Chapman and P. Rathjen (1999). "Formation of a primitive ectoderm like cell population, EPL cells, from ES cells in response to biologically derived factors." J Cell Sci 112 (Pt 5): 601-612.

Reya, T. and H. Clevers (2005). "Wnt signalling in stem cells and cancer." Nature 434(7035): 843-850.

Rosenquist, T. and G. Martin (1995). "Visceral endoderm-1 (VE-1): an antigen marker that distinguishes anterior from posterior embryonic visceral endoderm in the early post-implantation mouse embryo." Mechanisms of Development 49: 117-121.

Rossant, J. and P. Tam (2004). "Emerging Asymmetry and Embryonic Patterning in Early Mouse Development." Developmental Cell 7(2): 155-164.

Sadowski, I., J. Ma, S. Triezenberg and M. Ptashne (1988). "GAL4-VP16 is an unusually potent transcriptional activator." Nature 335: 563-564.

Santisteban, P., P. Recacha, D. Metzger and K. Zaret (2010). "Dynamic expression of groucho-related genes Grg1 and Grg3 in foregut endoderm and antagonism of differentiation." Developmental Dynamics 239(3): 980-986.

Sato, N., L. Meijer, L. Skaltsounis, P. Greengard and A. Brivanlou (2004). "Maintenance of pluripotency in human and mouse embryonic stem cells through activation of Wnt signaling by a pharmacological GSK-3-specific inhibitor." Nat Med 10(1): 55-63.

Sekiya, T. and K. S. Zaret (2007). "Repression by Groucho/TLE/Grg proteins: genomic site recruitment generates compacted chromatin in vitro and impairs activator binding in vivo." Mol Cell 28(2): 291-303.

Sekkai, D., G. Gruel, M. Herry, V. Moucadel, S. Constantinescu, O. Albagli, D. Roux, W. Vainchenker and A. Bennaceur-Griscelli (2005). "Microarray Analysis of LIF/Stat3 Transcriptional Targets in Embryonic Stem Cells." Stem Cells 23(10): 1634.

Shawlot, W., J. Deng, M. Wakamiya and R. Behringer (2000). "The cerberus-related gene, Cerr1, is not essential for mouse head formation." Genesis 26(4): 253-258.

Singh, A., T. Hamazaki, K. Hankowski and N. Terada (2007). "A Heterogeneous Expression Pattern for Nanog in Embryonic Stem Cells." Stem Cells 25(10): 2534-2542.

Singla, D., D. J. Schneider, M. LeWinter and B. Sobel (2006). "wnt3a but not wnt11 supports self-renewal of embryonic stem cells." Biochem Biophys Res Commun 345(2): 789-795.

Sinner, D., S. Rankin, M. Lee and A. M. Zorn (2004). "Sox17 and beta-catenin cooperate to regulate the transcription of endodermal genes." Development 131(13): 3069-3080.

Smith, A., J. Heath, D. Donaldson, G. Wongf, J. Moreau, M. Stahl and D. Rogers (1988). "Inhibition of pluripotential embryonic stem cell differentiation by purified polypeptides." Nature 336: 15.

Song, H., P. Hasson, Z. Paroush and A. Courey (2004). "Groucho oligomerization is required for repression in vivo." Molecular and Cellular Biology 24(10): 4341-4350.

Spemann, H. and H. Mangold (1924). "Über induktion von embryonalanlagen durch implantation artfremder organisatoren." Wilhelm Roux Arch. Entw. Mech. Org. 100: 599-638.

Spivakov, M. and A. Fisher (2007). "Epigenetic signatures of stem-cell identity." Nat Rev Genet 8(4): 263-271.

Srinivas, S., T. Rodriguez, M. Clements, J. Smith and R. Beddington (2004). "Active cell migration drives the unilateral movements of the anterior visceral endoderm." Development 131: 1157-1164.

Swingler, T., K. L. Bess, J. Yao, S. Stifani and P. Jayaraman (2004). "The proline-rich homeodomain protein recruits members of the Groucho/Transducin-like enhancer of split protein family to co-repress transcription in hematopoietic cells." J Biol Chem 279(33): 34938-34947.

Szymczak, A., C. J. Workman, Y. Wang, K. M. Vignali, S. Dilioglou, E. Vanin and D. A. Vignali (2004). "Correction of multi-gene deficiency in vivo using a single 'self-cleaving' 2A peptide-based retroviral vector." Nat Biotechnol 22(5): 589-594.

Takahashi, K. and S. Yamanaka (2006). "Induction of Pluripotent Stem Cells from Mouse Embryonic and Adult Fibroblast Cultures by Defined Factors." Cell 126(4): 663-676.

Tam, P. and K. Steiner (1999). "Anterior patterning by synergistic activity of the early gastrula organizer and the anterior germ layer tissues of the mouse embryo." Development 126(5171-5179).

Tam, W., C. Lim, J. Han, J. Zhang, Y. Ang, H. Ng, H. Yang and B. Lim (2008). "Tcf3 Regulates Embryonic Stem Cell Pluripotency and Self-Renewal by the Transcriptional Control of Multiple Lineage Pathways." Stem Cells 26: 2019-2131.

Tesar, P., J. Chenoweth, F. Brook, T. Davies, E. Evans, D. Mack, R. Gardner and R. D. McKay (2007). "New cell lines from mouse epiblast share defining features with human embryonic stem cells." Nature 448(7150): 196-199.

Thomas, P. and R. Beddington (1996). "Anterior primitive endoderm may be responsible for patterning the anterior neural plate in the mouse embryo." Current Biology 6: 1487-1496.

Thomas, P., A. Brown and R. Beddington (1998). "Hex: a homeobox gene revealing peri-implantation asymmetry in the mouse embryo and an early transient marker of endothelial cell precursors." Development 125: 85-94.

Thomson, J., J. Itskovitz-Eldor, S. Shapiro, M. Waknitz, J. Swiergiel, V. Marshall and J. Jones (1998). "Embryonic stem cell lines derived from human blastocysts." Science 282(5391): 1145.

Tsakiridis, A., E. Tzouanacou, O. Larralde, T. Watts, V. Wilson, L. Forrester and J. Brickman (2007). "A novel triple fusion reporter system for use in gene trap mutagenesis." Genesis 45(6): 353-360.

Vanhateren, N., A. Belsham, V. Randall and A. Borycki (2005). "Expression of avian -related genes during embryonic development." Gene Expression Patterns 5(6): 817-823.

Varlet, I., J. Collignon and E. Robertson (1997). "Nodal expression in the primitive endoderm is required for specification of the anterior axis during mouse gastrulation." Development 124(5): 1033-1044.

Waltzer, L. and M. Bienz (1998). "Drosophila CBP represses the transcription factor TCF to antagonize Wingless signalling." Nature 395(6701): 521-525.

Wang, J., M. Waltner-Law, K. Yamada, H. Osawa, S. Stifani and D. Granner (2000). "Transducin-like Enhancer of Split Proteins, the Human Homologs of Drosophila Groucho, Interact with" Journal of Biological Chemistry 275(24): 18418-18423.

Yaklichkin, S., A. Steiner, Q. Lu and D. Kessler (2007). "FoxD3 and Grg4 Physically Interact to Repress Transcription and Induce Mesoderm in Xenopus." Journal of Biological Chemistry 282(4): 2548.

- Yaklichkin, S., A. Vekker, S. Stayrook, M. Lewis and D. S. Kessler (2007).** "Prevalence of the EH1 Groucho interaction motif in the metazoan Fox family of transcriptional regulators." BMC Genomics 8(1): 201.
- Yamamoto, Y. Saijoh, A. Perea-Gomez, W. Shawlot, R. Behringer, S.-L. Ang, H. Hamada and C. Meno (2004).** "Nodal antagonists regulate formation of the anteroposterior axis of the mouse embryo." Nature 428: 387-392.
- Yamanaka, Y., T. Mizuno, Y. Sasai, M. Kishi, H. Takeda, C. H. Kim, M. Hibi and T. Hirano (1998).** "A novel homeobox gene, dharma, can induce the organizer in a non-cell-autonomous manner." Genes Dev 12(15): 2345-2353.
- Yao, J., Y. Liu, R. Lo, I. Tretjakoff, A. Peterson and S. Stifani (2000).** "Disrupted development of the cerebral hemispheres in transgenic mice expressing the mammalian Groucho homologue transducin-like-enhancer of split 1 in postmitotic neurons." Mechanisms of Development 93(1-2): 105-115.
- Ying, Q., J. Nichols, I. Chambers and A. Smith (2003).** "BMP induction of Id proteins suppresses differentiation and sustains embryonic stem cell self-renewal in collaboration with STAT3." Cell 115(3): 281-292.
- Ying, Q., M. Stavridis, D. Griffiths, M. Li and A. Smith (2003).** "Conversion of embryonic stem cells into neuroectodermal precursors in adherent monoculture." Nature Biotechnology 21: 183-186.
- Ying, Q.-L., J. Wray, J. Nichols, L. Batlle-Morera, B. Doble, J. Woodgett, P. Cohen and A. Smith (2008).** "The ground state of embryonic stem cell self-renewal." Nature 453(7194): 519-523.
- Yu, J., M. Vodyanik, K. Smuga-Otto, J. Antosiewicz-Bourget, J. Frane, S. Tian, J. Nie, G. Jonsdottir, V. Ruotti, R. Stewart, I. Slukvin and J. Thomson (2007).** "Induced pluripotent stem cell lines derived from human somatic cells." Science 318(5858): 1917-1920.
- Yu, X., P. Li, R. Roeder and Z. Wang (2001).** "Inhibition of androgen receptor-mediated transcription by amino-terminal enhancer of split." Molecular and Cellular Biology 21: 4614-4625.
- Zamparini, A., T. Watts, C. Gardner, S. Tomlinson, G. Johnston and J. Brickman (2006).** "Hex acts with β -catenin to regulate anteroposterior patterning via a Groucho-related co-repressor and Nodal." Development 133(18): 3709.
- Zernicka-Goetz, M. (1998).** "Fertile offspring derived from mammalian eggs lacking either animal or vegetal poles." Development 125(23): 4803-4808.

Zhang, H. and S. Emmons (2002). "Caenorhabditis elegans unc-37/groucho interacts genetically with components of the transcriptional mediator complex." Genetics 160: 799-803.

Zhou, H., S. Wu, J. Y. Joo, S. Zhu, D. Han, T. Lin, S. Trauger, G. Bien, S. Yao, Y. Zhu, G. Siuzdak, H. Scholer, L. Duan and S. Ding (2009). "Generation of Induced Pluripotent Stem Cells Using Recombinant Proteins." Stem Cell 4(5): 381-384.

Ziemer, A., K. Tietze, E. Knust and J. Campos-Ortega (1988). "Genetic analysis of Enhancer of split, a locus involved in neurogenesis in *Drosophila melanogaster*." Genetics 119(1): 63.